Christiana Opokuaah Appiah

Bone morphogenetic protein 4 and Gremlin-1 communication between mouse breast cancer cells and fibroblasts

Master's Thesis in Molecular Medicine
Trondheim, spring 2016
Principal supervisor: Geir Bjørkøy, PhD

Norwegian University of Science and Technology (NTNU)
Faculty of Medicine
Department of Cancer Research and Molecular Medicine

NTNU – Trondheim
Norwegian University of
Science and Technology

CEMIR
Centre of Molecular Inflammation Research

TABLE OF CONTENTS

ABSTRACT ..... **V**

ACKNOWLEDGEMENTS ..... **VII**

ABBREVIATIONS ..... **IX**

1. INTRODUCTION **1**

1.1BREAST CANCER 1

1.1.1 Stages of Breast Cancer 1

1.1.2 Breast Cancer Histology 2

1.1.3 Tumor Heterogeneity of Breast Cancer 3

1.1.4 Tumor Microenvironment of Breast Cancer 6

1.1.5 Tumor –Stroma Interaction in Breast Cancer 8

1.2 CANCER ASSOCIATED FIBROBLAST (CAF) 9

1.2.1 Signaling Pathway Associated with CAF Activation in Tumor Environment 10

1.2.2 Role of CAF in Breast cancer tumorigenesis and progression of breast cancer 11

1.4 TRANSFORMING GROWTH FACTOR β (TGF- β) SUPERFAMILY 13

1.4.1 Bone Morphogenic Protein (BMP) family 13

1.4.2 Bone Morphogenic Protein 4 (BMP4) and its Signaling 13

1.4.3 BMP4 Signaling Regulation 15

1.5. GREMLIN – BIOLOGICAL FUNCTIONS OF A BMP ANTAGONIST 16

1.6 BREAST CANCER MOUSE MODEL - BALB/CFC3H 18

2. AIM **21**

3. METHODOLOGY **23**

3.1 TRANSCRIPTOM ANALYSIS OF 66CL4 AND 67NR OF THE 4T1 BREAST CANCER MODEL 23

3.2 GENE CORRELATION WITH PROGNOSIS ANALYSIS 24

3.2.1 Kaplan-Meier (KM) Plotter Analysis 24

3.2.2 BreastMark Analysis 24

3.3 CELL CULTURE 25

3.3.1 Cell lines and Primary cells 25

3.3.2 Sub-Culturing of Cell lines and Primary cells 26

3.3.3 Recombinant mouse BMP4 and GREM1 activities in cultures 26

3.3.4 Transwell cultures 26

3.3.5 Condition medium (CM) treatment on cells 27

3.4 WESTERN BLOT 27

3.4.1 Cell harvesting and protein concentration 28
3.4.2 Gel electrophoresis and transfer of protein 28
3.4.3 Membrane blocking and immunostaining 30
3.5 ENZYME-LINKED IMMUNOSORBENT ASSAY (ELISA) 31
3.5.1 Sample analysis using Sandwich enzyme-linked immunosorbent assay (ELISA) 31
3.6 CELL PROLIFERATION ASSAY 32
3.6.1 Cell Counting Method 32
3.6.2 MTT (Methylthiazolyldiphenyl-tetrazolium bromide) Assay 32
3.7 xCELLigence REAL-TIME CELL ANALYZER (RTCA) MIGRATION ASSAY 33
3.8 STATISTICAL ANALYSIS 35
4. RESULTS 35
4.1 IDENTIFICATION OF PROMETASTATIC FACTORS IN TRANSCRIPTOM DATA AND THEIR CORRELATION WITH PROGRNOSIS 35
4.1.1 CAF associated markers and genes are differently expressed in 67NR and 66cl4 35
4.1.2 Bmp4 is highly expressed in 66cl4 on mRNA level 38
4.1.3 BMP4 correlation with breast cancer prognosis 38
4.1.4 Grem1 is highly expressed in 66cl4 on mRNA level 41
4.1.5 GREM1 correlation with Breast cancer prognosis 42
4.2 BMP4 AND GREM1 ARE EXPRESSED IN VARYING AMOUNT BY THE 4T1 BREAST CANCER CELL LINES. 45
4.3 ESTABLISING OPTIMUM CONDIITONS FOR RmBMP4 and RmGREM1 ON MEF 48
4.3.1 Mouse Embryonic Fibroblasts (MEF) respond to recombinant mouse BMP4 48
4.3.2 Recombinant mouse Grem1 (RmGREM1) can inhibit responses of recombinant mouse Bmp4 in MEFs 49
4.4 EVALUATION OF PARACRINE COMMUNICATION BETWEEN 4T1 BREAST CANCER CELL LINES AND MEF 51
4.4.1 67NR, 168FARN and 66cl4 of the 4T1 breast cancer model secrete soluble mediators that activate SMAD 1/5 signaling in MEF 51
4.4.2 168FARN antagonizes phosphorylated SMAD 1/5/9 signaling in MEF 53
4.4.3 MEF expressed BMP4 and GREM1 on protein level 54
4.4.4 MEF CM enhanced activation of SMAD1/5/9 signaling in 67NR and 4T07 of the 4T1 breast cancer cell lines via secreted mediators 55
4.4.5 Transwell culture of tumor cells and MEF enhances their ability to secrete GREM1 55
4.4.6 MEFs proliferation are influenced by soluble mediators via paracrine crosstalk. 58
4.5 FIBROBLAST ISOLATED FROM LUNGS DISPLAYED ENHANCED MIGRATION ACTIVITY IN RESPONSE TO SOLUBLE MEDIATORS VIA PARACRINE CROSSTALK. 61

5. DISCUSSION 65
5.1 mRNA expression of CAF markers are upregulated in 66cl4 compared to 67NR 65
5.2 Tgf-β superfamily member, Bmp4 is expressed on mRNA level in 66cl4 cell line in culture and primary tumor 66
5.3 BMP4 is associated with good prognosis in lymph node negative breast cancer patients 67
5.4 GREM1 expression correlates with poor prognosis in breast cancer patients 68
5.5 BMP4 and GREM1 expressions in 4T1 Breast cancer model:66cl4 express BMP4 whiles 168FARN and 66cl4 express GREM1 69
5.6 Interplays of BMP4 and GREM1 in 4T1 breast cancer model and MEFs 70
5.7 BMP4 and GREM1 are co-expressed in MEF 71
5.8 Influence of BMP4, GREM1 and tumor soluble mediators on fibroblast proliferation and migration properties 72
6. CONCLUSION AND FUTURE PLANS 75
6.1 Conclusion 75
6.2 Future Plans 75
REFERENCE 77
APPENDIX 89

ABSTRACT

Breast cancer (BC) metastasis is the leading cause of death in breast cancer patients. Interactions between breast cancer tumors and stromal cells allow the microenvironment surrounding the tumor to co-evolve into an activated state leading to tumor progression and metastasis. The 4T1 breast cancer mouse model which consists of five cell lines with different metastatic propensities was used to identify mechanisms of tumor-stroma communication that might facilitate metastasis. It was hypothesized that the breast cancer cell lines which can leave the primary tumor (168FARN, 4T07, 66cl4 and 4T1) are better equipped to attract and communicate with fibroblasts than the non- metastasizing 67NR cell line. Transcriptome analysis found some fibroblast associated genes and markers as well as the TGF-β family member *Bmp4* and its antagonist *Grem1* to be upregulated in 66cl4 as compared to 67NR. Immunoblotting and ELISA showed that the micrometastatic cell line 168FARN, had the highest GREM1 protein levels. BMP4 was expressed only by the metastatic 66cl4 at protein level. Meta-analysis identified correlation between high GREM1 expression levels and poor prognosis in BC patients in KM plot and BreastMark. The paracrine crosstalk between the tumor cell lines and fibroblasts was further analyzed in vitro. Treatment of Mouse Embryonic Fibroblasts (MEFs) with condition medium (CM) from the tumor cells showed that, 67NR CM, 168FARN CM and 66cl4 CM increased SMAD 1/5/9 phosphorylation on MEFs, indicating activation of BMP4 signaling. Interestingly, the tumor cells ability to stimulate migration of fibroblasts was in line with the degree of expression of GREM1. In conclusion, this study indicates that, the metastatic cell lines in the 4T1 model have a higher propensity to recruit fibroblasts. Moreover, GREM1 expression might aid the recruitment of fibroblasts that facilitates metastasis. These findings can be further researched into to aid in improving BC therapy.

ACKNOWLEDGEMENTS

This work was carried out at the Center of Molecular Inflammation Research from August 2015 to May 2016 for the Master's degree in Molecular Medicine at the Norwegian University of Science and Technology (NTNU).

I wish to express my heartfelt gratitude to my supervisor professor Geir Bjørkøy for his immense help and suggestions in carrying out this work and giving me the opportunity to work with the group. I am also very grateful to Ulrike Neckmann and Jennifer Mildenberger for their great ideals, suggestions and help they showed towards this work. Much thanks to my colleague Camilla Wolowczyk for being there through thick and thin during our laboratory activities and with collaboration of some work during the initial stages of our thesis. My appreciation goes to all members of the autophagy and oxidative defense group who helped out in a various way especially Unni Nonstad.

My sincere thanks to my parents, Mr. Emmanuel K. Appiah and Mrs Cecilia Appiah, and my siblings Mary, Jonathan, Abigail, Gabriel, Aaron and Kofi for their untiring support, prayers and motivation which have paved the way for me to reach this height. I dedicate this work to you all. Also, my gratitude is expressed to Micheal Ohene-Nyako for his love, support, advice and encouragement given throughout my studies in NTNU. I am also grateful to all my friends and colleagues in class who encouraged me and helped in one way or the other throughout this project.

May the good Lord richly bless you all and thank you.

Christiana Opokuaah Appiah
Trondheim, June 2016

ABBREVIATIONS

°C	Degrees celcius
µl	Microliter(s)
µm	Micrometer(s)
ACTA2	Smooth muscle alpha-actin
ACTB	Beta-actin
ACTR	Activin type 2 receptors
ALK	Anaplastic lymphoma kinase
BAMBI	Bone morphogenetic protein and activin membrane-bound inhibitor
Bambi-ps1	BMP and activin membrane-bound inhibitor, pseudogene
bFGF	basic fibroblast growth factor
BC	Breast cancer
BMDC	Bone marrow-derived cells
BMP	Bone morphogenetic protein
Bmper	BMP Binding Endothelial Regulator
BMPR	Bone morphogenetic protein receptor
CAF	Cancer associated fibroblasts
CCL2	Chemokine (C-C Motif) Ligand 2
CDC42	Cell Division Cycle 42 homolog
Cer1	Cerberus 1
Chrd	Chordin
CIF	Cancer invasion front
CIM plate	Cell Invasion and Migration plate
CM	Condition medium
CO_2	Carbon dioxide
Co-Smad	Common mediator Smad
Crim1	Cysteine Rich Transmembrane BMP Regulator 1
Csf	Colony Stimulating Factor
CXCL12	C-X-C motif chemokine
CXCR4	C-X-C chemokine receptor
DCIS	Ductal carcinoma in situ
ECM	Extracellular matrix
EDTA	Ethylenediaminetetraacetic acid
Dcn	Decorin
DMEM	Dulbecco's modified eagle medium
DPBS	Dulbecco Phosphate buffered saline
DMFS	Distant Metastasis Free Survival
DTT	Dithiothreitol
ELISA	Enzyme-linked immunosorbent assay
EMT	Epithelial-mesenchymal transition
ER	Estrogen receptor
ERK	Extracellular signal–regulated kinases
Fap	Fibroblast Activation Protein
FCS	Fetal Calf Serum
Fgf	Fibroblast growth factor

Fsp1	Fibroblast-specific protein 1
Fst	Follistatin
Fstl	Follistatin-related protein 1
G1	Gap 1
GDF	Growth Differentiation Factor
Grem1	Gremlin-1
HER2	Human epidermal growth factor receptor 2
HGF	Hepatocyte growth factor
Hr(s)	Hour(s)
Igf	Insulin-like growth factor
IL-6	Interleukin 6
I-SMADs	Inhibitory SMADs
JNK	c-Jun NH_2-terminal kinases
Kcp	Kielin/chordin-like protein
kDa	KiloDalton
KM	Kaplan–Meier
LDS	Lithium Dodecyl Sulfate
Lefty1	Left-Right Determination Factor 1
Lox	Lysyl Oxidase
M	Molar
MAP3K1	Mitogen-Activated Protein Kinase 1
MAPK	Mitogen Activated Protein Kinases
MDSC	Myeloid-derived suppressor cells
MEF	Mouse Embryonic Fibroblast
mg/ml	Milligram/milliliter
Min(s)	Minute(s)
ml	Millimeter(s)
MMP	Matrix metalloproteinases
MOPS	3-(N-morpholino) propanesulfonic acid
mRNA	Messenger RNA
MTT	Methylthiazolyldiphenyl-tetrazolium bromide
NADH	Nicotinamide adenine dinucleotid
NADPH	Nicotinamide adenine dinucleotide phosphate
NF-kB	Nuclear factor-kappaB
ng/ml	Nanogram/milliliter
NG2	Neural/glial antigen 2
nm	Nanometer
NODAL	Nodal Growth Differentiation Factor
Nog	Noggin
OS	Overall Survival
Pald1	Phosphatase Domain Containing, Paladin 1
PCR	Polymerase chain reaction
PDGF	Platelet- derived growth factor
PDGFR	Platelet- derived growth factor receptor
pg/ml	Picogram/milliliter
PI3K	Phosphoinositide 3-kinase

PIC	Phosphatase inhibitors cocktail
Plau	Plasminogen activator, urokinase
PPS	Post rogression Survival
PR	Progesterone receptor
p-SMAD	Phosphorylated SMAD
PVDF	polyvinylidene fluoride
RAC	Ras-related C3 botulinum toxin substrate 1
RFS	Relapse Free Survival
Rgmb	Repulsive guidance molecule B
RhoA	Ras homolog gene family, member A
RmBMP4	Recombinant mouse BMP4
RmGREM1	Recombinant mouse Gremlin-1
Rpm	Resolutions per minutes
R-Smad	Receptor-regulated SMAD
RTCA	Real-Time Cell Analysis
SD	Standard deviation
SDF-1	Stromal cell-derived factor 1
Sec(s)	Seconds
SEM	Standard error of mean
ShcA	Src Homology 2 Domain Containing Transforming Protein
SMURF	SMAD Specific E3 Ubiquitin Protein Ligase
Sost	Sclerostin
Sostdc1	Sclerostin Domain Containing 1
Sparc	Secreted Protein, Acidic, Cysteine-Rich
TAK1	Transforming growth factor beta-activated kinase 1
TBS	Tris Buffered saline
Tbx1	T-box transcription factor
Tdgf1	Teratocarcinoma-Derived Growth Factor 1
TGF β	Transforming growth factor -β
TGFβR	Transforming growth factor –β receptor
Thy1	Thy-1 Cell Surface Antigen
Tll1	Tolloid-Like 1
TME	Tumor microenvironment
Tnc	Tenascin C
Tob1	Transducer of ERBB2, 1
TRAF6	TNF Receptor-Associated Factor 6
Tris-HCl	Tris(hydroxymethyl)aminomethane- hydrochloric acid
TSG	Twisted gastrulation
Tsku	Tsukushi Small Leucine Rich Proteoglycan Homolog
Tsp1	Thrombospondin 1
Twsg1	Twisted gastrulation BMP signaling modulator 1
V	Volt(s)
VEGF	Vascular endothelia growth factors
VEGFR2	Vascular endothelial growth factor receptor-2
Vim	Vimentin
Vwc2	Von Willebrand Factor C Domain Containing 2

Wisp1	WNT1 Inducible Signaling Pathway Protein 1

The nomenclature of proteins and genes written in this thesis followed the rules and guidelines of *International Committee on Standardized Genetic Nomenclature* for Mice and *HUGO Gene Nomenclature Committee* for humans.

1.INTRODUCTION

Worldwide, breast cancer is a major public health issue as it is the second most commonly diagnosed cancer in women with about 1.67 million new cases and the fifth cause of death from all cancer (522,000 deaths) as of 2012 (1). Breast cancer is a heterogeneous disease with regards to its responses to treatment and prognosis and biological behavior with poor early diagnosis, high incidence rates, ineffective therapeutic approaches and aggressive metastasis (2,3). Amongst these, metastasis is known to be a complicated pathological process and the single greatest cause of mortality in cancer patients (4,5). This is reflected in the five year survival rate of 24-25% among patients with metastatic breast cancer as compared to the 100% survival of patients with localized tumor (6,7). Thus, diving into the concepts of metastasis and fully understanding it is a critical step for us to tackle this major public health issue.

1.1BREAST CANCER

1.1.1 Stages of Breast Cancer

The mammary gland is a highly organized organ comprising of milk-producing glands called the lobules, the ducts that convey the milk from the lobules to the nipple and the stroma (**Figure 1.1A**). The stroma consist of the adipose tissue and connective tissue (8,9). The initiation of breast cancer begins in cells of the duct, the lobules and other tissues. Breast cancer initiation in the duct is however the most common form of breast cancer with ductal carcinoma in situ (DCIS) making up 90% of the forms of breast cancer that are not invasive (9–11). The duct is lined with both myoepithelial and luminal epithelial surrounded by basement membrane (**Figure 1.1B**) and initiation of breast cancer in the duct begins with the normal epithelial cells in the duct becoming atypical hyperplasia, a stage of the epithelial cell proliferating (10). This then evolves to In-Situ carcinoma, invasive carcinomas and then metastatic cancer (**Figure 1.1C**) (9–11).

Among the stages, metastasis is the major determinant of mortality in breast cancer patient. It involves few critical steps yet is one of the most complex pathological process that exit (4,5,12). These step includes: 1) the primary cancer first developing and/or extending blood vessels (angiogenesis) 2) detachment of the primary cancer cells 3) migration and invasion of the cells to adjacent tissues 4) penetrating the extracellular matrix (ECM) and blood vessels (intravasation) 5) penetrating out of the vessels (extravasation) and finally 6) settling and proliferating in a secondary site (13,14).

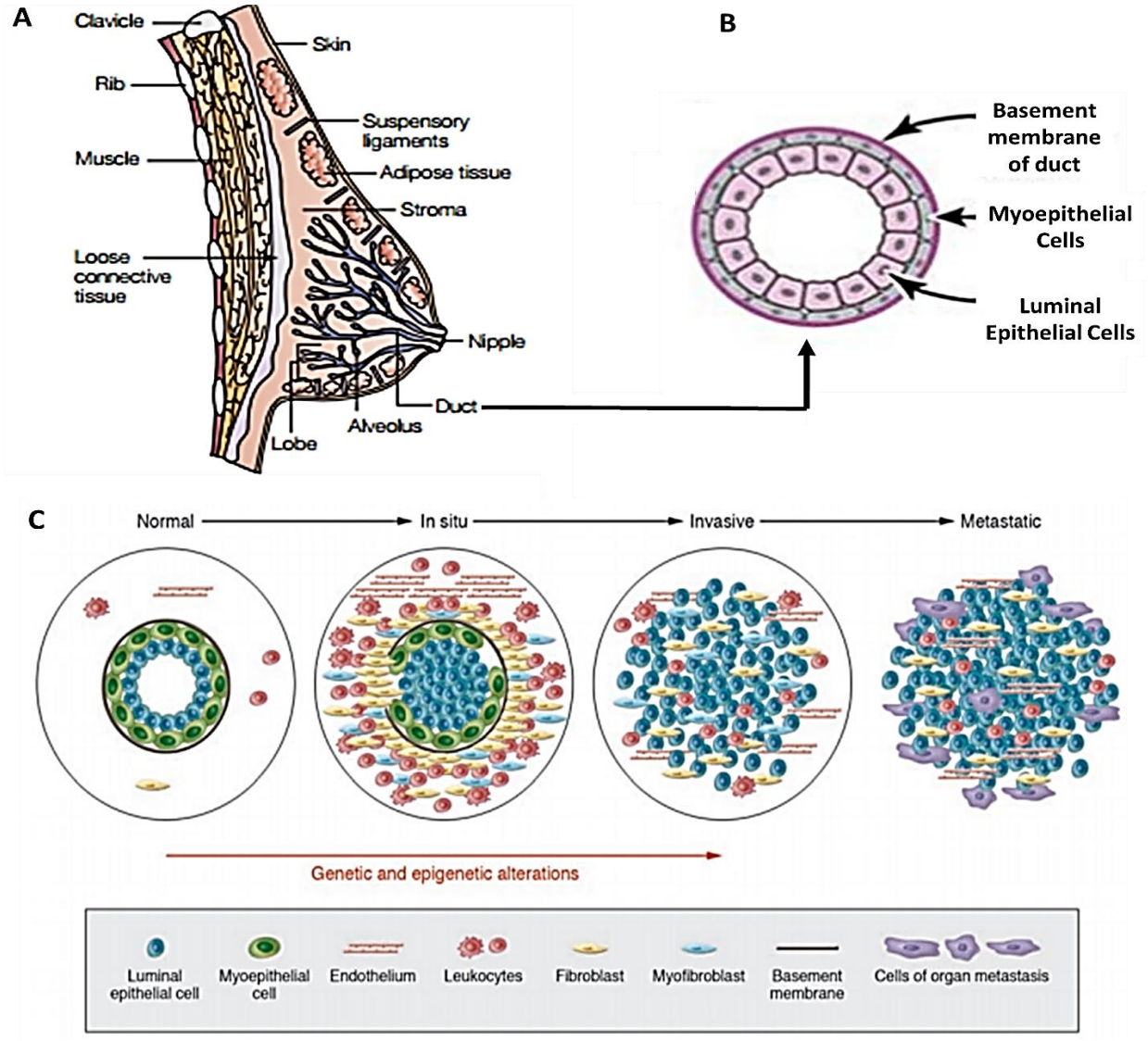

Figure1.1: The anatomy of mammary gland and breast cancer progression in the duct.
A) *The mammary gland consists of adipose tissue, muscles, alveolus and duct that are branched out from lobes. Each mammary gland contains about 15- 20 lobes.* ***B)*** *The ducts which is responsible for milk production are lined with both myoepithelial and luminal epithelial surrounded by basement membrane.* ***C)*** *The normal duct epithelial structure breaks down when cancer is initiated and this begins as ductal in-situ that is associated with proliferation luminal epithelial cells. The myoepithelial layer is degraded during invasive ductal carcinoma which is the next stage. The final stage which is the metastasis involves in the complete loss of the epithelial cells of the duct and basement membrane that leads to the invasion to other organs (9–11).*

1.1.2 Breast Cancer Histology

Breast cancer with its heterogeneous complexity has a spectrum of subtypes with distinct biological behavior and features which attribute to different forms of clinical outcomes (7,15). Initially, breast cancer was traditionally classified based on hormone receptor positive and

hormone receptor-negative types which involved expression of hormone receptors such as estrogen receptor (ER), progesterone receptor (PR) and human epidermal growth factor receptor 2 (HER2) among other factors (16,17). Development of microarray techniques such as gene expression profiling studies has however characterized further subtypes beyond the hormone receptor positive and hormone receptor-negative types (15,17–19). For instance, a study showed that luminal epithelial/estrogen receptor positive group based on distinct gene expression profile could be divided into subgroups (19). Currently, the molecular subtypes of breast cancer are luminal (luminal A and luminal B), HER2-enriched, basal-like, normal breast-like, claudin-low and molecular apocrine based on the expression of specific biomarker (**Table 1.1**) (17). The metastatic potential and aggressiveness of the breast is based on its hormone receptor status with less aggressiveness being attributed to hormone receptor positive subtypes. Basal like tumors on the other hand is usually triple negative and are highly metastatic hence are usually life threatening due to its difficulty to detect and poor prognosis (7).

Table 1.1: Molecular subtype of Breast cancer and their major biomarker expressed.
Where, ER = estrogen receptor. PR = progesterone receptor and HER2 = human epidermal growth factor receptor 2. "+" = positive. "-" = negative. Adapted and modified from (17).

Subtype	Immunohistochemistry markers		
Luminal A	ER+:91–100% Ki67:low	PR+:70–74% Basal markers: –	HER2+:8–11%
Luminal B	ER+:91–100% Ki67:high	PR+:41–53% Basal markers:-	HER2+:15–24%
Basal-like	ER+: 0–19% Ki67: high	PR+: 6–13% Basal markers: +	HER2+: 9–13%
HER2-enriched	ER+:29–59% Ki67:high	PR+:25–30% Basal markers: –/+	HER2+:66–71%
Normal breast-like	ER+:44–100% Ki67:low/intermediate	PR+:22–63% Basal markers: –/+	HER2+:0–13%
Claudin-low	ER+:12–33% Ki67:intermediate	PR+:22–23% Basal markers: +/	HER2+:6–22%
Molecular apocrine	ER– Ki67:high	PR– Basal markers: –/+	HER2+/–

1.1.3 Tumor Heterogeneity of Breast Cancer

The various histology showing heterogeneity above has been associated with diverse clinical outcomes, survival rates, responses to treatment and metastasis potential (20,21). There are two forms of the breast cancer heterogeneity that is; the intra-tumor heterogeneity and the inter-tumor

heterogeneity (**Figure 1.2 A-C**). Inter- tumor heterogeneity is when there is variation between patients with regards to morphological different, expression of subtypes, among other differences (21) (**Figure 1.2 A**). Inter- tumor heterogeneity occurrence has been linked to two proposed models The first model is the genetic model which results from tumor originating from the same cell but have different initiation events that lead to different molecular subtype (10,21).The second proposed model involves tumor originating from different cells leading to diversified molecular subtype. Combination of the two models has also been acknowledged (10,21)

Intra-tumor heterogeneity on the other hand is the variation within a tumor characterized by genetic differences observed among tumor subpopulation, as well as difference in morphology and staining behavior of the different sections of the same tumor (**Figure 1.2 B)** (21). Intra-tumor heterogeneity occurrence is importantly explained based on tumor progression. Proposed Intra-tumor heterogeneity occurrence models include clonal evolution, cancer stem cell and mutator phenotype models (**Figure 1.2 D**) (21). Clonal evolution involves tumor evolving by expansion of monoclonal or polyclonal subpopulation of tumors to form the total tumor mass. Cancer stem cell model on the other hand suggest precursor cells giving rise to different subpopulation in a tumor. The last model which is the mutator phenotype suggest evolution of tumors by gradual and random accumulation of mutation as tumor progression (21).

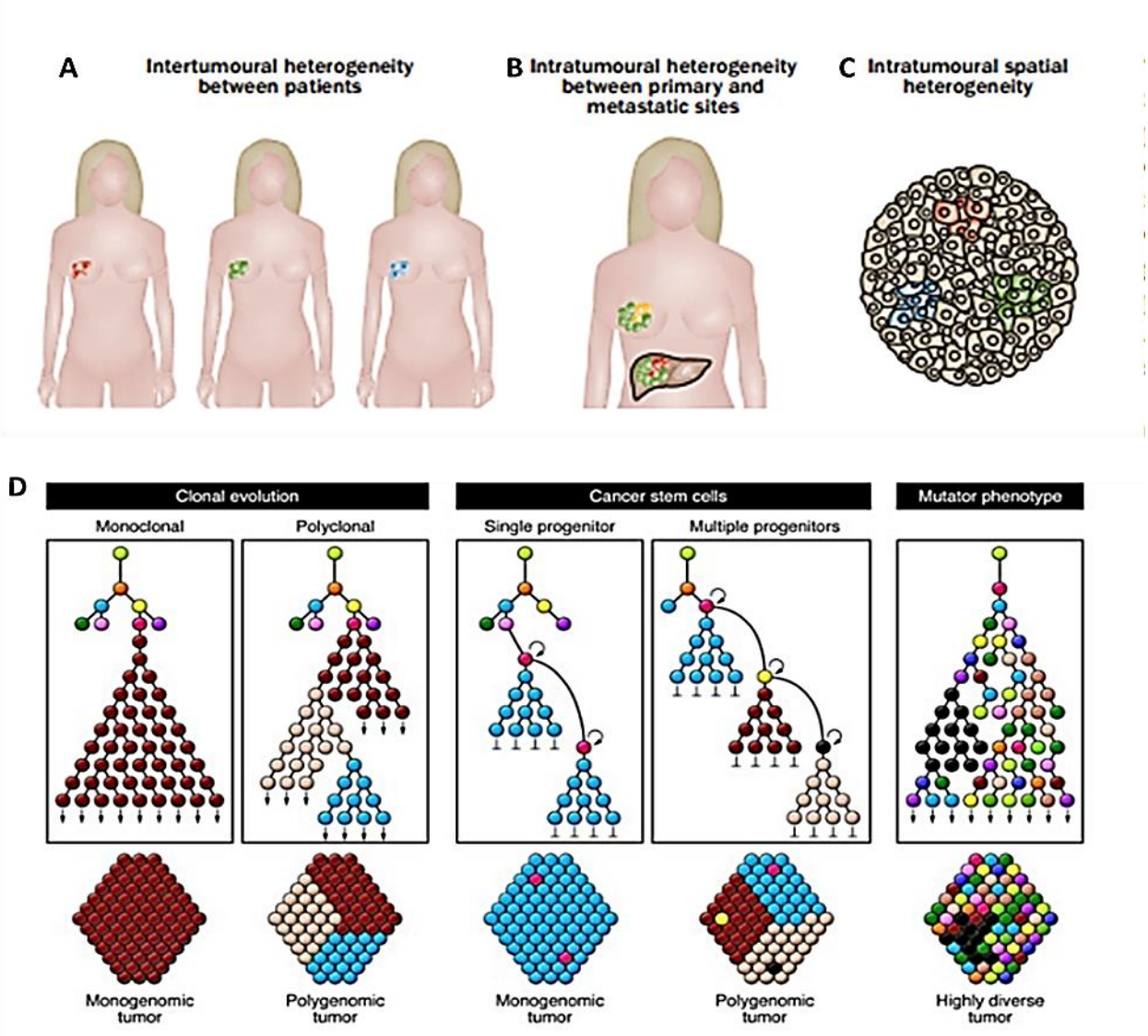

Figure 1.2: Tumor heterogeneity and proposed models explaining heterogeneity

A) *Inter-tumor heterogeneity showing patients with similar histology but differences in genetic mutation status and other molecular characteristics.* ***B)*** *Intra-tumor heterogeneity exhibiting variation within primary tumors occurring as a result of genetic difference (red clone – genomic alteration) and/or lose of alteration (yellow clone) occurring in metastatic tumor site.* ***C)****Intra-tumor spatial heterogeneity have common initiation genomic events in all the tumor cells but have spatially heterogeneity due to copy number changes or somatic mutation (green, red and blue clones).* ***D)****Proposed models explaining intra-tumor heterogeneity – clonal evolution, cancer stem cell and mutator phenotype models results in spatial distributions of subpopulations. Adapted and modified from* (21,22).

These heterogeneity mention above has posed many challenges with regards to diagnosis and treatment which lead to the concepts of personalized cancer therapy. Personalized cancer therapy takes the persons cellular and metabolic products as well as the molecular characteristics of the tumor into paly during the diagnostic phase (22,23). This is because it is believed that people

respond differently to a particular medicine as a result of their genetic makeup and their metabolism ability. Due to this, making medicine or structuring therapies for the general population will result in different outcomes (**Figure 1.3**). Breast cancer is one of the few cancers in which the molecular classification of the tumor has been used to designed personalized therapy that lead to improved effects (24) . It is therefore important to understand the role of heterogeneity in treatment response, tumor evolution and the microenvironment surrounding the tumor as it is critical for the survival of each cancer patient.

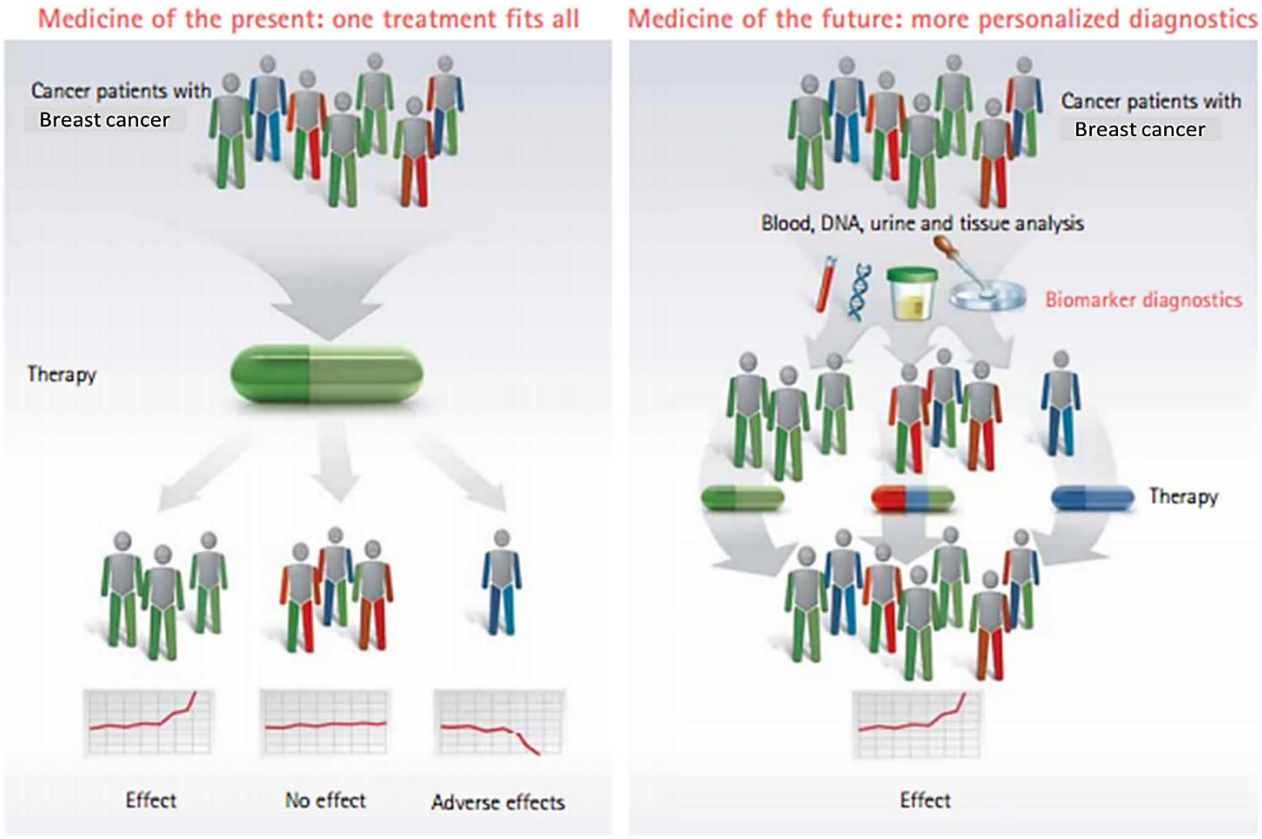

Figure 1.3: Tailored treatment – Personalized medicine
Individuals respond differently to the same therapy: whiles it might yield the desired result for one individual, it can lead to adverse effects in another individual or no effects at all (left). The differences in effect is because of the tumor heterogeneity and also the differences in the genetic makeup and metabolic profile of patient. Personalized medicine (right) takes into account all this different factors to establish therapy that will give the best effect in the individual being treated. Adapted and modified from (23).

1.1.4 Tumor Microenvironment of Breast Cancer

Tumor microenvironment (TME) includes the non- cancerous cells present in the tumor and it's an attributing factor for increase in heterogeneity in tumor cells (25). The TME which consists of cancer associated fibroblasts (CAFs), extracellular matrix , inflammatory cells, blood vessel cells

and immune cells has been associated with initiation, progression and metastasis of cancer (26–28). In breast, the normal mammary duct environment (**Figure 1.4**) is composed of the luminal epithelial cells (inner layer), myoepithelial cells (outer layers) and normal fibroblast that is enclosed by a continuous basement membrane/ECM (10,29). In comparison with the tumor mammary duct microenvironment, one can find in addition to the composition stated for the normal mammary, the tumor itself, lymphocyte/white blood cells, CAFs as well as bone marrow-derived cells (BMDC) such as macrophages (**Figure 1.4**) (29). However, the integrity of the normal organized structure cannot be seen in the tumor mammary microenvironment as it is distorted when tumorigenesis leading to invasion occurs in the mammary. This is as a result of transformation of cells due to genetic/epigenetic changes the leads to the loss of epithelial polarity, reduction in the myoepithelial cells as well as the degradation of the basal membrane /ECM (29). Thus, the interaction between the tumor cells and stroma cells creates a crosstalk that results in the production of cytokines and growth factors that modifies ECM and other factors secretion that support survival, proliferation and invasion of tumor cells (5).

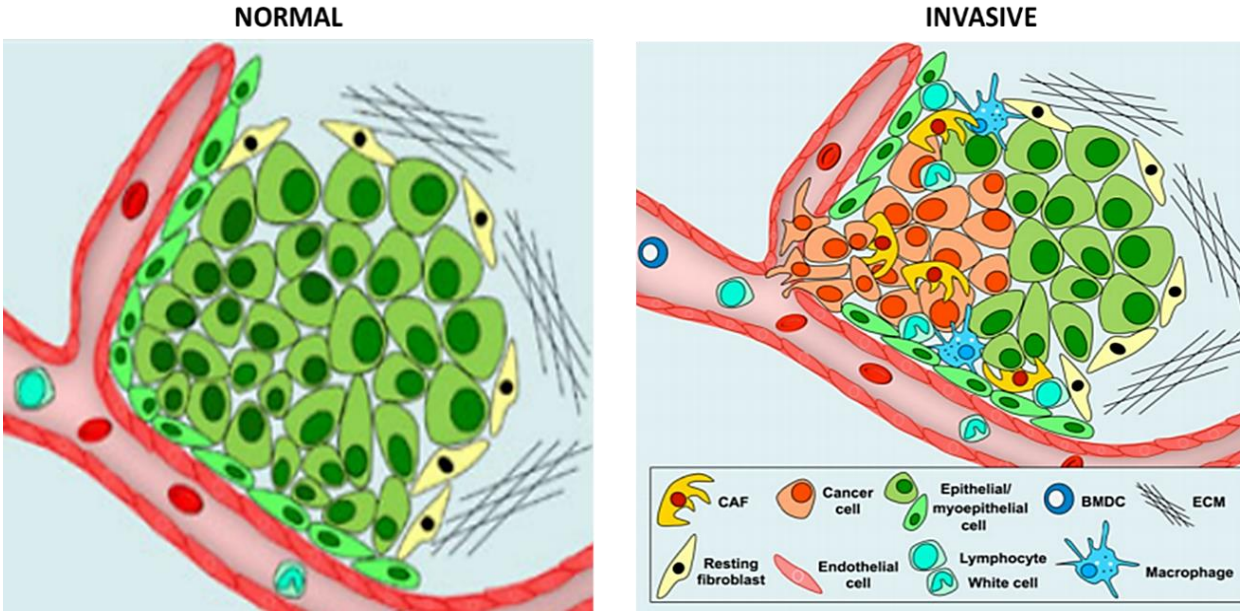

Figure 1.4: Normal environment of breast versus tumor microenvironment of breast cancer.
Normal mammary duct of the breast is made of luminal epithelial cells (inner layer) and myoepithelial cells (outer later) that is surrounded by a basement membrane. In a tumor related mammary duct, there exist both the tumor and the stroma cells which includes fibroblast, pericytes and immune cells. They also consist of non-cellular components such as the extracellular matrix and growth factors. \ When the mammary duct becomes over burden after tumorigenesis, the myoepithelial becomes alters and distorts the normal frame organization of the duct leading to tumor cells escaping and invading other sites other than their primary site. Adapted and modified from (29).

1.1.5 Tumor –Stroma Interaction in Breast Cancer

Tumor cells and its microenvironment exist in an interrelation network that aid in the various stages of cancer (30). Tumor cells are known to produce stroma - modulating growth factors and proteases that disrupt normal tissue homeostasis in an attempt to generate a conduction microenvironment. This growth factors includes transforming growth factor -β (TGF β), vascular endothelia growth factors (VEGF), platelet- derived growth factors (PDGF), basic fibroblast growth factor (bFGF) among other (31,32). These factors allow the microenvironment surrounding the tumor to co-evolve into activated state via continuous autocrine and paracrine communication that forms a complex signaling network as cancer progresses (**Figure 1.5**) (33–35).

The activated microenvironment made up of the stroma cells causes the cells to further produce additional growth factors and protease. For instance, stroma cells such as the CAF are activated to secret proteolytic enzymes such as MMP that initiates the degradation of extracellular matrixes leading to tumor invasion (**Figure 1.5**). The growth factors produced also leads to the proliferation of the tumor cells and eventually the induction of angiogenesis factor (29,31). Thus, the hallmark of cancer such as inducing angiogenesis and activation of invasion and metastasis as stated by Hanahan and Weinberg (36) are attributed to various stromal components including extracellular matrix, endothelial cells , pericytes, various leukocytes, macrophages and fibroblast (33). The various stroma cells has individual function they perform and it's been shown that during tumor progression the number of cancer associated fibroblast (CAF) is increased (29).

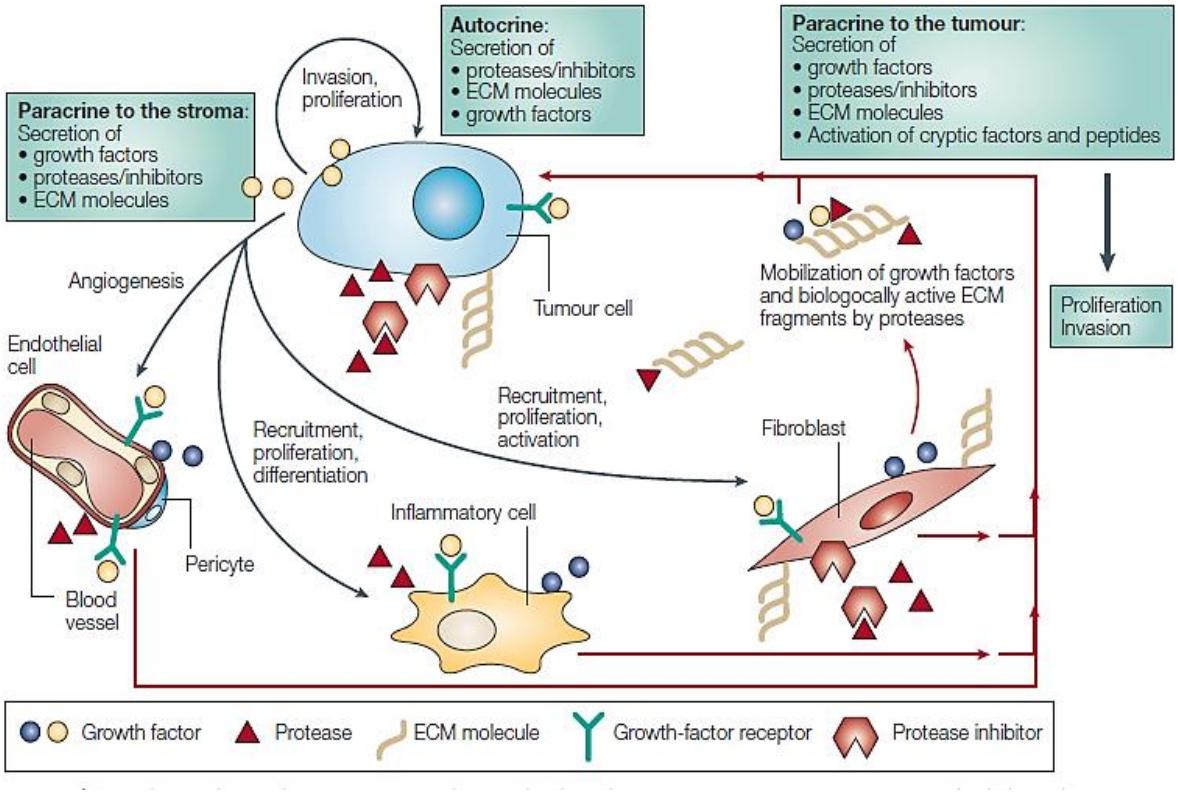

Figure 1.5 Tumor-stromal crosstalk in Breast cancer.
Tumor-stromal crosstalk is initiated when tumor cells produce growth factors and proteases that activate the stroma cells in an autocrine and paracrine fashion. Concurrently, they produce specific pro-migratory ad invasive extracellular- matrix components together with their receptors whiles suppressing the protease inhibitor expression. This leads to the stroma cells such as the CAF secreting proteolytic enzymes such as MMP that initiates the degradation of extracellular matrixes leading to tumor invasion. The degradation of the ECM leads to the release of matrix- bound growth factor. The total growth factors produced leads to the proliferation of the tumor cell, recruitments of inflammatory cells and eventually the induction of angiogenesis factors. All these factors facilitate tumor cell invasion and metastasis. Adapted and modified from (29,31)

1.2 CANCER ASSOCIATED FIBROBLAST (CAF)

Fibroblast is the most prominent cells in the stroma and is usually in a normal inactive quiescent state until activated by activities that require tissue remodeling such as wound healing (35,37,38). Fibroblast are usually elongated cells with a spindle-like shape morphology but have heterogeneous morphology with different forms of appearance based on their location and activity(39). Studies have showed that human fibroblast cultures isolated from different sites exhibit gene expression patterns distinct from the different anatomical sited it was isolated form. The differences are evident in the different growth factors, differentiation factors and different extracellular matrix constituent they secrete (39,40) .

Normal fibroblast are associated with maintaining the structural integrity of extracellular matrix through secreting precursors of the extracellular matrix which includes collagen, vimentin, proteoglycan, glycoproteins and actin (38,41). Normal fibroblasts also play a role in wound healing process by recruiting endothelia precursors cells and aiding in angiogenesis healing (42). In the tumor stroma environment, fibroblast is activated by tumor cells into CAF. CAF is a subpopulation of fibroblast that is of most interest to researchers because CAF in comparison to normal stromal fibroblast are more effective in promoting cell survival, growth and progression of tumor cells (37,42). However, due to CAFs poor lack of specific markers and their high heterogeneity, they remain poorly defined by researchers (42). The activation of normal fibroblast into CAF is as a result of tumor cells interacting with its microenvironment thereby creating a conductive environment to serve their benefits by activation of various signals (33).

1.2.1 Signaling Pathway Associated with CAF Activation in Tumor Environment

The microenvironment surrounding the tumor co-evolves into activated state through continuous autocrine and paracrine communication that forms a complex signaling network as cancer progresses (33–35). CAF is not an exception as it is activated in the presence of breast cancer cells in order to be able to affect or interact with breast cancer cells through various molecular signaling pathways.

CAFs are activated by tumor cell-derived factors such as transforming growth factor beta (TGF-β) and stromal cell-derived factor 1 (SDF-1) also known as C-X-C motif chemokine 12 (CXCL12) in an autocrine signaling loop as demonstrated by Kojima and colleagues (37,41,43). TGF-β is however the major mediator of activation of CAF. TGF-β is a pleotropic cytokine stored as a reservoir in ECM which is usually secreted by various cells types including fibroblast (44). The TGF- β family is a broad family and per sequence similarities they are divided into two ligand subfamilies: the BMP family and the TGFβ–Activin–Nodal subfamily. Their receptors are transmembrane receptors in all cell types with for example TGF-β1 binding to its receptor TGFβRII on fibroblast membrane. Upon binding, they form heterodimeric activated receptor complex with a second receptor a factor important for their activation since these ligands are disulphide-linked dimers (45). This complex leads to SMAD dependent and independent signal activation which ends up in the transcription of factors of genes in the nucleus that encode factors such as PDGF, VEGF, MMPs and other factors involved in CAF activation (42,44). Also, TGF-β triggers the activation of SMAD independent signaling cascades including TRAF6, TAK1, PI3K,

MAP3K1, ShcA, RAC/CDC42, RAS, and RhoA pathways (42,44). These signals interplay with CAFs are attributing factors leading to CAFs association to tumorigenesis and tumor progression (30). Thus, CAF are involved from initiation through progression to metastasis as a result of direct or indirect association with activities such as angiogenesis, enhancing epithelial cell growth, epithelial to mesenchymal transaction and suppression of antitumor immune responses (4,30).

1.2.2 Role of CAF in Breast cancer tumorigenesis and progression of breast cancer

CAF involvement in the initiation of cancer involving resident fibroblast has been seen in studies where CAF co-injected with tumor cells in mouse models has led to more efficient tumor formation (39). To compliment this, prostatic epithelial cells grown with CAF lead to growth stimulation as compared to the prostatic epithelia cells grown on its own or together with normal human fibroblast (46). The sensitivity of Human mammary epithelial adenocarcinoma cells MCF7 to tumor stroma derived factors was observed when the tumorigenicity of MCF7 was improved when cultured with fibroblast than it standing alone (47). These influences of fibroblast in tumorigenesis was proven when numerous protein extracted from normal fibroblast was seen to be involved with breast tumorigenesis (48). An example was also seen with CAF association with breast cancer cells stimulating the production of Hepatocyte growth factor (HGF) known to be associated to tumorigenesis (49). These indicate that fibroblast supports the initial phase of tumor development through by their production of various cytokines and proteins to support processes such as angiogenesis and immune suppression (**Figure 1.6**) (48).

CAF is involve in creating the niche for cancer cells where they proliferate and sustain their dissemination. Cancer metastasis invovling multistep is said to be regulated intrinsically by tumor cells and extrinsically by stromal cells surrounding it (42). It has been demonstrated that CAF association with metastasis is based both on their release of soluble factors and physical attributes (42,50). An example was seen when myofibroblast was observed to create tunnels in extracellular matrix to pave way for cancer cells to follow suite (51). CAF manage to pave the way by the release of extracellular proteases such as matrix metalloprotineases (MMP) that remodels the ECM (42,52). Matrix metalloprotineases production by CAF includes MMP1, MMP3 and plasmongen acitvator (PLAU) which converts plasminogen to plasmin, a ECM degrader. Cancer incidence increment with age might be attributed to the fact that senescence fibroblast is associated with upregulation of MMPs among other factors(31).

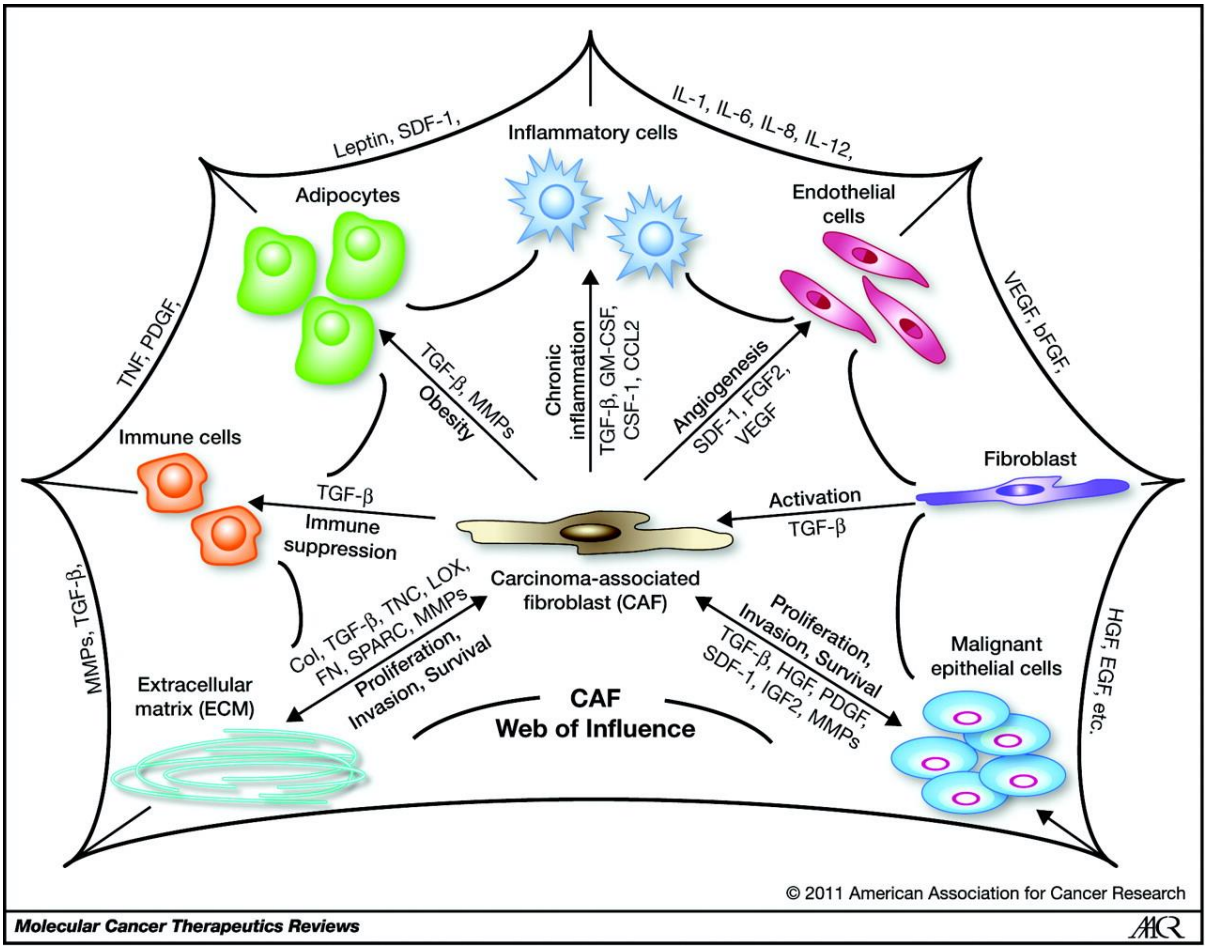

Figure 1.6: Overview of CAF involvement in tumorigenesis and tumor progression through multiple mechanisms.
Normal fibroblast in the tumor environment become stimulated into CAFs through an autocrine/paracrine means by TGF-β and CXCL12. Upon activation, CAF mediate direct and indirect tumorigenesis and tumor progression effects through secretion and expression of several growth factors (e.g.IGF-2, HGF, FGF-2, PDGF), proteases (e.g. MMPs), extracellular matrix proteins (e.g. COL), cytokines (eg.IL-6, IL-4) and other mediators (e.g. CCL-2, IL-4, CXCL9, CXCL10, CXCL12) that cause the recruitment and influence on other cells such as immune and inflammatory cells. Paracrine signals derived from these cells recruited cells (examples listed around the perimeter of the web) promote in a feedback loop. Adapted from (30)

CAF in comparison to normal stromal fibroblast is more efficient in promoting tumor progression by secretion of growth factors which is known to regulate EMT in cancer cells (37). A study showed that CAF generated from invasive human mammary carcinomas secreted eminent levels of proangiongenic chemokine SDF-1/CXCL12 (53). SDF-1/CXCL12 is known to aid in the proliferartion, invasion and survival of malignant epithelial cells and also promote angiogenisis by signalling through its associated receptor CXCR4 which are normally expressed on tumor cells (53,54). SDF-1/CXCL12 contribute to cancer progression by up-regulation of protease such as MMPs being modulated by CXCL12 – CXCR4 interaction (27). CAF also promote progression

of tumor by secreting pro- migratory ECM elements such as tenascin(31).With regards to tumor invasion, CAF aid in the production of Vascular endothelial growth factor which is a precursor for angiogenesis and invasion (30). Furthermore, it has been shown that CAF is involve in metastasis by a study that reported the presence of CAF of brain metastasis from primary tumors of breast and lung (55).

1.4 TRANSFORMING GROWTH FACTOR β (TGF- β) SUPERFAMILY

The transforming growth factor-β (TGF-β) superfamily includes about 33 cytokines that are structurally related. The major members of the family are the TGF-β, activins (Acts)/inhibins (Inhs), Nodal proteins (Noldals), bone morphogenic protein (BMP), Müllerian inhibiting substance (MIS), and the growth differentiation factors (GDFs) (56,57) These family is present in both vertebrate and invertebrate and regulate a large number of biological functions such as inflammation, tissue repair, proliferation, apoptosis, cell differentiation as well as organism development.. Their dysregulation leads to several pathological outcomes including cancer(56,57).

1.4.1. Bone Morphogenic Protein (BMP) family

BMP which belongs to the TGF-β superfamily are cytokine that plays a role in bone and cartilage formation and morphogenetic activity hence its name origin (58–61). BMP has however been associated with diverse body morphogenesis function and it is the largest subfamily of the TGF-βs superfamily (60,62). Cancer has also been associated with impairment and/or abnormalities of BMP signaling pathways (58) with BMP playing a dual role by activation and suppression of cell proliferation associated with tumor (59). BMPs has also been established as an exogenous stimuli that control EMT of tumor cells which is a determinant in tumor invasion and progression (39). Among the member of BMP family, BMP4 has been well studied.

1.4.2 Bone Morphogenic Protein 4 (BMP4) and its Signaling

BMP4 at the protein level can be seen in two forms: the inactive form that has a molecular weight of 50-kDa which is found within the cells and the active carboxyl-terminal mature BMP4 protein dimer with 25kDa for each monomer which is secreted as the growth factor and found outside the cells (63). BMP4 plays several roles in adult tissue such as embryogenesis, hematopoiesis , skeletal formation, neurogenesis as well as controlling cellular behaviors that includes apoptosis, differentiation, proliferation and motility(64). BMP4 is also involved in developmental processes which is dependent on the concentration of the active form secreted. Thus, it can be said that the

regulation of the activation and how much matured BMP4 is secreted determines the cell fate decision that are mediated by BMP4 (63). The developmental role in relation to cell fate decision was for instant seen when a study showed that $Bmp4^{tm1}$ homozygous null mutant mouse embryos lacked lens formation in the eye an indication that BMP4 together with other factors play a significant role in eye lens formation (65).

Like most BMPs, BMP4 also play a dual role of suppression and proliferation of tumor cells as it has been associated with reduction of prostate and breast cancer cells as well as increase in migration and invasion of ovarian, melanoma, pancreatic and breast cancer (66). The importance of BMP4 in breast cancer was captured when a survey of seven BMPs showed it as one of the ligands with the highest expression among 39 primary tumor samples and 22 cell lines (62). A similar outcome was seen in another study that had 66% of breast cancer tissue from 486 patient expressing BMP4 expression (66).

The BMP4 signaling pathway (**Figure 1.7**) is activated when extracellular BMP4 ligand is cleaved and processed by proprotein peptidases to form its active dimers that binds two copies of the type I and type II BMP receptors (67,68). The type 1 receptors for bmp4 includes ALK3 (BMPR1A) and ALK6 (BMPR1B) whiles that of type II receptors includes ACTRII, ACTRIIB and BMPR2. (69,70).This forms a hexameric receptor–agonist complex leading to the type1 receptor phosphorylation initiated by type II receptor on the GS domain. The type 1 receptor which is now activated phosphorylates cytoplasmic signal transduction proteins such as R-SMAD, which dimerize with Co-SMAD 4 and then translocated to the nucleus where they promote transcription of BMP target genes (61,67,71,72). It is important to note that BMP4 can have a downstream signaling that is SMAD independent which includes NF-kB, ERK, JNK and Mitogen Activated Protein Kinases (MAPK) (72,73) .

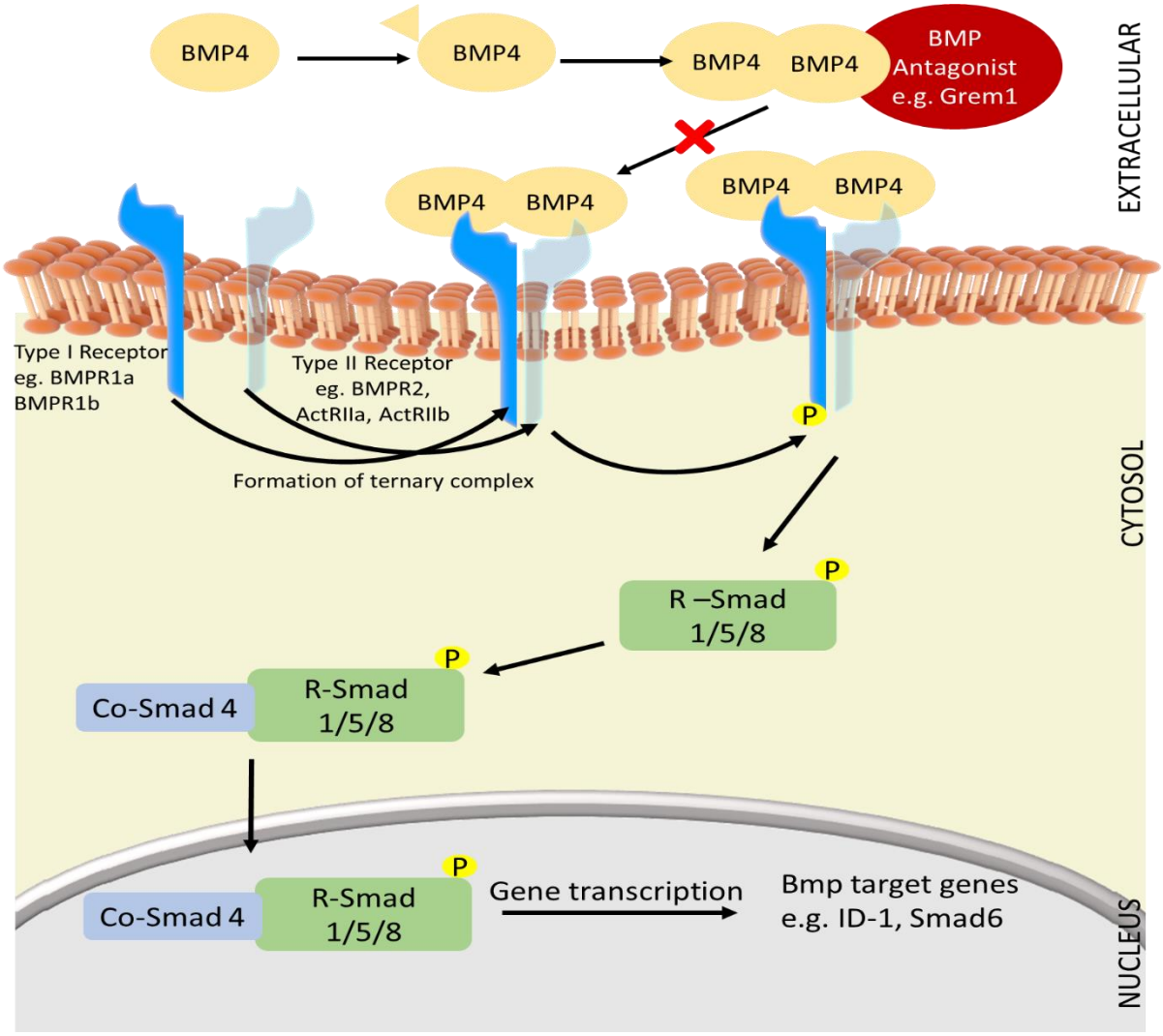

Figure 1.7 BMP4 Signal Transduction.

The BMP4 signaling pathway is activated when extracellular BMP4 ligand is cleaved and processed by proprotein peptidases to form its active dimers that binds two copies of the type I and type II BMP receptors. This forms a hexameric receptor–agonist complex leading to the type1 receptor phosphorylation initiated by type II receptor on the GS domain. The type 1 receptor which is now activated phosphorylates cytoplasmic signal transduction proteins such as R-SMAD, which dimerize with Co-SMAD 4 and then translocated to the nucleus where they promote transcription of BMP target genes. The pathway can be regulated both intracellular and extracellularly. An example of an extracellular regulation is the binding of extracellular antagonist such as Grem1. Abbreviations: BMP, bone morphogenetic protein; BMPR, bone morphogenetic protein receptor; Co-SMAD, common-mediator SMAD; GS domain, glycine–serine domain; R-SMAD, receptor-regulated SMAD. Grem1, Gremlin. Adapted and modified from (67,68)

1.4.3 BMP4 Signaling Regulation

The BMP4 signaling can be regulated at various stages in their pathway. They can be extracellularly regulated by the BMP4 ligand being inhibited by a number of BMP antagonist such as the Noggin, DAN family members, the chordin family members, Twisted gastrulation (TSG)

and Follistatin (69,74,75). These extracellular BMP antagonists such as Gremlin-1(GREM1) function by preventing ligand-receptor interaction by binding to the BMP receptor or to the BMP ligand itself. Another stage by which regulation can occur is via the distortion of BMP4 signaling by plasma membrane bind proteins such as the pseudo-receptors known as BMP and Activin Membrane Bound Inhibitor (BAMBI) (67,74). In addition, Cysteine Rich Transmembrane BMP Regulator 1 (CRIM 1) affects the actions of BMP4 signaling by affecting the ligand processing of the BMP4 in the Golgi compartment (74).

Intracellularly, BMP4 signaling can be regulated by inhibitory SMADs (I-SMADs) which includes SMAD6 and SMAD7. SMAD 6 and SMAD7 is known to have similar structure with R-SMADs and SMAD4. SMAD6 is known to compete with SMAD4 hence preventing the active complex formation of SMAD4 with receptor-activated SMAD1 whiles SMAD7 competes with R-SMAD (76). R-SMAD degraded by proteasome mechanism by SMURF1 and SMURF2 also inhibits BMP signaling (76,77).

1.5. GREMLIN – BIOLOGICAL FUNCTIONS OF A BMP ANTAGONIST

Gremlin-1 (GREM1) also known as downregulation by mos (Drm) is a 20.7 kDa protein with 184 amino acid that has been mapped to the human chromosome 15q13-q15(78)t (78,79). Identification of GREM1 was first observed when it was isolated from a v-mos- transformed rat fibroblast cell line which was only present in the normal fibroblast but not the oncogenic fibroblast (80). GREM1 exists as a cell – associated (on external cell surface) and secreted form (within endoplasmic reticulum - Golgi compartments) and with regards to protein analysis they are present in glycosylated and non-glycosylated form. The glycosylated form is usually slow in migration as compared to the non- glycosylated form (81,82). Despite its molecular weight of 20.7kDa, GREM1 has a molecular weight between 20-30 kDa during protein analysis such as immunoblotting as a result of its post translational modification such as phosphorylation and glycosylation (79–81) .

GREM1 belongs to BMP antagonist family known as the DAN family which have eight member ring with regards to the size of cysteine-knot (60,78,79). It performs its BMP antagonistic activities by binding to BMP2, BMP4 and BMP7 preventing ligand – receptor interaction to activate their signaling via SMAD (79,83). Aside its BMP antagonism activity, GREM1 also have other signaling capabilities independent of the BMP antagonism (**Figure 1.8**)(67). GREM1 also plays a

critical role in early development with regards to embryo patterning and limb development and tissue – specific differentiation (81). Due to its significant role in development, Mice that have GREM1 knockout (GREM1-/-) have been associated with deficiency in growth, skeletal phenotype and in some cases failure to complete development of kidney and lung septation with its associated outcomes (84,85).

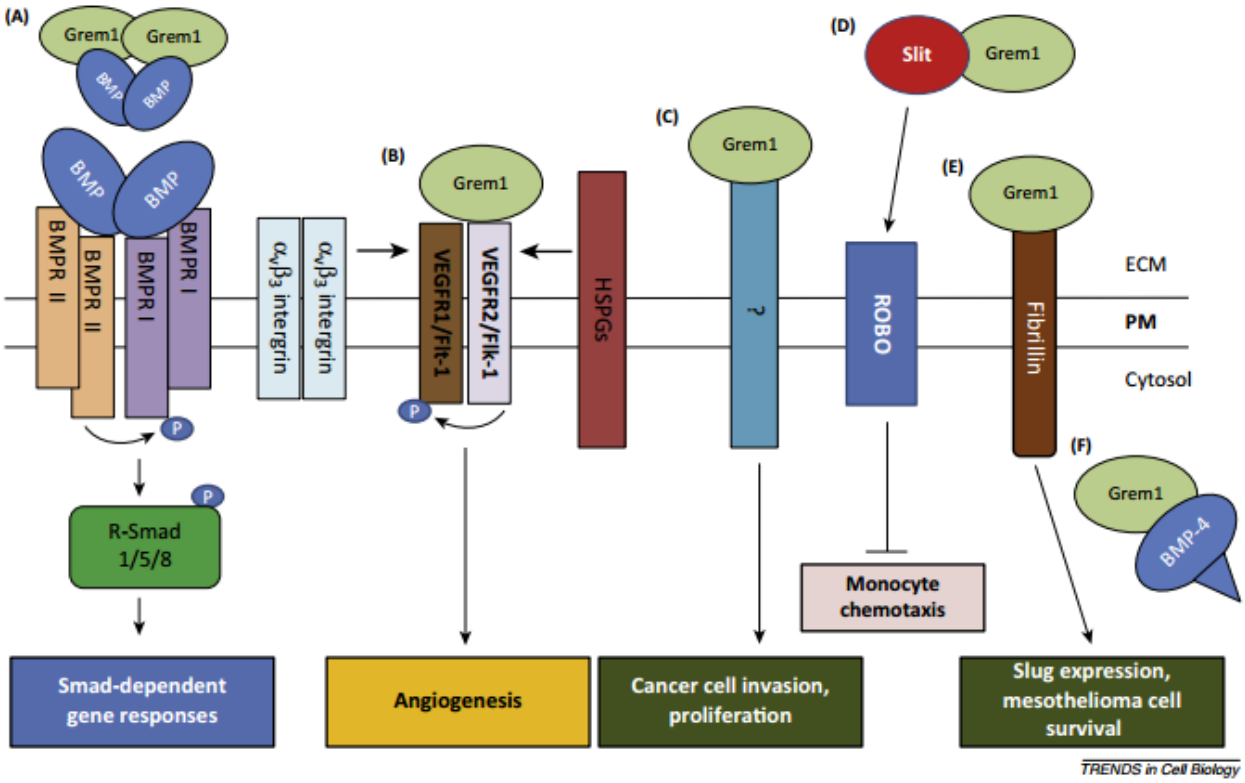

Figure 1.8: Mechanisms of Grem1 signaling in cells
A) *Prevention of BMP signaling and gene expression by Grem1 dimers binding to BMP dimers and prevents the BMP ligand from binding its receptor.* ***B)*** *Grem1 promotes angiogenesis in endothelial cells by binding to Vascular Endothelial Growth Factor Receptor 2 (VEGF2). This response requires both* $\alpha_v\beta_3$ *integrin and Heparin sulphate proteoglycan.* ***C)*** *Grem1 using an unidentified mechanism activates cancer cell invasion and proliferation.* ***D)****Grem1 inhibits monocyte chemotaxis by binding to slit1/2 to facilitate their binding to Robo receptor.* ***E)*** *Grem1 associates with fibrillin microfibrils leading to slug expression that triggers epithelial mesenchymal transition and mesothelioma cell survival.* ***F)*** *Grem1 prevents secretion of matured BMP4 by binding to BMP4 precursor proteins. Adapted from*(67).

GREM1 has been associated with many activities that are detrimental to human health such as fibrotic disease which includes Diabetes nephropathy, immune glomerulonephritis, chronic allograft nephropathy, human idiopathic pulmonary fibrosis among others (83). For instance, GREM1 gene is upregulated in response to TGF- β in renal dysfunction and human chronic kidney disease (82). A study on GREM1 association with Epithelial Mesenchymal Transition found out

that GREM1 activates SMAD 2/3 signaling pathway similar to TGF- β since both belong to the cysteine knot superfamily and this induced EMT in tubular epithelial cells which could be linked to renal fibrosis (82).

Oncogenic roles has been linked also with GREM1 as it has been shown to be overexpress in several human tumor such as cervix, ovary, lung, kidney , colon , pancreases and breast (86,87). An attribute of the oncogenic role was shown by increment in cell proliferation of normal lung fibroblast and epithelial cell lines after they have been transfected with GREM1 (88). In addition to its cell proliferation capabilities, GREM1 transfected into a human lung adenocarcinoma epithelial cell line (A549 cells) increased their migration and invasion (87). Angiogenesis, a hallmark of cancer has also been found to be initiated by GREM1 in a BMP independent manner (89,90). Vascular endothelia growth factor, a proangiogenic factor known to modulate angiogenesis belongs to the same cysteine knot family that Grem1 belong to. As a result of this, VEGF and GREM1 may have similarities in their structures and/or function. This similarities was proven when a study reported GREM1's ability to function as an agonist and bind to vascular endothelial growth factor receptor-2 (VEGFR2) to activate the VEGF-mediated angiogenic signaling pathway (90).

1.6 BREAST CANCER MOUSE MODEL - BALB/CFC3H

In order to understand mechanisms such as signaling pathways leading to breast cancer and its fetal metastasis, many forms of mouse model systems has been established to aid in research in respect to that (91,92). Mouse model studies has given us better insights into molecular pathways that leads to tumorigenesis and metastasis. Mouse models thus can be said to be more efficient in comparison to tissue and cell cultures studies which gives operative with single cells as it incorporates the complexity of the various organ and cells and other physiological status that can be related more in humans system (93). The mouse model also enables the study of cells in vivo in mice with a functional immune system as there is evident of role of the immune systems in the initial stages of breast cancer and metastasis (94).

One of such model to be currently use in this study that plays a fundamental clinically role in examining breast cancer metastatic progression is the 4T1 breast cancer mouse model. It consists of several isogenic tumor lines which has different propensity of metastatic phenotype generated from a spontaneous mammary primary tumor in a BALB/cfC3H mouse after injection into the

mammary gland of the mice (**Figure 1.8**) (95,96).

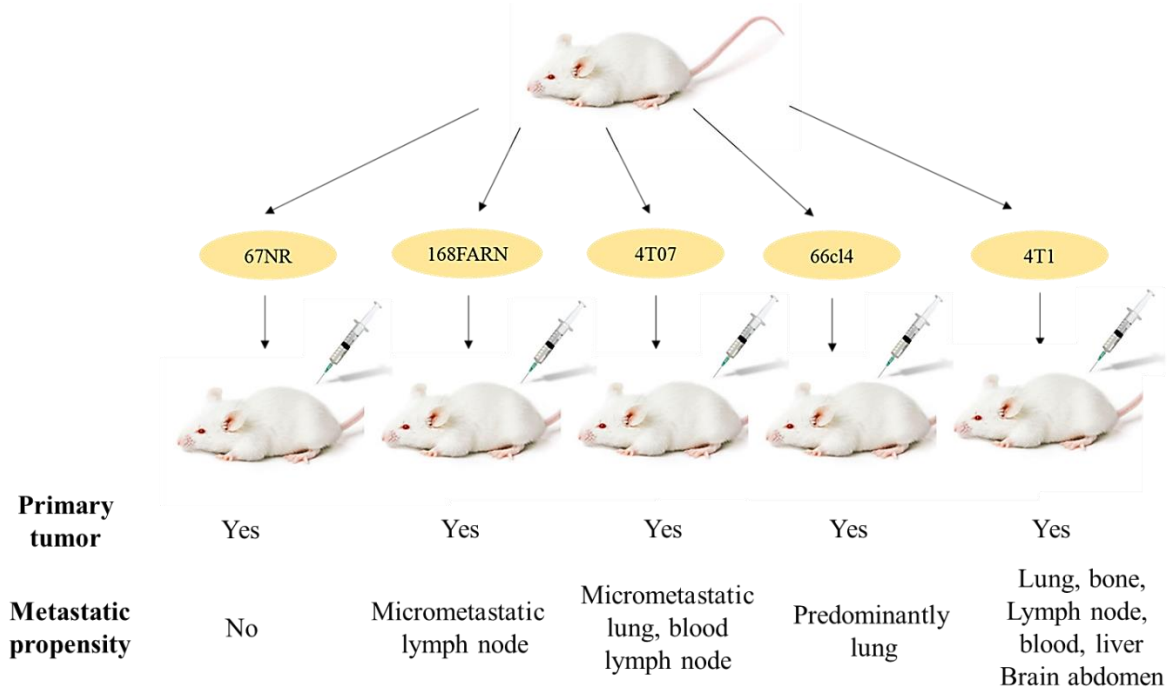

Figure 1.9: BALB/cfC3H breast cancer mouse model.

All the five cell lines form primary tumors when implanted back into a BALB/c mouse, but they have different metastatic propensity (95,96).

Some mouse model studies including the 4T1 model with regards to metastasis have their shortfalls as they cannot be used for complete metastasis studies (97). This is as a result of it not covering all the requirement step in establishing metastasis as mostly the invasion and intravasation steps are omitted by tumor cell injection directly into circulation through the tail vein as seen in this present 4T1 mouse model (97)

2.AIM

Previous studies have shown that tumor cells exist in an interrelation network with stroma cells, including fibroblasts. The interrelation between the tumor and stromal cells are the key players which allows the microenvironment surrounding the tumor to co-evolve into activated state through continuous autocrine and paracrine communication. The communication forms a complex signaling network leading to tumor progression and metastasis (31,33–35,39). The tumor ability to communicate and reprogram stroma cells in their favor likely varies from tumor cell to tumor cell. Some tumor cells have higher propensity in attracting and polarizing stroma cells than other and the concept behind that is not completely understood.

To understand this process, the 4T1 mouse mammary tumor model was chosen, which consists of five cell lines isolated from the same primary tumor. All five cell lines form primary tumors when injected into BALB/c mice, but have different metastatic ability. It was therefore aimed to get a better understanding of interplays between the 4T1 mouse mammary tumor model and stroma cells that attributes to their different metastatic potential. The main hypothesis is that the breast cancer cell lines which can leave the primary tumor (168FARN, 4T07, 66cl4 and 4T1) are better equipped to attract and/or polarize and communicate with stroma cells than the non- metastasizing 67NR cell line.

The overall hypothesis was divided it into several working hypotheses. Firstly, if the main hypothesis is valid, it would be expected that tumors of the metastasizing 66cl4 cell line contains more fibroblasts than primary tumors formed by the non-metastasizing 67NR cell line. The hypothesis was tested by analysis of fibroblasts markers in the RNA-sequencing data of 66cl4 and 67NR primary tumors.

Secondly, if the metastatic cell line 66cl4 differ from the non-metastatic cell line 67NR in their ability to recruit and/or polarize fibroblasts, this may be due to differences in secreted chemokines and cytokines. Tumor associated fibroblasts can be regulated by a multitude of different signaling compounds, including members of the TGF-β super family. Many of these signaling molecules are tightly regulated to maintain cellular homeostasis. Thus, the RNA-sequencing data of 66cl4 and 67NR was analyzed for differences in the expression levels of selected chemokines and cytokines; in particular members of the TGF-β super family and selected antagonists. If expression

of some of these chemokines/cytokines is important for recruitment and/or polarization of fibroblasts one could expect a direct correlation between high expression levels of these chemokines/cytokines and poor prognosis in breast cancer patients. To test this hypothesis, two online databases (BreastMark and Kaplan-Meier plotter) were used to analysis such a possible correlation.

Finally, based on the findings of the RNA-sequencing data and database analysis, two cytokines were selected. The effect of the cytokines on the tumor cell lines and different types of fibroblasts was tested in vitro. The interaction of tumor cells and fibroblasts was also studied in vitro by the help of transwell cell culture inserts and conditioned medium. These methods were used to mimic some aspects of the interaction between tumor cells and fibroblasts in a primary tumor.

3. METHODOLOGY

All methods used in this study were standardized methods which have been used in various studies. Slight modification might apply to some as this was done to suit the cells and condition related to the work.

3.1 TRANSCRIPTOM ANALYSIS OF 66CL4 AND 67NR OF THE 4T1 BREAST CANCER MODEL

To get better understanding of mechanisms such as signaling pathways leading to breast cancer metastasis, the 4T1 breast cancer model was used. Transcriptome analysis of the second aggressive metastatic cell line 66cl4 and the non-metastatic cell line 67NR of the 4T1 breast cancer model has been carried out. The sequencing was carried out at Norwegian University of Science and Technology (NTNU) faculty of medicine Genomics Core Facility (GCF) (http://www.ntnu.edu/dmf/gcf) and bioinformatics was spearhead by a group led by is Prof. I. Skotheim. RNA-sequencing data were produced from RNA isolation of three replicates of the 66cl4 and 67NR cell line in culture, seven primary tumours 66cl4 and four primary tumours for 67NR. A total of 23,965 genes were generated from the RNA–sequencing. Quality check of the sequence showed that the individual sequenced samples had between 85% and 92% of the sequence reads to the mouse genome allowed. The mapped reads with multiple hits to the genome accounted for between 4.71% and 6.76%. These outcomes indicated that the quality of the RNA-sequencing data is high with no contamination in the sequence. Differential analysis was then carried out using the cufflinks software. The Fragment per kilobase of exon per million reads mapped (FPKM) values were then assigned to all the 23,965 genes based on University of California Santa (UCSC) genome mouse mm10 assembly (https://genome.ucsc.edu/). A comparison done for both the primary tumors and cell lines showed 534 genes were highly expressed in the metastatic 66cl4 phenotype than 67NR while 548 genes were highly expressed in 67NR in comparison to 66cl4. Also comparison of 67NR versus 66cl4 cell lines in culture and 67NR versus 66cl4 primary tumor was done to obtain Log_2 value and p-value. Log_2 value was the expression difference between primary tumours or cell lines in culture from 67NR and 66cl4 whiles p-value was obtained via student t-test.

3.2 GENE CORRELATION WITH PROGNOSIS ANALYSIS

Databases have been established that enables researchers to associate genes, various markers and other factors relevance to clinical outcome for various cancer. In this current study, Kaplan –Meier plotter and BreastMark database have been used. Both enables us to compute the survival outcomes of breast cancer patients over time taking into consideration the event that has been entered.

3.2.1 Kaplan-Meier (KM) Plotter Analysis

The prognostic property of relevant genes associated with breast cancer and fibroblast was analyzed using Kaplan-Meier Plotter (http://kmplot.com/analysis/). The KM plot is a database that integrates gene expression data and clinical data with sources obtained from Gene Expression Omnibus (GEO) (Affymetrix microarrays only), European Genome-phenome Archive (EGA) and The Cancer Genome Atlas (TCGA)(98). KM Plotter currently contains information on 22,277 genes (54,675 probe sets) and their effect on survival in 4,142 breast cancer patients with mean follow-up of 69months (98). This meta–analysis based biomarker incorporates both gene expression data and clinical data and assesses the candidate gene of interest by splitting the patient samples into two groups. The two patient groups which are representative of higher and lower expression levels were compared by the KM plot. The plot then computes hazard ratio with 95% confident intervals and p-value from log rank test. The analysis was done with the Jet Set probes that recognized the genes of interest.

3.2.2 BreastMark Analysis

BreastMark Analysis was also used to analyze the prognostic property of relevant genes as done with the Kaplan Meier plotter analysis to serve as confirmation since both have different assessment of data. Gene of interest was checked in total cancer and several subtypes such as luminal A, luminal B and Basal. BreastMark integrates gene expression microarrays and clinical data that is correlated with clinical outcomes. BreastMark currently incorporates gene expression and survival data from 26 datasets from 12 different microarray platforms. This leads to a total of approximately 17,000 genes in 4738 samples (16,99).

3.3 CELL CULTURE

3.3.1 Cell lines and Primary cells

Below are the various cell lines and primary cells that were incorporated in this current study. All the cell lines and primary cells were cultured in Dulbecco's Modified Eagle's medium (DMEM) (Sigma-Aldrich, D5796) supplemented with 10% Fetal Calf Serum (FCS) (Gibco, Life Technologies 10270-106), 1X L-Glutamine with stock concentration of 200mM (Lonza, DE-17-605E) and 1X Penicillin/streptomycin with stock concentrations 5000 units/mL of penicillin and 5000 µg/mL of streptomycin. (GIBCO, Invitrogen 15070-063). Cell lines and primary cells were all incubated at 37°C in 5% CO_2.

4T1 breast cancer mouse model cell lines

The 4T1 breast tumor model comprised of different isogenic cell lines, was obtained from Barbara Ann Karmanos Cancer Institute. The cell lines include 67NR that is non-metastatic, the weakly to moderately metastatic 168FARN, 4T07 and 66cl4 and the highly metastatic 4T1 lines

Mouse embryonic fibroblast (MEF)

MEFs were obtained from Noboru Mizushima laboratory and the maximum passage number used in this work was twenty.

Isolation of primary fibroblasts from the lungs and skin of BALB/c mice

The isolation of the fibroblast was carried out as described by Seluanov and colleagues with slight modification (100). Lung and skin tissues were harvested aseptically from BALB/c mice and transferred into Dulbecco's phosphate buffered saline (DPBS) (Sigma-Aldrich, D8537) on ice which was then transported from the animal facility to the Laboratory. The lung and skin tissues were then sliced into about 1mm pieces using sterile blade and then transferred into 4ml and 8ml digestion solution respectively. The digestion solution was made up of equal amount of collagenase (Worthington, LS002592, 750 U/ml) and hyaluronidase (Worthington, LS004154, 750 U/ml). Digestion was carried out for a total of 50mins at 37°C with gentle rotation and making sure to check on it every 10mins after 30mins. This was to ensure that the lung and skin tissue was not over digested. A complete digestion was identified by the sticky nature of the minced tissue. The digestion process was seized by transferring the mixture into a 50ml tube and then topping it up to the 50ml mark with medium. The obtained solution was then span at 1500rpm for 5mins,

supernatant removed and then pellets re-suspended into 30ml medium. This process was repeated thrice with the final pellet suspended into fresh DMEM and transferred into 10cm tissue culture dish. The incubated cultured dish was checked on every day for adhering and proliferating fibroblasts. Fibroblast was seen to emerge from the various tissue usually from the third day which was a bit longer for the skin tissue. The cells were then sub-cultured at about 80% confluence and used directly seeded out for experiments. All lung and skin fibroblasts used did not go beyond two passages.

3.3.2 Sub-Culturing of Cell lines and Primary cells

Cells were sub-cultured at 80-90% confluence by firstly removing the respective growth medium by aspiration. The cells were washed two times with DPBS for cell lines and three-five times for primary cells to ensure that all trace of medium with serum has been removed. Trypsination was then used in splitting the cells to their appropriate split ratios.

3.3.3 Recombinant mouse BMP4 and GREM1 activities in cultures

Recombinant mouse (Rm) BMP4 (R&D systems, 5020- BP) and rmGREM1 (R&D systems, 956-GR) were used on MEFs and the five cell lines of the 4T1 breast cancer mouse model (67NR, 168FARN, 4T07, 66cl4 and 4T1) to determine their responses. Cells were seeded in accordance to the experimental plan and were cultured for 24-48hrs until they were treated with the appropriate recombinant agent at about 80-90% confluence. RmBMP4 was given to cells for a duration of 30mins whiles rmGREM1 for a duration of 1hr

3.3.4 Transwell cultures

Transwell-culture of MEFs with the five cell lines of the 4T1 breast cancer models cancer cells in transwell system was also used to study interactions between fibroblast and tumor cells. The transwell plate was prepared by adding the appropriate volumes of medium to the multiple wells and then incubated for an hour in order to aid cell attachment. MEFs were grown in the bottom of a 6-well plate in 2.6 ml medium and the various five tumor cell lines were seeded in 1.5 ml of the same medium on the 0.4-µm polyester membrane transwell insert (Corning, 3450) (**Figure 3.1**). The cells were allowed to grow for 48hrs upon which the appropriate treatment pertaining to the experiment planned are carried out.

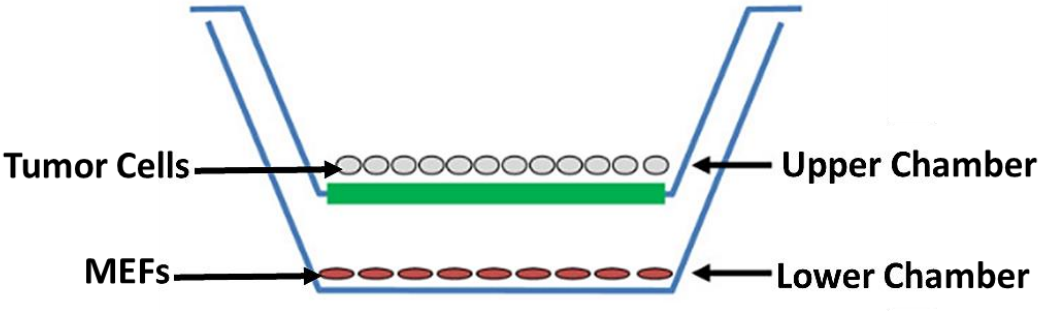

Figure 3.1: Overview of transwell setup
The transwell consists of two chambers separated by 0.4µm polyester membrane. The MEFs were placed on the bottom of the lower chamber while the tumor cells were placed on the membrane of the upper chamber. Adapted and modified from (101).

3.3.5 Condition medium (CM) treatment on cells

Condition media were prepared by growing the appropriate cells and the media was collected on the third day. The cells were usually about 80-100% confluent on the third day when the media was collected. The cultured medium was cleared up by centrifugation at 1500rpm for 5mins and then filtered through 0.2µm filter. The condition medium was aliquoted and stored at -20°C until usage. The CM was treated on cells at a concentration of 50% or 100% depending on the experiment set up. The incubation time for the CM was usually 1hr unless otherwise stated.

3.4 WESTERN BLOT

In this current study, Western blotting was used to determine the protein levels of BMP4, GREM1 and p-SMAD1/5/9 for various experiment. Western blotting also referred to as immunoblotting was introduced by Towbin, *et al.* in 1979 (102). It is a protein analysis technique which enables one to identify specific protein of interest from a pool of protein mixture extracted form cells. Western blotting enables one to obtain qualitative and semi quantitative data about the protein of interest. The technique involves four major steps in accomplishing the task. The first step is the separation of the macromolecules by size using gel electrophoresis. This involves the denaturing of the proteins to introduce a negative charge on the protein which migrates to the anode during the electrophoresis. The second step is electro-transfer of the proteins to a second matrix.(103,104) This second matrix is usually a nitrocellulose or polyvinylidene fluoride (PVDF) membrane. The membranes are then blocked to prevent nonspecific binding of antibody on the membrane and thus

increasing the signal-to-noise ratio. The proteins are then detected on the membrane by incubation of primary and secondary detection reagents (103,104).

3.4.1 Cell harvesting and protein concentration

Cells seeded in the 6-well plate or transwell that are confluent or that have been successfully treated as described in the previous section were harvested by initially washing with sterile DPBS. The cells were then lysed by adding 40µl of 8M Urea lysis buffer for 6-well and 35µl for transwell insert. The lysis buffer comprised of 8M Urea (Sigma Aldrich, U4883) and 0.50% triton X-100 (Sigma Aldrich, T8787) prepared in MilliQ water in addition with 0.1M Dithiothreitol (DTT) (Sigma Aldrich, 43816). Complete protease inhibitor cocktail (1X) (Roche, 11873580001) and 2X phosphatase inhibitors cocktail (PIC) 2 &3 (Sigma Aldrich, P4726 & P0044) was also added to make up the lysis buffer. The cell cultures were then scarped and the cell lysates were transferred into appropriated labeled 1.5ml Eppendorf tubes. The tubes were vortexed three times for 15secs after which it was centrifuged at 13000rpm for 15mins at 4 °C (Eppendolf, Centrifuge 5427R) and supernatants of the cell lysates collected into a newly labeled 1.5ml Eppendorf tubes.

The concentration of the total protein extract was determined by Bio-Rad protein assay. The Bio-Rad solution was prepared by diluting 1 part Bio-Rad concentrated (Bio-Rad laboratories 500-0006) with four parts of distilled water. The protein extracts were diluted 1:1000 with the Bio-Rad solution with the lysis buffer being used as blank. The obtained sample mixture was mixed and incubated at room temperature for 10mins shielding it from light. Visible Spectrophotometer (Thermo Scientific, Genesys 20) was used to measure the absorbance of the samples at 595nm and the protein concentration was calculated. Protein extract were stored at -80°C when not in use or were worked on immediately.

3.4.2 Gel electrophoresis and transfer of protein

Equal protein concentration for all samples to be run on a particular gel was obtained by appropriate protein sample dilution with 10mM Tris-HCl. The diluted sample was then mixed with 4X Lithium Dodecyl Sulfate (LDS) sample buffer (NuPage, Life Technologies, NP0007) and 1M DTT in the ratio 5:1. The samples were then incubated at 80°C on heating block (VWR Digital heatblock) for 10mins to denature the protein. The ladder was prepared by mixing Odyssey two-color protein molecular weight marker (IR dye 4000, LI-COR Biosciences, 928-40000) with loading mix. The loading mixed comprised of LDS and 10mM Tris-HCL mixture in 1:4 ratio.

Equal amount of protein samples were loaded and separated in NuPAGE® 4–12%, 10% and 12% gradient sodium dodecyl sulfate polyacrylamide gel electrophoresis (SDS-PAGE) gels (NuPAGE®, Novex, NP0335BOX, NP0321BOX, NP0341BOX, NP0302BOX) using a MOP buffering system (NuPAGE Life Technologies, NP0001-02) (**Appendix I**) for 1hr at 200V.

Following gel electrophoresis, proteins were transferred to membranes using the electrophoretic transfer method also called electroelution transfer method. The electrophoretic transfer involved placing the 0.45 µm pore size nitrocellulose membrane (GE Healthcare Life Sciences, 10600016) and PDVF (EMD Millipore Immobilon, IPVH304F0) in direct contact with the polyacrylamide gel supporting it with blotting pad together with filter paper (**Figure 3.2**). This was sandwiched between two electrodes and submerged into NuPAGE 20X transfer buffer (ThermoFisher Scientific, NP0006-1) (**Appendix I**). The transfer was carried out at 30V for 1hr (Invitrogen, PowerEase 500).

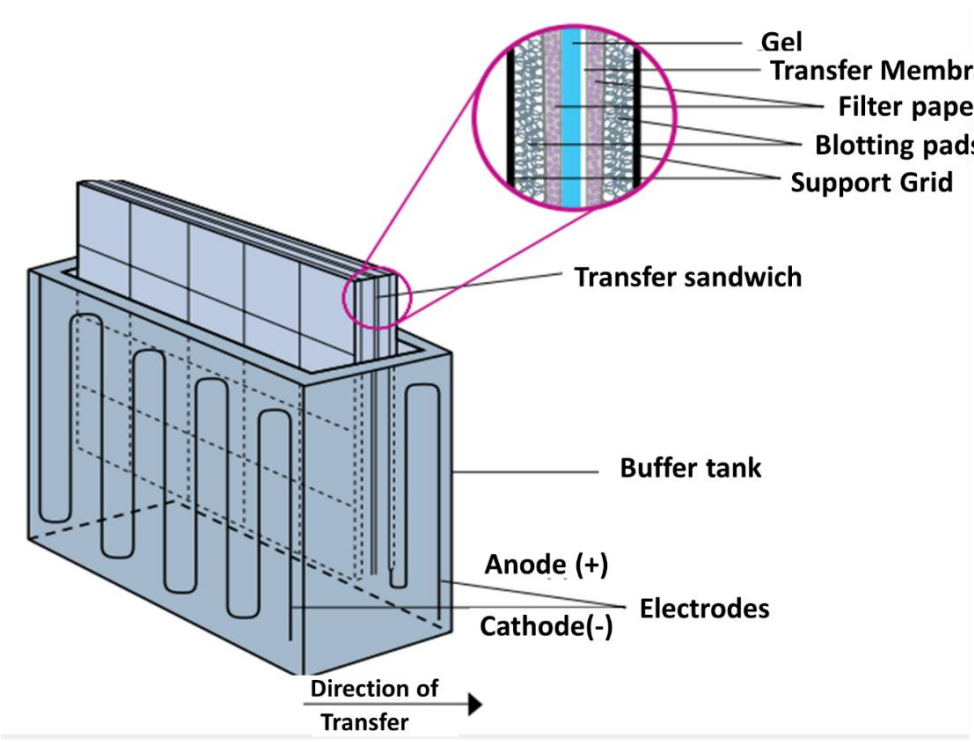

Figure 3.2: Electrophoretic transfer method setup overview.
This illustrates how proteins are transferred from gel matrix to nitrocellulose or PDVF membrane using wet (Tank) transfer. The highlighted insert shows the "transfer sandwich" that consist of the gel, transfer membrane, blotting pads and filter papers. Electrical current subjection results in protein transfer from gel to the membrane. The entire set up is placed on ice throughout the entire transfer. Adapted and modified from (103).

3.4.3 Membrane blocking and immunostaining

The membrane was then blocked with Odyssey blocking buffer (LI-COR Biosciences, 927-50000) prepared at a 1:1 dilution with Tris Buffered saline with Tween-20 (sigma, P1379) (TBS-T) for 1hr on a roller mixer (Stuart, SRT6D) at 50rpm. Afterward, it was incubated overnight with primary antibody per specific dilutions (**Table 3.1**). To remove unbound primary antibody and reduce background, the membrane was washed with TBS-T (**Appendix 1**) 3 x 10mins on a roller mixer at 50rpm after staining with the primary antibodies. The membrane was then stained with labelled secondary antibody (**Table 3.2**) after which the membrane was washed with Tris Buffered saline (TBS) for 3x10mins. Infrared fluorescence of the secondary antibody, representing the amount of the protein of interest, was quantified using ImageStudio. To correct for concentration variation in each sample lane, detected proteins of interest were normalized with loading controls (**Table 3.1**) which were expressed in all cells. After developing, the membrane was visualized with Odyssey CLx infrared imaging system (LI-COR Biosciences, USA) and Image Studio software.

Table 3.1: Primary antibodies for Western blot staining

Antigen	Host – Antibody type	Size (kDa)	Manufacturer	Dilution
p-SMAD 1/5/9	Rabbit mAb	60	Cell Signaling (9511)	1:1000
GREM1	Rabbit pAb	21	Abcam (ab189267)	1:1000
BMP4	Mouse mAb	47	Abcam (Ab93939)	1:1000
Vimentin (loading control)	Guinea Pig	57	Progen Biotechnik(GP57)	1:1000
Beta Actin (loading control)	Mouse mAb	42	Abcam (ab6276)	1:5000

Table 3.2: Secondary antibodies for Western blot staining

Secondary Antibody	Manufacturer (LI-COR Biosciences)	Dilution
Goat anti-guinea pig IgG - IRDye 800	925-32411	1:5000
Goat anti-mouse IgG - IRDye 800	925-32212	1:5000
Goat anti-rabbit IgG - IRDye 800	925-32213	1:5000
Goat anti-guinea pig IgG - IRDye 680	925-68077	1:5000
Goat anti-mouse IgG - IRDye 680	925-68072	1:5000
Goat anti-rabbit IgG - IRDye 680	926-68073	1:5000

3.5 ENZYME-LINKED IMMUNOSORBENT ASSAY (ELISA)

ELISA was used in this study to determine GREM1 antigen in supernatant solutions of various samples to confer if GREM1 is secreted by that samples. ELISA incorporates the specificity of antibody to an antigen and vice versa. It is a very sensitive enzyme assay that involves usage of antibodies or antigens coupled with enzymes used in the measurement of antigen and antibody concentration (105,106). Sandwich ELISA was used in this study which involves the immobilization of the specific antigen of interest. The sensitivity of the assay is based on the amount of antigen immobilized. This particular assay requires two antibodies to detect the antigen of interest. The primary is called the capture antibody whiles the secondary is called the detection antibody(105).

3.5.1 Sample analysis using Sandwich enzyme-linked immunosorbent assay (ELISA)

Conditioned medium from cultured cells was analyzed for mouse GREM1 levels using kit from DuoSet ELISA development systems an R&D systems product (Cat# DY956). Samples to be analyzed were performed according to the manufacture's instruction with slight modification. The modification was the incubation time of the samples and standards which was modified from 2hrs to overnight incubation at 4^{o}C. After the whole assay was done and reactions stopped, the optical density for each well was measured immediately at 450nm wavelengths using an iMark Microplate Absorbance Reader (Bio-Rad, catalog #168-1130) with aid of Microplate Manager 6 Software (Bio-Rad, catalog # 168-9520). The standard curve generated was usually a seven-point standard curve with serial dilution having at least a high standard of 6000pg/ml (**Appendix II**)

3.6 CELL PROLIFERATION ASSAY

The effects of various treatment on the rate of growth of fibroblast was determined using cell proliferation assay. Cell proliferation assay is accomplished by several methods but will be restricted to the direct cell counting method and the use of Methylthiazolyldiphenyl-tetrazolium bromide (MTT) method in this study.

3.6.1 Cell Counting Method

In this study, the automatically counting procedure using the Z1 Beckman counter was used. Experiments were performed in 24-well plates with 8000 MEFs seeded per well. The cells were incubated for about 4-6 hrs to allow the cells ample time to attach. Afterward, the cells were treated with various conditions such as RmBMP4 and RmGREM1 as well as condition medium from the various five cell lines of the 4T1 breast cancer cell model. The treated cells were then incubated for 24hrs. For the counting, trypsination was used to detach the cells making sure all cells were detached and in single colonies. The obtained cell suspension was then transferred into Eppendorf tubes and counted using Z1 Beckman counter. Each cell condition was performed in triplicate.

3.6.2 MTT (Methylthiazolyldiphenyl-tetrazolium bromide) Assay

The principle of this colorimetric method is correlating the number of cells with the relative metabolic activity of the cell MTT, a soluble yellow tetrazolium salt is reduced to its equivalents such as NADH and NADPH as a result of metabolic activity of the cells by action of dehydrogenase enzymes. The reduction leads to formation of intracellular purple formazan which is dissolved and then quantified by measuring absorbance (107).

For the experiment using MTT assay, the optimal cell counts were first determined by seeding out MEFs ranging between 250 – 12000 cells per well and then determining which of the cell number will give an optimal absorbance whiles in the range of 80-100% confluent. This was achieved by plotting the absorbance against the cell number (cell/ml) and then selecting the number of cells that yield a higher absorbance without being over confluence within 48hrs. After establishing that, MEFs were seeded using the optimal cell number and the experimental condition were run in parallel of eight in a 96 well plate. The cells were incubated overnight to allow cell attachment. The medium was carefully taken out and the various appropriated treatments in medium were added to make up a volume of 200µl. The plate with the treated cells was then incubated for 24hrs after which 20µl of the 5mg/ml MTT reagent (Thiazolyl Blue Tetrazolium Bromide, Sigma

M2128) was added and again incubated for 4hrs at 37^{o}C. An amount of 150µl of the medium on the cells was taken off after the 4hrs incubation, followed by addition of 100µl of the detection reagent, acidic isopropanol (0.1N HCl in absolute isopropanol). The plate was then mixed on a shaker for 1hr after which each well was pipetted up and down to ensure total dissolving of the purple formazan. The optical density for each well was measured immediately at 570nm wavelengths using an iMark Microplate Absorbance Reader (Bio-Rad, catalog #168-1130) with aid of Microplate Manager 6 Software (Bio-Rad, catalog # 168-9520). All procedure during the addition of MTT towards the end was done away from direct light.

3.7 xCELLigence REAL-TIME CELL ANALYZER (RTCA) MIGRATION ASSAY

Influence of soluble factors secreted from the five cell lines of the 4T1 breast cancer mouse model on migration of fibroblast was to be determined. xCELLigence RTCA (ACEA bioscience Inc.) was used to monitor cell migration in a real-time setting. The method involves correlating impedance to the number of migrated cells (cell index). Thus, an increment in impedance is an indication of increase in migration of the cells (108,109). As illustrated in **Figure 3.3A,** the Cell Invasion and Migration plate (CIM plate) consists of two chambers: cells on upper chamber and chemoattractant in bottom chamber. Cells migrate from the upper chamber through the micropore membrane at the bottom surface of the upper chamber to the bottom chamber. The migration is as a result of chemoattractant in the lower chamber and the impedance is measured when cells come in contact and adhere to the gold microelectrodes attached to the bottom surface of the upper chamber. The attachment interrupts the flow of electrons as a result of electric potential across the electrons as described in **Figure 3.3B** which causes impedance (108,109).

In the RTCA migration experiments, the lower chamber was filled with chemoattractant that consisted of both CM from the tumor cells and tumor cells itself. With regards to the cells, 67NR, 168FARN and 66cl4 were seeded at 10000cells/well. Medium used in this experiment contained 2% FCS with the exception of the positive control that contained 10% FCS. The various 20% condition medium were prepared from lung fibroblast, skin fibroblast, 67NR, 168FARN and 66cl4 cultures. These cell suspension and condition medium were transferred in volume of 160µl to the lower chamber as designated in duplicate. To validate the system, media supplemented with and without FBS was used as controls. The lower chamber was then closed with the upper chamber compartment which was then filled with 50µl of medium with 2% FBS. The plate was then placed

in the RTCA DP instrument, allowed to stand for 30mins to allow cells to attach and for equilibrium to be established. The background measurement was then done. Afterwards, 100µl of lung/skin fibroblast seeded at 10000cells/well was added to the upper changer making sure to avoid air bubbles. The chamber was then covered with the lid and allowed to stand for 30mins at room temperature to allow settlement of the cells. The plate was then placed in the RTCA DP instrument and the cell index was measured every 10mins for the total length of time.

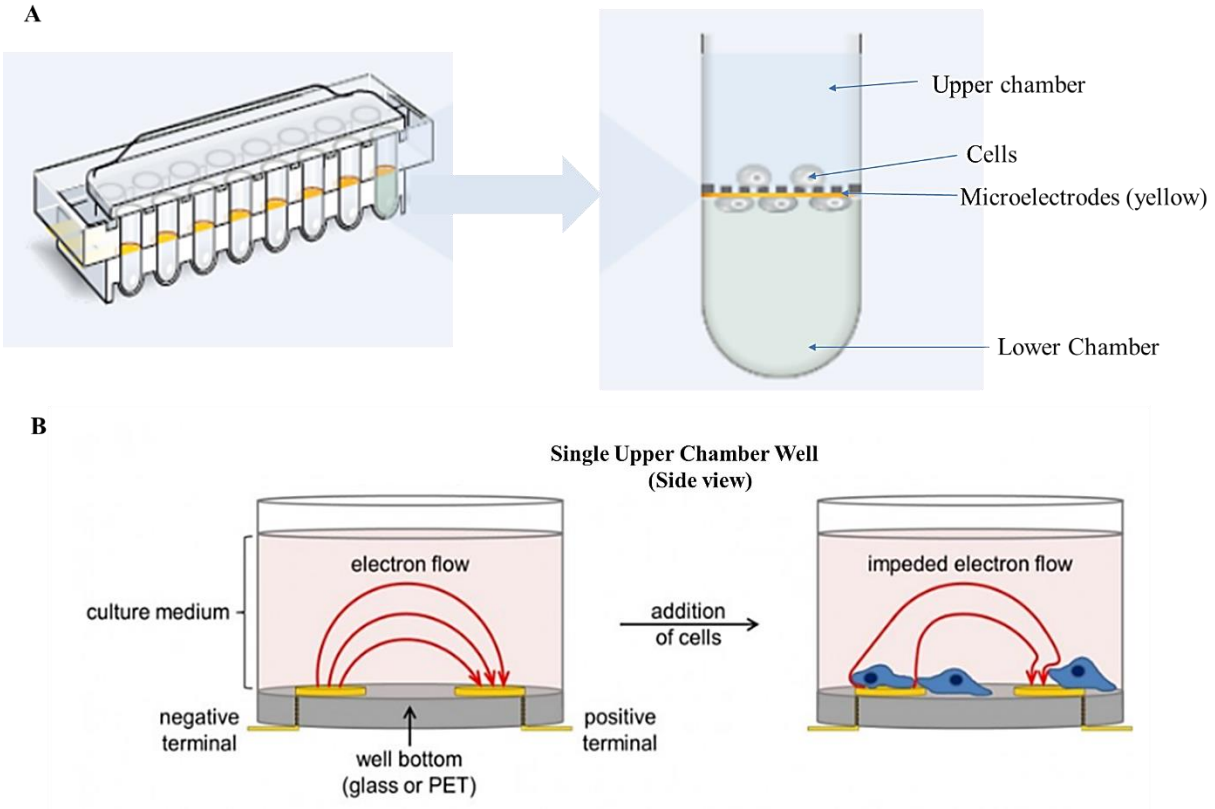

Figure 3.3: Overview of setup and mechanism of impedance measurement in RTCA migration assay. ***A)*** *CIM-plate details. The left image shows cross sectional view of the 8-wells of the CIM-plate. The right image is an extended view of a single well showing both the upper and lower chambers. The bottom of the upper chamber is made up of microporous membrane that the cells can migrate through. Underneath the membrane is the gold microelectrodes that detects the presence of adherent cells.* ***B)*** *A side view of a single well (upper chamber) before and after cells have been added to illustrate impedance measurement. The bottom of the well contains a set of gold microelectrodes which when submerged in solution and powered up creates an electric potential across the electrodes. Upon establishing the electric potential, electrons move from the negative terminal to the positive terminal. However, when cells in solution become adherent to the electrodes, they interfere with the electron flow and cause impedance. The magnitude of the impedance is dependent on the number of cells that migrate. In contrast, the absence of cells leads to electric current flowing freely through culture medium, completing the circuit between the electrodes. Adapted and modified from* (108,110).

3.8 STATISTICAL ANALYSIS

Graph Pad prism 5 software was used in the statistical analysis. Data were expressed as mean ± standard error of mean (SEM) unless stated otherwise. For comparison of the differences between different treatment and control, Student's t-test and the statistical significance was determined by the p-value. $P < 0.05$ is an indication of significance.

4. RESULTS

The aim of this study was to get a better understanding of the interplay between 4T1 mouse mammary tumor model and stroma cells that might attribute to their different metastatic potential. The main hypothesis was that the breast cancer cell lines which can leave the primary tumor (168FARN, 4T07, 66cl4 and 4T1) are better equipped to attract, polarize and communicate with stroma cells than the non- metastasizing 67NR cell line. In this respect, fibroblasts were used as an important part of the stroma cells. RNA-sequencing data of the non-metastatic 67NR and metastatic 66cl4 tumors was analyzed for fibroblast markers and other cytokines. Relevant genes expressed were tested for clinical relevance and outcomes in breast cancer patients with two online databases (BreastMark and KM plotter). Finally, several interactions of tumor cells and fibroblasts were also studied in vitro with focus on two relevant cytokines, BMP4 and GREM.

4.1 IDENTIFICATION OF PROMETASTATIC FACTORS IN TRANSCRIPTOM DATA AND THEIR CORRELATION WITH PROGRNOSIS

In this section RNA- sequencing data analysis of marker and genes that might be attributed to the different metastatic ability of 67NR and 66cl4 was identified. Relevant genes clinical relevance was then checked to ascertain its importance.

4.1.1 CAF associated markers and genes are differently expressed in 67NR and 66cl4

Tumor growth is known to be dependent on interaction with multiples of cell types known collectively as stroma cells (26–28). Transcriptome analysis of 67NR and 66cl4 has been done previously in the group and this data can be used to identify candidates that may be involved in the interplay of tumor cells and stroma. The group has also demonstrated the presence of stroma cells in the 67NR and 66cl4 primary tumor of the 4T1 breast cancer mouse model. The unpublished data showed approximately 40% of 66cl4 and 67NR primary tumors are made up of stroma cells.

CAF is a stroma cell that has been associated with production of autocrine and paracrine factors that influences tumor growth and metastasis. To get a better view of the interplay of fibroblasts and tumor cells in the 4T1 breast cancer model, markers and genes obtained from literature were compiled and extracted from the transcriptome data of 67NR and 66cl4 **(Appendix III**). The genes and markers included fibroblast markers (e.g. *Vim*, *Fap*, *Fsp1* and *Acta2*), fibroblast activation markers (e.g. *Tgfb1*and *Pdgfb*), growth factors (e.g. I*gf2, Hgf, Fgf2,* V*egfa*), proteases (e.g. *Mmp*

and *Plau*) and other cytokines (e.g. *Cxcl9*, *CxcL10*, *Cxcl12*). To streamline the genes and markers to those that were most informative, genes and markers that were expressed in primary tumors of 67NR and/or 66cl4 but were not expressed or significantly lower in cell culture were selected (**Table 4.1**). This made it more probable that those markers are expressed in the fibroblasts in the tumor. Smooth muscle alpha-actin (*Acta2*), Platelet-derived growth factor receptor alpha (*Pdgfra)* and Platelet-derived growth factor receptor, beta (*Pdgfrb*) were the three fibroblast markers that met the criteria and were selected out of the six identified. *Acta2*, *Pdgfra* and *Pdgfrb* were all upregulated in primary tumors from 66cl4 cells compared to 67NR induced primary tumors. This suggested that the metastatic cell line had a higher propensity in recruiting fibroblasts than the non-metastatic cell line 67NR.

Table 4.1: Transcriptome Data - CAF associated marker and gene mRNA expression in 66cl4 and 67NR tumors

Where Log_2 = Log2(66cl4 /67NR). This indicates the differential expression between 66cl4 and 67NR of either the cell line or tumor. A positive number indicates higher expression in 66cl4 whiles a negative number indicated higher expression in 67NR. p-value= p-value from t-test of the comparison of 66cl4 and 67NR in the cell lines or tumor

		Comparison of cell lines				Comparison of primary tumors			
	Gene	**66cl4**	**67NR**	**Log2**	**p-value**	**66cl4**	**67NR**	**Log2**	**p-value**
Markers	Acta2	0.02	0.00	2.72	1.0000	8.73	3.46	1.34	0.0002
	Pdgfra	4.01	14.25	-1.83	0.0001	60.65	28.86	1.07	0.0002
	Pdgfrb	5.87	4.13	0.51	0.0001	27.58	6.24	2.14	0.0002
Activation Markers	Cxcl12	143.02	31.62	2.18	0.0001	205.08	75.16	1.45	0.0002
	Tgfb1	18.74	3.16	2.57	0.0001	44.65	24.64	0.86	0.0002
	Pdgfb	1.11	0.01	7.40	0.0042	8.54	5.26	0.70	0.0005
Proteases	Plau	0.01	0.02	-0.89	1.0000	51.62	27.86	0.89	0.0002
	Mmp3	3.83	21.23	-2.47	0.0001	68.83	38.26	0.85	0.0002
	Mmp9	0.97	0.18	2.44	0.0001	33.53	14.20	1.24	0.0002
	Mmp11	3.15	0.79	2.00	0.0001	11.77	1.66	2.82	0.0002
Growth Factors	Vegfa	14.34	19.12	-0.41	0.0016	16.64	24.96	-0.58	0.0010
	Fgf2/bFgf	0.01	1.24	-6.96	0.0001	0.14	1.92	-3.80	0.0045
	Igf2	0.20	0.09	1.23	0.0001	3.21	0.93	1.78	0.0002
	Pdgfc	0.06	1.13	-4.17	0.0001	3.41	5.96	-0.81	0.0002
Others	Sparc	161.94	557.21	-1.78	0.0001	424.48	629.78	-0.57	0.0016
	Cxcl9	0.04	0.02	0.92	1.0000	13.44	29.55	-1.14	0.0002

CAFs are required to be activated in order to perform functions such as ECM degradation that could promote breast cancer growth and metastasis. After observing the higher expression of fibroblast markers in metastatic 66cl4 as compared to 67NR in primary tumor, we next looked at the fibroblast activation markers. The fibroblast activation markers Chemokine (C-X-C Motif) Ligand 12 (*Cxcl12*), transforming growth factor (*Tgf-β1*) and Platelet derived growth factor B (*Pdgfb*) selected were all higher expressed in 66cl4 than 67NR tumors. This means that 66cl4 do not only seem to recruit more CAFs in comparison with 67NR but they might activate them through an autocrine/paracrine means by *Cxcl12*, *Tgf-β1* and *Pdgfb*. *Cxcl12* is also known as stromal cell-derived factor 1 (*Sdf1*), aside being a fibroblast activation marker, and has been shown to recruit bone marrow- derived cells to promote tumor growth (53).

Upon activation, CAF mediate direct and indirect tumorigenesis and tumor progression through secretion of several growth factors (30). Proteins that function in promoting the growth of cancer cells such as Fibroblast growth factor 2 (*Fgf*), Platelet derived growth factor C (*Pdgfc*) and Insulin-like growth factor 2 (*Igf2*) (38,111) were found to be higher expressed in the non-metastatic 67NR in primary tumor than 66cl4 with the exception of *Igf2* that portrayed a high expression in 66cl4 as compared to the 67NR. Vascular endothelial growth factor A (*Vegfa*) that stimulates angiogenesis (111) however, was highly expressed in 67NR as compared to 66cl4.In addition, proteases secreted by CAFs that function in the distraction of ECM, an indicator that aids in tumor invasion and metastasis (29,31) were also selected. The proteases plasminogen activator urokinase (*Plau*), matrix metalloproteinase-3 (*Mmp3*), *Mmp9* and *Mmp11* were highly expressed in 66cl4 as compared to 67NR in primary tumor.

Based on these results, it can be speculated that fibroblasts contribute to the metastatic ability of 66cl4 since the majority of CAF associated markers and genes were highly expressed in 66cl4 as compared to 67NR. To better understand why fibroblasts were recruited more and activated in 66cl4 as compared to 67NR, fibroblast activation markers was further investigated. CAFs are functional in promoting breast cancer progression and metastasis upon their activation. Since CAF are known to be majorly activated by Tgf-β1 (37,41,43,45), TGF-β superfamily was then investigated.

4.1.2 Bmp4 is highly expressed in 66cl4 on mRNA level

The TGF-β superfamily is made up of the TGFβs, NODAL, activins, bone morphogenetic proteins (BMPs), growth and differentiation factors (GDFs) and anti-Müllerian hormone(AMH) (70). From the transcriptome data it was noticed that among the Tgf-β subfamily, *Bmp4*, *Tgf-β1,2&3*, *Inhba* and *Gdf15* were the only ones that were significantly expressed in both the cell lines and primary tumors (**Table 4.2**). *Bmp4* and *Tgf-β1* had the highest expression amongst them which were higher expressed in 66cl4 than 67NR. It was observed that *Bmp4* was upregulated in the cell lines than the primary tumors. *Tgf-β1* was also noted to be significantly elevated in the 67NR tumor compared to the same cells grown in culture making this factor more difficult to follow in further experiments. Therefore, *Bmp4* was selected and the clinical relevance checked, before studying this cytokine in more detail.

4.1.3 BMP4 correlation with breast cancer prognosis

We verified the clinical significance of BMP4 to patient survival by obtaining a prognosis curve for breast cancer patients (n=4142) (**Figure 4.1**) using Kaplan Meier (KM) plotter (98,112). The Affymetrix ID was 211518 (BMP4). BreastMark was also use to determine the clinical significance of BMP4(**Figure 4.2**). The cutoff point used in determining clinical significance was Hazard Ratio (HR) > 1.2 and HR < 0.83. High expression of BMP4 with HR > 1.2 and a p-value <0.05 is associated with poor clinical outcome. On the other hand, high expression of Bmp4 with HR < 0.83 and a p-value <0.05 is associated with good prognosis. From the KM prognostic curve, it was observed that BMP4 mRNA expression was not correlated to prognosis with respect to Overall Survival (OS), Relapse Free Survival (RFS), Distant Metastasis Free Survival (DMFS) and Post Progression Survival (PPS) (**Figure 4.1**).

Table 4.2: Transcriptome analysis showing significant upregulation of Bmp4, Tgf- β1 and Tgf- β3 in 66cl4 compared to 67NR among the Tgf- β superfamily

Where Log_2 = Log2(66cl4 /67NR). This indicates the differential expression between 66cl4 and 67NR of either the cell line or tumor. A positive number indicates higher expression in 66cl4 whiles a negative number indicated higher expression in 67NR. p-Value= p-value from t-test of the comparison of 66cl4 and 67NR in the cell lines or tumor. Abbreviation: Bmp – Bone morphogenetic protein, Gdf- Growth differentiation factors, Tgf- β -Transforming growth factor beta, Inhb- inhibin beta/Activin.

	Comparison of cell lines				Comparison of primary tumors			
Gene	**66cl4**	**67NR**	**Log_2**	**p-value**	**66cl4**	**67NR**	**Log_2**	**p-value**
Bmp2	0.0	0.0	0.00	1.0	2.2	0.8	1.52	0.0
Bmp3	0.0	0.0	-1.16	1.0	0.1	0.1	0.01	1.0
Bmp4	47.4	0.0	10.75	0.0038	38.8	0.4	6.58	0.00020
Bmp5	0.0	0.0	3.36	1.00	0.2	0.0	2.39	1.0
Bmp6	0.0	0.0	1.41	1.0	0.2	0.1	0.69	1.0
Bmp7	0.0	0.0	1.32	1.0	0.1	0.0	2.13	1.0
Bmp8a	0.0	0.0	1.74	1.0	0.0	0.0	1.61	1.0
Bmp8b	0.0	0.0	-0.10	1.0	0.0	0.0	-1.27	1.0
Bmp10	0.0	0.0	-1.04	1.0	0.0	0.0	-2.34	1.0
Bmp15	0.0	0.0	0.00	1.0	0.0	0.0	-1.44	1.0
Gdf1	0.0	0.0	-2.23	1.0	0.1	0.0	2.56	1.0
Gdf10	0.0	0.0	0.00	1.0	0.1	0.0	1.19	1.0
Gdf11	10.6	8.0	0.40	0.0054	6.0	6.8	-0.16	0.6
Gdf15	0.0	1.3	-4.77	0.00048	0.5	2.7	-2.34	0.0
Gdf3	0.0	0.0	0.00	1.0	0.4	0.3	0.61	0.3
Gdf5	0.8	0.0	7.20	0.31	0.1	0.0	2.96	1.0
Gdf6	0.0	0.0	0.00	1.00	0.0	0.0	-0.49	1.0
Gdf7	0.0	0.0	0.39	1.0	0.1	0.0	3.79	1.0
Gdf9	0.0	0.2	-2.02	1.0	0.3	0.3	-0.06	0.9
Tgfb1	18.7	3.2	2.57	0.00012	44.6	24.6	0.86	0.00020
Tgfb2	0.4	0.1	2.63	0.00012	0.6	0.1	2.99	0.00020
Tgfb3	1.9	6.7	-1.78	0.00012	26.8	12.7	1.08	0.00020
Inhba	3.7	1.9	0.95	0.00012	3.6	1.4	1.38	0.00055
Inhbb	0.0	0.0	-0.13	1.0	4.9	7.5	-0.61	0.00055
Inhbc	0.0	0.0	-1.72	1.0	0.0	0.0	-2.27	1.0
Inhbe	0.0	0.0	0.76	1.0	0.0	0.0	1.25	1.0
Nodal	0.0	0.0	0.00	1.0	0.0	0.0	1.84	1.0

BreastMark (**Figure 4.2**) also showed that BMP4 mRNA expression was not correlated to prognosis with whole cancer with HR =0.8801(0.7819-0.9991) and p-value=0.26. However high expression of BMP4 was associated with good prognosis with lymph node negative breast cancer

patient with HR =0.7793(0.603-0.9034) and p-value=0.0209. It is also important to note that lymph node positive patient and breast cancer tumor subtype luminal A, luminal B, basal and Her2 did not correlate BMP4 mRNA expression to clinical outcomes (**Appendix IV**)

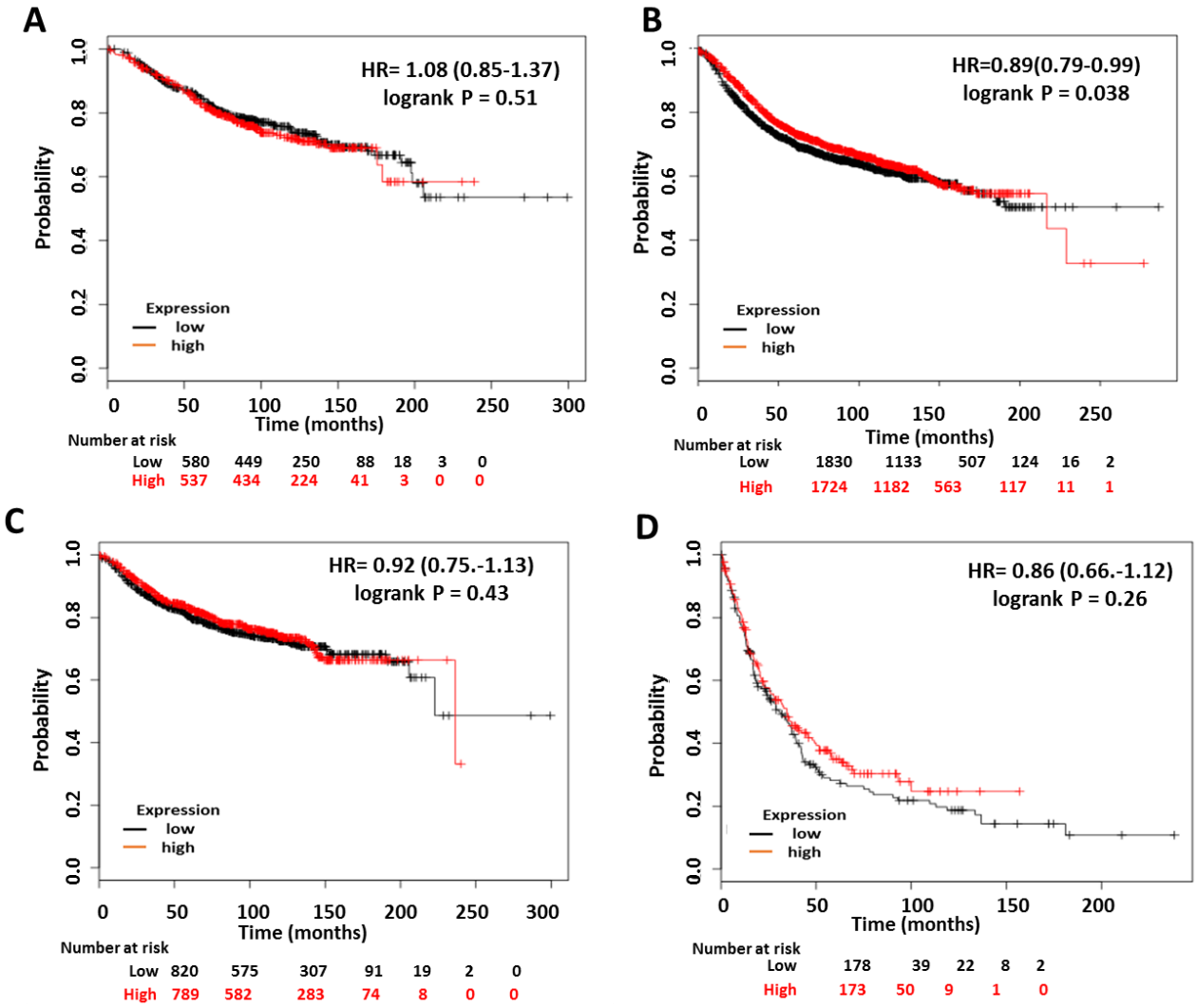

Figure 4.1: Kaplan – Meier survival curve does not correlate BMP4 expression with prognosis
Kaplan – Meier (KM) survival curve for breast cancer patients stratified by their expression level of BMP4 showing prognosis in breast cancer for ***A.*** *Overall Survival,* ***B.*** *Relapse free survival,* ***C.*** *Distant Metastasis Free Survival and* ***D.*** *Post Progression Survival. The breast cancer was classified into low (Black) or high (red) expression groups based on whether the expression of BMP4 was greater than the median expression of BMP4. The p-value obtained from log-rank tests by comparison of the two KM curves is shown on the top right corner of the plot together with Hazard Ratio (HR) with 95% confidence intervals. The cutoff point was (HR > 1.2 and HR < 0.83). HR > 1.2 and a p-value <0.05 is associated with poor clinical outcome and HR < 0.83 and a p-value <0.05 is associated with good prognosis. The total number of patients with available clinical data was: OS, n=1117; RFS, n=3557 DMFS, n=1610; and PPS, n=351.*

Collectively, these results suggest that BMP4 might be relevant in the metastatic potential of 66cl4 since it is higher expressed 66cl4 than 67NR. Even though we did not find a convincing clinical significance for Bmp4. The role of BMP4 in breast cancer metastasis has been document (64,74).Thus, we speculated that in the complex tumor microenvironment there could also be inhibitors of Bmp4 signaling that modulate the responses. Therefore, we checked the mRNA expression of Bmp antagonist family in the transcriptome data of the 4T1 breast cancer model.

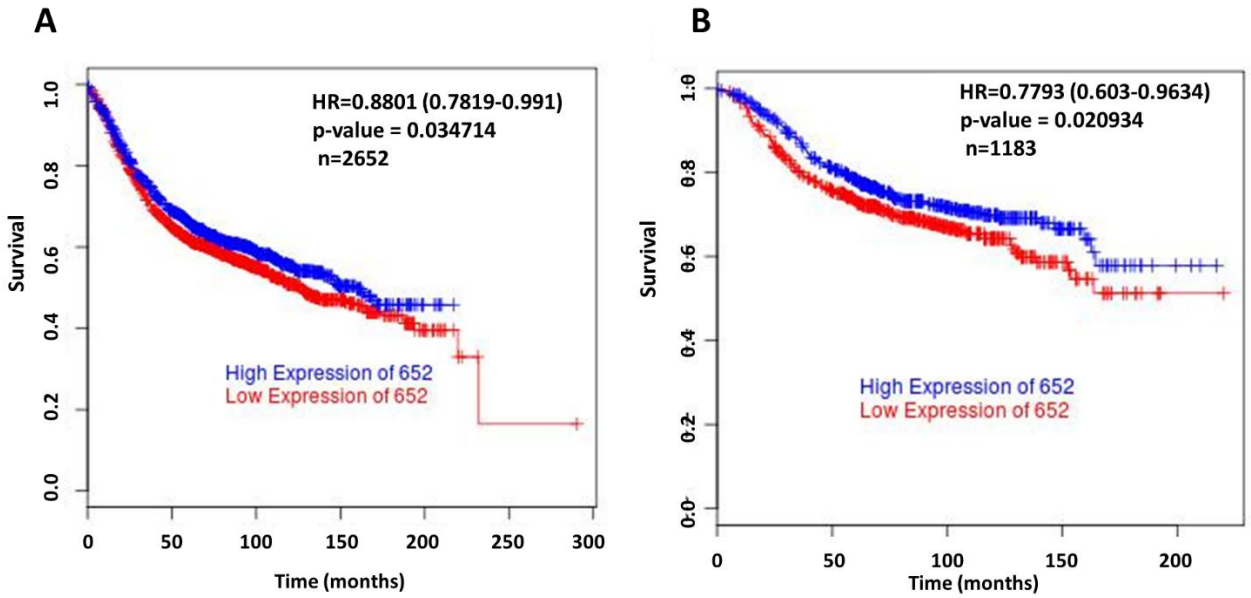

Figure 4.2: BreastMark survival curve correlates BMP4 high expression with good prognosis for lymph node negative breast cancer patient
BreastMark survival curve for breast cancer patients stratified by their expression level of BMP4 showing prognosis in breast cancer for ***A.*** *Whole Cancer* ***B.*** *lymph node negative patient. The breast cancer was classified into low (Red) or high (blue) expression groups based on whether the expression of BMP4 was greater than the median expression of BMP4. The p-value is shown on the top right corner of the plot together with Hazard Ratio (HR) with 95% confidence intervals and number of patients involved. The cutoff point was (HR > 1.2 and HR < 0.83). HR > 1.2 and a p-value <0.05% is associated with poor clinical outcome whiles HR < 0.83 and a p-value <0.05% is associated with good prognosis with regards to high expression of Bmp4.*

4.1.4 Grem1 is highly expressed in 66cl4 on mRNA level

BMP4 is known to be regulated at various stages of its pathway by antagonist such as the Noggin, DAN family members, the chordin family members, Twisted gastrulation (TSG) and Follistatin (FST). (69,74,75). About thirty-four *Bmp4* antagonists could be identified in the transcriptome data. About nine (*Coco, Twsg1, Bambi, Fst, Fst1, Bmper, Rgmb, Tobi,* and *Tsku*) were significantly expressed in 67NR or 66cl4. The expression could be in either cell line in culture or primary tumor or even both. Among the nine, Follistatin-Like 1 (*Fstl 1*), *Fst*, BMP Binding Endothelial Regulator

(*Bmper*), Tsukushi, Small Leucine Rich Proteoglycan (*Tsku*) and BMP and Activin Membrane-Bound Inhibitor (*Bambi*) was upregulated in 66cl4 as compared to 67NR in either cell line or primary tumor or both (**Table 4.3**). *Grem1* on the other hand did show upregulation in 66cl4 as compared to 67NR but was not significant. It was however interesting to see there was practically no expression in the 67NR cell line since *Grem1* has been shown to be overexpressed in various forms of cancer such cervix, ovary, lung, kidney, colon , pancreases and breast (86,87). Due to *Fstl 1, Fst, Bmper, Tsku, Bambi* and *Grem1* upregulation in 66cl4 as compared to 67NR as seen in *Bmp4* above, their significance in breast cancer patient survival outcome was important to be analyzed.

4.1.5 GREM1 correlation with Breast cancer prognosis

FSTL1, FST, BMPER, TSKU, BAMBI and GREM1 clinical relevance was checked by obtaining a prognosis curve for breast cancer patients (n=4142) using KM plotter (112) and BreastMark(99). With the exception of GREM1, the remaining showed no significant correlation with prognosis ($p>0.05$) (**Appendix V**). GREM1 with the Affymetrix ID-218468 showed a significant correlation between high GREM1 mRNA expression and poor OS with HR= 1.4(1.1-1.78) and p=0.0054 (**Figure 4.3**). This correlation extended to RFS, DMFS and PPS with HR 1.35(1.21-1.52), $p=1.7e^{-07}$; HR 1.52(1.25-1.87), $p=3.8e^{-05}$and HR 1.43(1.1-1.85), p=0.0068 respectively.

BreastMark showed that GREM1 high expression was correlated with poor prognosis for basal subtype breast cancer and lymph node negative patients (**Figure 4.4**). GREM1 expression for whole cancer, luminal A, luminal B, lymph node positive patients and Her2 showed no correlation with clinical outcomes (**Appendix IV**). GREM1 being highly expressed in 66cl4 and also its high expression being correlated with poor prognosis of breast cancer patients might suggest that it plays a significant role in metastasis. This is because 66cl4 is a metastatic cell line and metastasis of breast cancer has been associated with most death of breast cancer patients (4,5).

Table 4.3: Transcriptome analysis showing comparison of 66cl4 and 67NR mRNA expression of Bmp antagonist family.

Where Log_2 = Log2(66cl4 /67NR). This indicates the differential expression between 66cl4 and 67NR of either the cell line or tumor. A positive number indicates higher expression in 66cl4 whiles a negative number indicated higher expression in 67NR. p-value= p-value from t-test of the comparison of 66cl4 and 67NR in the cell lines or tumor.

	Comparison of cell lines				Comparison of primary tumors			
Gene	**66cl4**	**67NR**	**Log_2**	**p-value**	**66cl4**	**67NR**	**Log_2**	**p-value**
Cer1	0.0	0.0	0.00	1.0	0.0	0.1	-2.93	1.0
Dand5 (coco)	2.2	3.7	-0.74	0.0001	3.6	3.4	0.07	0.8716
Nbl1 (DAN)	0.1	0.2	-0.72	0.0667	2.5	1.6	0.67	0.0736
Grem1	15.5	0.0	11.91	0.1969	6.1	0.0	9.05	0.0958
Grem2	0.0	0.0	-0.20	1.0	0.1	0.3	-1.30	0.0670
Sost	0.0	0.0	0.00	1.0	0.0	0.0	0.00	1.0
Sostdc1	0.0	0.0	0.00	1.0	0.0	0.0	-2.03	1.0
Chrd	0.0	0.1	-3.40	1.0	0.0	0.4	-2.96	0.0644
Chrdl1	0.0	0.0	1.18	1.0	0.2	0.1	0.92	1.0
Chrdl2	0.0	0.0	1.14	1.0	0.0	0.0	-1.00	1.0
Nog	0.0	0.0	0.00	1.0	0.0	0.0	-0.41	1.0
Twsg1	18.0	26.5	-0.55	0.0001	35.0	47.9	-0.45	0.0016
Bambi	0.5	0.0	5.77	0.0001	0.9	0.3	1.52	0.0002
Bambi-ps1	0.0	0.0	0.00	1.0	2.4	1.4	0.75	0.0899
Fst	1.8	0.1	5.01	0.0001	5.3	0.3	4.33	0.0002
Fstl1	4.9	0.1	6.30	0.0001	50.8	9.7	2.39	0.0002
Fstl3	1.0	1.7	-0.73	0.7434	0.0	0.0	0.00	1.0
Fstl4	0.0	0.0	1.34	1.0	0.0	0.0	0.23	1.0
Fstl5	0.0	0.0	0.61	1.0	0.0	0.0	3.37	1.0
Bmper	13.8	7.6	0.86	0.0001	6.1	1.7	1.86	0.0002
Tdgf1	0.0	0.0	0.00	1.0	0.0	0.0	0.04	1.0000
Dcn	0.0	0.0	-0.62	1.0	11.3	34.5	-1.61	0.0002
Rgmb	7.9	11.6	-0.56	0.0001	39.4	19.1	1.05	0.0002
Nodal	0.0	0.0	0.00	1.0	0.0	0.0	1.84	1.0
Lefty1	0.0	0.0	-1.12	1.0	0.8	0.6	0.36	0.5334
Kcp	0.0	0.0	2.76	1.0	0.1	0.0	0.22	1.0
Crim1	21.3	16.5	0.37	0.0580	12.5	12.5	0.00	0.9909
Vwc2	0.0	0.0	0.00	1.0	0.0	0.0	-0.23	1.0
Vwc2l	0.0	0.0	0.00	1.0	0.0	0.0	3.51	1.0
Tbx1	0.0	0.0	0.00	1.0	0.0	0.0	1.15	1.0
Tll1	0.0	0.0	2.87	1.0	0.6	0.4	0.71	0.0882
Wisp3	0.0	0.0	-0.15	1.0	0.1	0.0	1.62	1.0
Tob1	11.3	23.6	-1.06	0.0001	12.7	22.1	-0.80	0.0002
Tsku	9.4	6.9	0.44	0.0010	7.5	7.2	0.06	0.7947

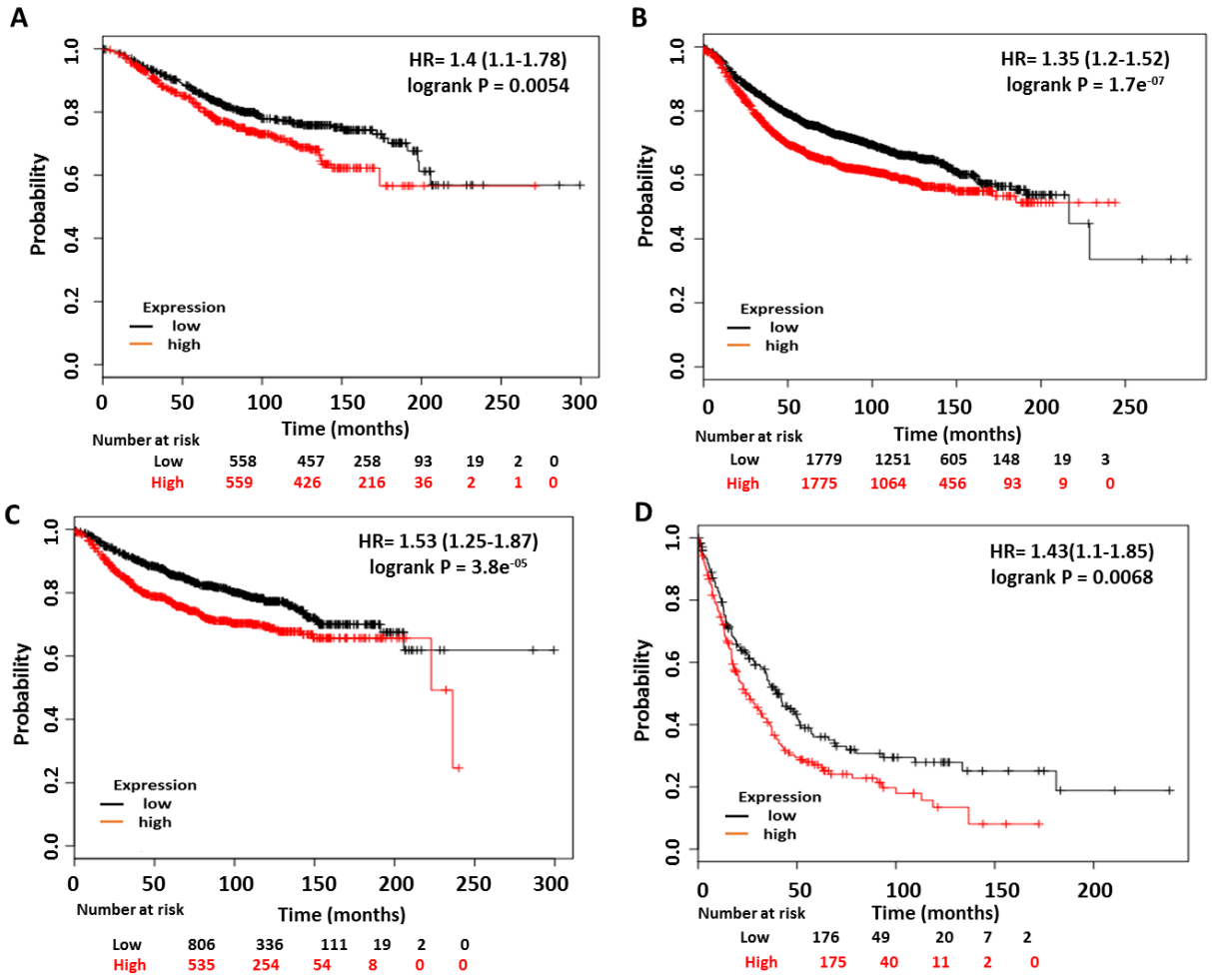

Figure 4.3: Kaplan – Meier survival curve correlates highly expressed GREM1 with poor prognosis
Kaplan – Meier (KM) survival curve of breast cancer patients stratified by their expression level of GREM1 showing prognosis in breast cancer for ***A.*** *Overall Survival (OS),* ***B.*** *Relapse Free Survival (RFS),* ***C.*** *Distant Metastasis Free Survival(DMFS) and* ***D.*** *Post Progression Survival (PPS). The breast cancer was classified into low (Black) or high (red) expression groups based on whether the expression of Grem1 was greater than the median expression of Grem1. The p-value obtained from log-rank tests by comparison of the two KM curves is shown on the top right corner of the plot together with Hazard Ratio (HR) with 95% confidence intervals. The total number of patients with available clinical data was: OS, n=1117; RFS, n=3557 DMFS, n=1610; and PPS, n=351.*

BMP4 and its antagonist GREM1 being highly expressed in the metastatic 66cl4 as compared to the non-metastatic 67NR together with their correlation to breast cancer prognosis, lead this study to focus on these parameters. mRNA expression that was seen in transcriptome data for 66cl4 and 67NR cell lines may not necessarily be portrayed on the protein level (113,114). We therefore decided to check the expression of BMP4 and GREM1 on a protein level for the 4T1 breast cancer model cell lines.

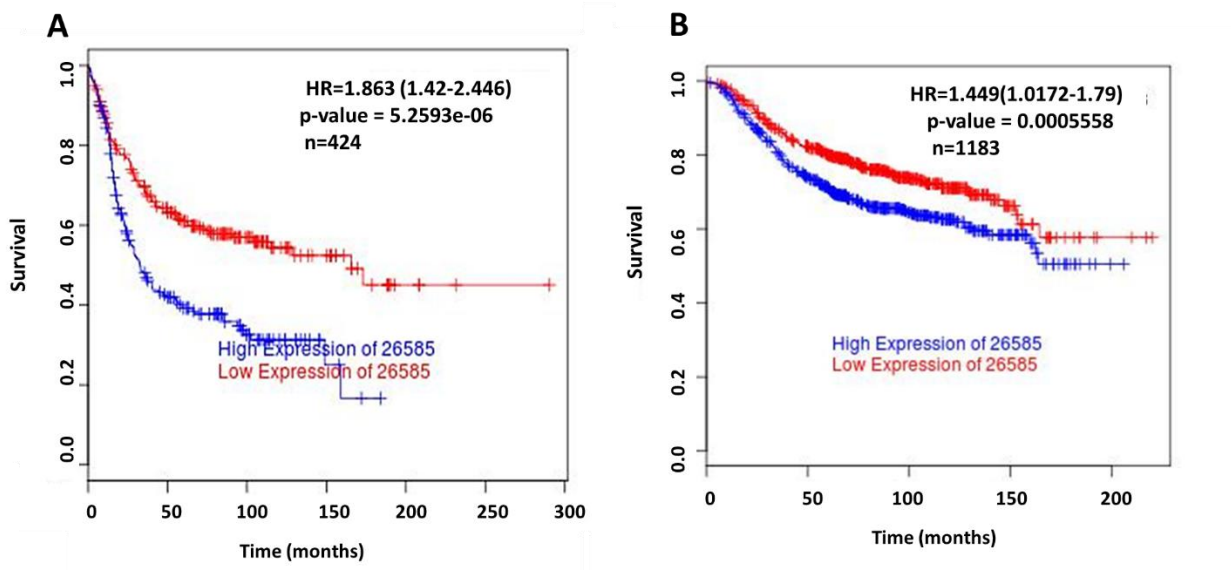

Figure 4.4: BreastMark survival curve correlates GREM1 high expression with poor prognosis
BreastMark survival curve for breast cancer patients stratified by their expression level of BMP4 showing prognosis in breast cancer for ***A.*** *Basal subtype* ***B.*** *lymph node negative patient. The breast cancer was classified into low (Red) or high (blue) expression groups based on whether the expression of GREM1 was greater than the median expression of GREM1. The p-value is shown on the top right corner of the plot together with Hazard Ratio (HR) with 95% confidence intervals and number of patients involved. The cutoff point was (HR > 1.2 and HR < 0.83). HR > 1.2 and a p-value <0.05% is associated with poor clinical outcome whiles HR < 0.83 and a p-value <0.05% is associated with good prognosis with regards to high expression of GREM1.*

4.2 BMP4 AND GREM1 ARE EXPRESSED IN VARYING AMOUNT BY THE 4T1 BREAST CANCER CELL LINES.

We investigated the five cell lines (67NR, 168FARN,4T07, 66cl4 and 4T1) of the 4T1 breast cancer model for their BMP4 and GREM1 protein level via immunoblotting. This showed that the micrometastatic cell line 168FARN and the second most aggressive metastatic cell line 66cl4 produce GREM1.The 168FARN cell lines producing the highest amount however was not significantly different ($p \geq 0.05$) from the non-metastatic 67NR (**Figure 4.5 A and B**). Having the knowledge that GREM1 exists both as cell – associated and secreted form (81,82), we treated the cells with protein transport inhibitor (PTI) to observe if the intracellular levels of GREM1 will change. There was an upsurge of GREM1 level in both 66cl4 and 168FARN observed that was significantly different from each other and from the non-metastatic 67NR ($p<0.05$). The secretion of GREM1 of the five cell lines of the 4T1 breast cancer model was further verified by ELISA. The same pattern of GREM1 activities as seen in the immunoblotting was seen in the supernatant of the cells analyzed with ELISA **(Figure 4.5 C**). 67NR, 4T07 and 4T1 showed no secretion of

GREM1 whiles 66cl4 and 168FARN secreted GREM1 with 168FARN being the highest between them ($p<0.05$).

BMP4 on the other hand was only observed in the 66cl4 cell line which increased with PTI treatment (**Figure 4.5 D**). In comparison with the non-metastatic cell lines, it was significantly different $p<0.05$ with and without PTI treatment respectively. The PTI treatment increasing BMP4 in 66cl4 was a confirmation that BMP4 is secreted (63). To further verify secretion of BMP4 in 66cl4, ELISA for BMP4 detection was attempted but failed to work. From the observations, we can conclude that the protein level of BMP4 and GREM1 with regards to 66cl4 and 67NR was a correlation to the mRNA expression seen in the transcriptome data with 66cl4 having higher expression than 67NR.

Tumor cells and their microenvironment exist in an interaction network that aids in the various stages of cancer (30). Also, it is known that cytokine- mediated crosstalk between CAFs and tumor cells influences all aspects of tumor stages (29,31). Thus, it was important to study the interplay of BMP4 and GREM1 between fibroblast and the 4TI breast cancer model cell lines.

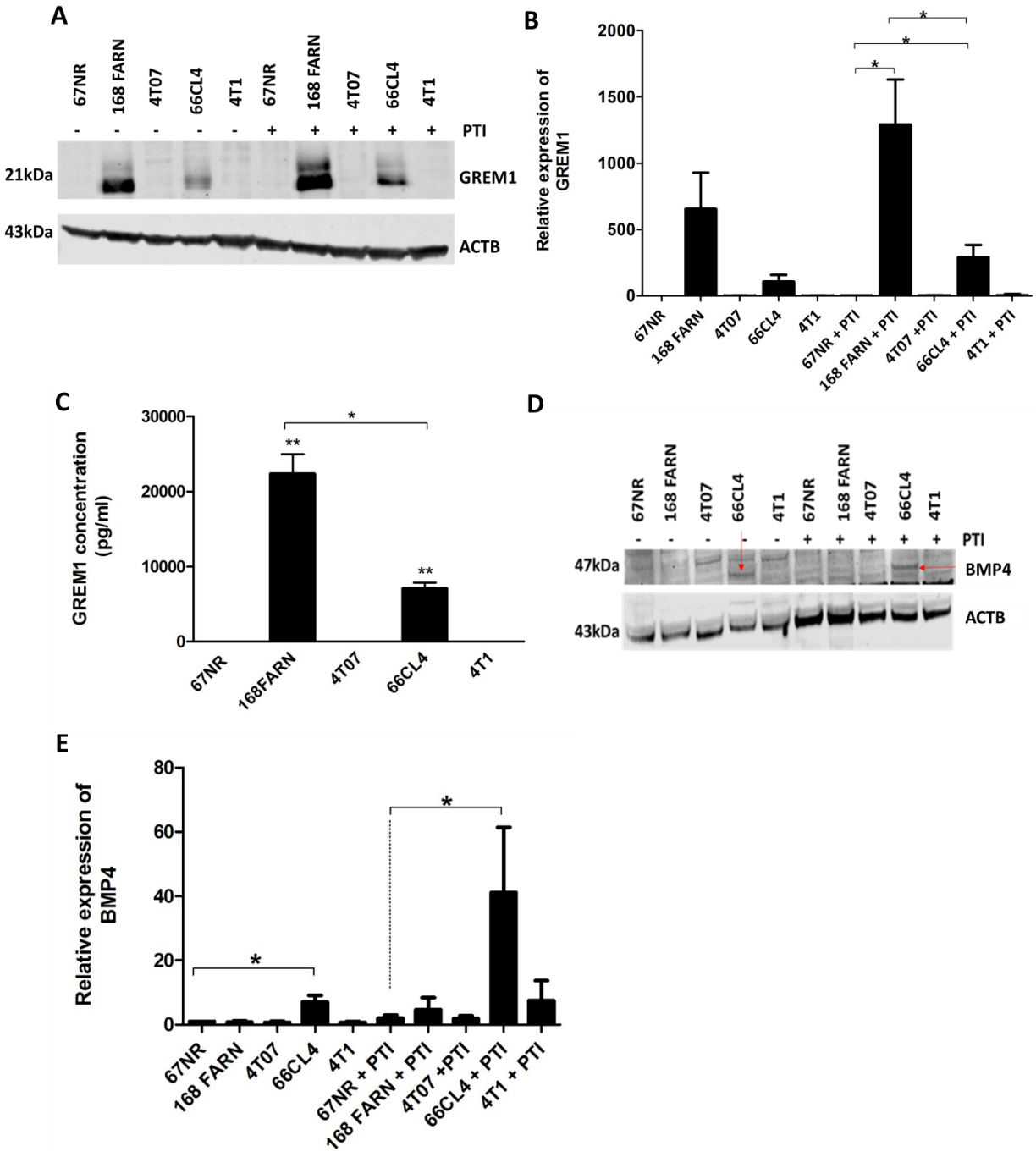

Figure 4.5 BMP4 and GREM1 are expressed by the five cell lines of the 4T1 breast cancer model at varying amount on protein level

A. *Immunoblot analysis of GREM1 protein level for the five cell lines of the 4T1model. The cells were seeded with and without treatment with protein transport inhibitor for 6hrs. The data represents one blot out of three independent experiments carried out.* ***B.*** *Relative level of GREM1 when "**A**" is normalize with β-actin and 67NR set at 1.* ***C.*** *GREM1 ELISA for Supernatant from the five cell lines.* ***D)*** *Immunoblot of Bmp4 protein level for the five cell lines with the relative expression of Bmp4 obtained via normalizing with β-actin* ***(E)****. All results are mean ± SEM. from 3 independent experiment. All p-value were obtained via student t-test. *p≤0.05 and ** p≤0.01.*

4.3 ESTABLISING OPTIMUM CONDIITONS FOR RmBMP4 and RmGREM1 ON MEF

We aimed to verify if BMP4 and GREM1 interaction studies can be achieved with MEF. Various concentration of rmBMP4 and rmGREM1 was treated on MEF to find optimum response. Kinetic profiles were also checked.

4.3.1 Mouse Embryonic Fibroblasts (MEF) respond to recombinant mouse BMP4

GREM1 and BMP4 interaction in the tumor stoma environment with respect to 5 cell line 4T1 breast cancer model was aimed to be studied. Fibroblast was the primary focus for stroma cells. Mouse Embryonic Fibroblast (MEF), Lung Fibroblast and Skin Fibroblast were the types of fibroblast used in the study. Fibroblasts were selected as interesting stroma cells because it is the most prominent cell type in the tumor microenvironment and fibroblasts have been used to establish assays to study Bmp activities (35,115). Also, presence of fibroblasts has been associated with tumor progression and metastasis (31,33,39).

We firstly investigated the ability of MEFs to respond to rmBMP4. The responsiveness of rmBMP4 following stimulation of MEFs for 1hr was identified by p-SMAD 1/5/9 on Western blot **(Figure 4.6A**) as BMP4 signaling activation at protein level is measured by Smad 1/ 5 / 8 phosphorylation (77,115). Results obtained showed that that MEFs were responsive to rmBMP4 as shown by the strong detection of the 60kDa p-SMAD 1/5/9 protein bands. RmBMP4 dose response curve was then generated from the signal of the p-SMAD 1/5/9 protein bands.

The rmBMP4 dose response graph showed an increase in p-SMAD 1/5/9 level from 0-1ng/ml which then rose steadily (**Figure 4.6B**). A steady increase with concentration up to 10ng/ml was observed, therefore 5ng/ml was chosen for further experiments. The difference between the response of absence and presence of rmBMP4 stimulant implies that we have established a scope to attempt inhibition of BMP4 activity with GREM1.

Deciding on 5ng/ml concentration of rmBMP4, the kinetic profile of its stimulation was tested. RmBMP4 induced highest phosphorylation of SMAD1/5/9 from 0.5hr which gradually decreased until 24hrs (**Figure 4.6C and 4.6D**). It can therefore be inferred that rmBMP4 has a stimulus – response lag time between 0.5hr -1hr. It is however important to note that this conclusion is based on the minimal set response time 0.5hr used in the experiment since it could be below 0.5hr. The results were consistent with other studies that used measuring of SMAD1/5/9 phosphorylation as a form of detecting BMP activation showing a BMP stimulus- response lag time between 0.5hr–

1hr (116,117). After establishing BMP4 response in MEF, the next step was to access whether that response could be antagonized by rmGREM1.

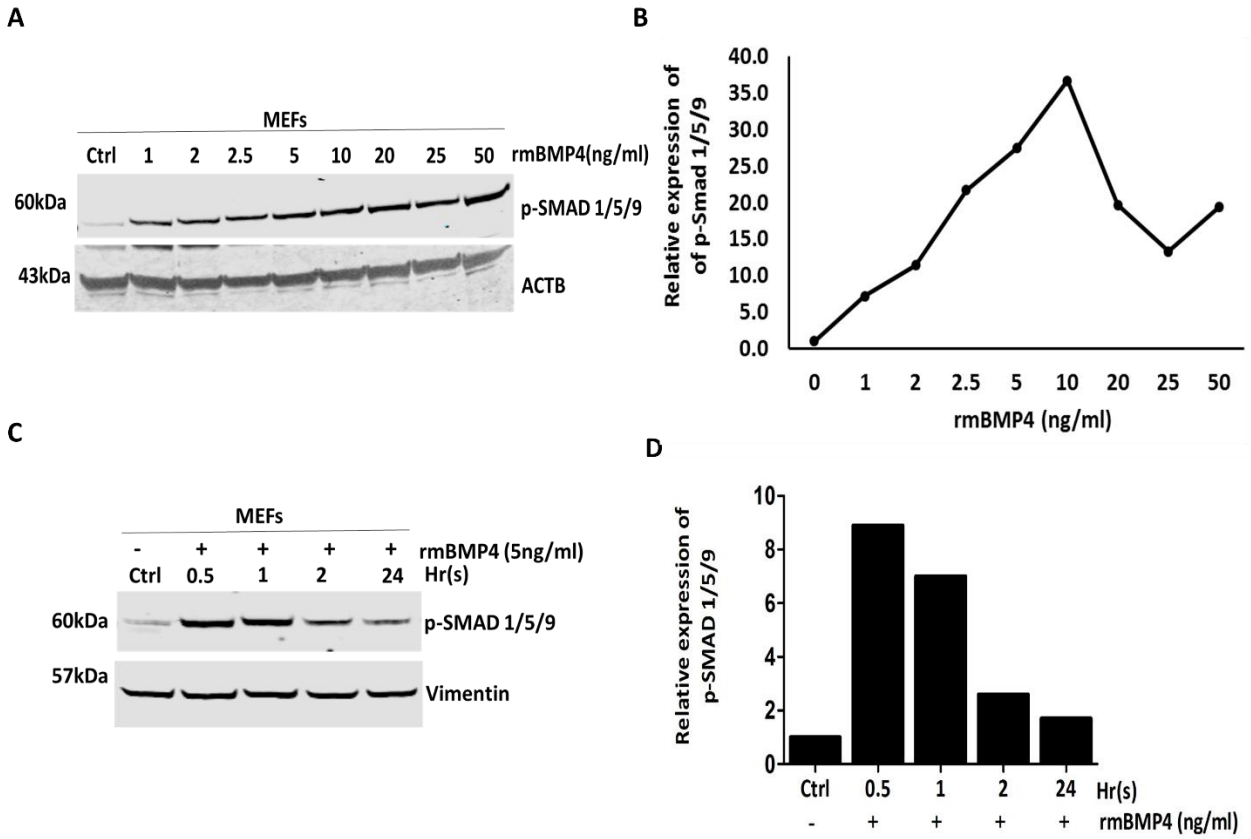

Figure 4.6 MEFs displays a transiently elevated p-SMAD 1/5/9 signal in response to rmBMP4
MEFs were treated for 1hr at 37 °C with different concentration of rmBmp4 and harvested. ***A)*** *Immunoblot detection of p-SMAD1/5/9 at 60 kDa to determine activation of Bmp4 was achieved using a polyclonal p-SMAD1/5/9 primary antibody* ***B)*** *Relative level of p-SMAD1/5/9 when "**A**" is normalize with β-actin and Ctrl set at 1. (**A**).* ***C)*** *Immunoblot detection of kinetic profiles of rmBMP4 (5ng/ml) induction of SMAD 1/5/9 phosphorylation on MEFs.* ***D****) Relative level of p-SMAD1/5/9 when "**C**" is normalize with vimentin with Ctrl set at 1.*

4.3.2 Recombinant mouse Grem1 can inhibit responses of recombinant mouse Bmp4 in MEFs

GREM1 is an extracellular antagonist that inhibits BMP4 signaling by preventing BMP4- BMP4 receptor binding (69,74). After observing the rmBMP4 response in MEFs, we further investigated rmGREM1 ability to antagonize the Bmp4 mediated phosphorylation of Smad 1/5/9 in the MEFs and with the corresponding dosage requirements. To achieve this, we treated the MEFs with different concentration of rmGREM1 for 1hour after which 5ng/ml recombinant Bmp4 was added for 30mins at 37 °C. We observed that 250ng/ml of GREM1 was enough to antagonize 5ng/ml rmBMP4 since it was equivalent to the activity of the control (**Figure 4.7 A and B**). The dosage of rmGREM1 required to antagonized 5ng/ml rmBMP4 activation

response on MEF was equivalent to 50 folds of 5ng/ml rmBMP4. We also validated the kinetic profile of rmGREM1 in antagonizing the rmBMP4. It was observed that the intensity of the bands decreased during the first 30min, however, it was equivalent to the control basal level within 1hr and completely disappeared at 6hrs (**Figure 4.7 C and D**). This was similar to a study that determined the half- life of cell associated GREM1 to be about 1hr and secreted form to be detectable for up to 4-5hrs (81). We could also see that rmGREM1 had some effect on the MEFs when compared with untreated MEFs. The level of p-SMAD 1/5/9 decreased in a time related manner when rmGREM1 alone was treated on MEF. This was indicative of the fact that MEF might express factors that activate p-SMAD 1/5/9 and which were inhibited by the rmGREM1.

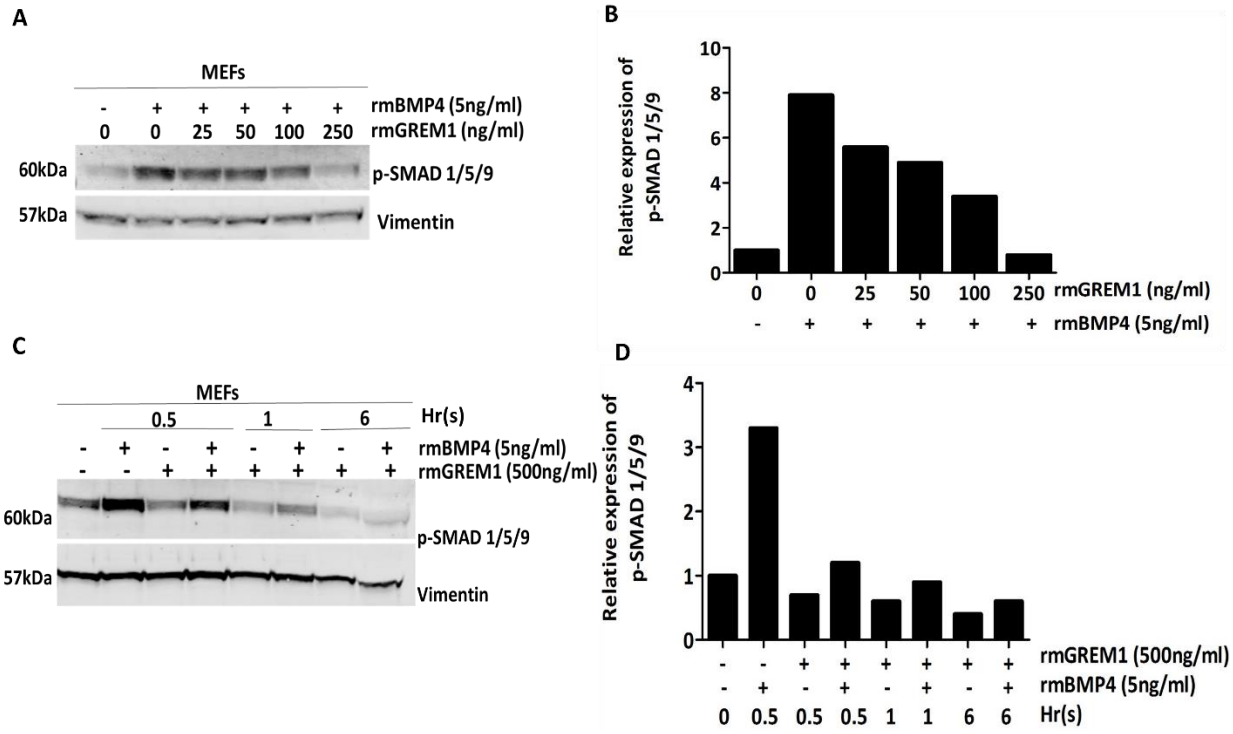

Figure 4.7: Recombinant Gremlin1 antagonizes Bmp4 response in MEF

To antagonize the Bmp4 activation on MEFs, rmGREM1 of different concentration was added to the MEFs cell cultures for 1hr hour at 37 °C, followed by Bmp4 for 30min after which cells were harvested. ***A)*** *Immunoblot detection of how much Grem1 is required to antagonize 5ng/ml Bmp4 which was normalized to loading control – vimentin* ***(B)****. The kinetic profile of the Grem1 required to antagonized 5ng/ml was also established via Immunoblot* ***(C)*** *and normalized to vimentin* ***(D).***

MEF responding to rmBMP4 by induction of p-SMAD 1/5/9 that was able to be antagonized by rmGREM1indicated BMP4 and GREM1 interaction studies can be achieved with MEF. We have also observed BMP4 and GREM1 expression in 168FARN and 66cl4 on protein level. It was therefore important to establish whether the BMP4 and GREM1 expressed by the tumors interaction will be seen on MEF.

4.4 EVALUATION OF PARACRINE COMMUNICATION BETWEEN 4T1 BREAST CANCER CELL LINES AND MEF

We aimed at studying the interplays between 4T1 breast cancer cell lines and MEF.

4.4.1 67NR, 168FARN and 66cl4 of the 4T1 breast cancer model secrete soluble mediators that activate SMAD 1/5 signaling in MEF

In order to determine if BMP4 produced by the tumor cell lines response will be seen in MEF, 100% CM from all the five cell lines of the 4T1 breast cancer model were treated on MEF for 1hr using MEF CM as control. SMAD 1/5/9 activations were then checked. Detection of the 60kDa band of the p-SMAD 1/5/9 band showed that 66cl4 CM on MEF had the highest p-SMAD 1/5/9 signaling however, 67NR CM and 168FARN CM on MEF also activated SMAD 1/5/9 signaling above the control MEF CM set to 1 (**Figure 4.8 A and B**). Even though we can say that both 67NR and 168FARN do not express Bmp4 at protein level (**Figure 4.5 D and E**) and mRNA level (**Table 1.2**) for 67NR, the activated p-SMAD1/5/9 with their CM treatment on MEF is an indication of other secreted parameters that signal through Smad 1/5/9.

4T07 and 4T1 CM on MEF on the other hand had levels of p-SMAD 1/5/9 that were below MEF which was the control with 4T07 CM on MEF difference being significant ($p<0.05$) This might be as a result of 4T07 and 4T1 not secreting factors into their CM that enables p-SMAD 1/5/9 activations. It is however important to note that 4T07 CM and 4T1 CM being below the control MEF CM might be an indication that MEF secret soluble mediators that activates a higher level of SMAD 1/5/9 pathway than 4T07 and 4T1.

67NR and 66cl4 were also cultured in transwell with MEF to check if SMAD1/5/9 activation will be observed. In transwell, the cells will share their medium but be separated from each other, so that secreted factors can reach both cell types. MEF induction of p-SMAD 1/5/9 was increased in transwell with 67NR and 66cl4 as compared to MEF monoculture (**Figure 4.8 C and D**). The induction of the p-SMAD 1/5/9 was however higher with 66cl4 transwell culture as compared to the 67NR transwell culture. We cannot make much conclusion since this experiment was done once. However, what is currently observed is an indication that the tumor cells might produce soluble mediators that activates p-SMAD 1/5/9 in MEFs.

In conclusion, the results suggest that CM from 67NR, 168FARN and 66cl4 contains soluble mediators that activate p-SMAD 1/5/9 whiles CM from 4T07 and 4T1 seems not to contain SMAD

1/5/9 activation mediators but rather antagonizes p-SMAD 1/5/9 soluble mediators. Bearing also in mind that GREM1 was expressed and secreted on a protein level in 168FARN and 66cl4, we hypothesized that 168FARN, 4T07, 66cl4 and 4TI has the ability to secrete soluble proteins that have BMP4 antagonistic property Thus, we decided to verify the tumor cell lines ability to secret soluble mediators that antagonize p-SMAD 1/5/9 in MEFs.

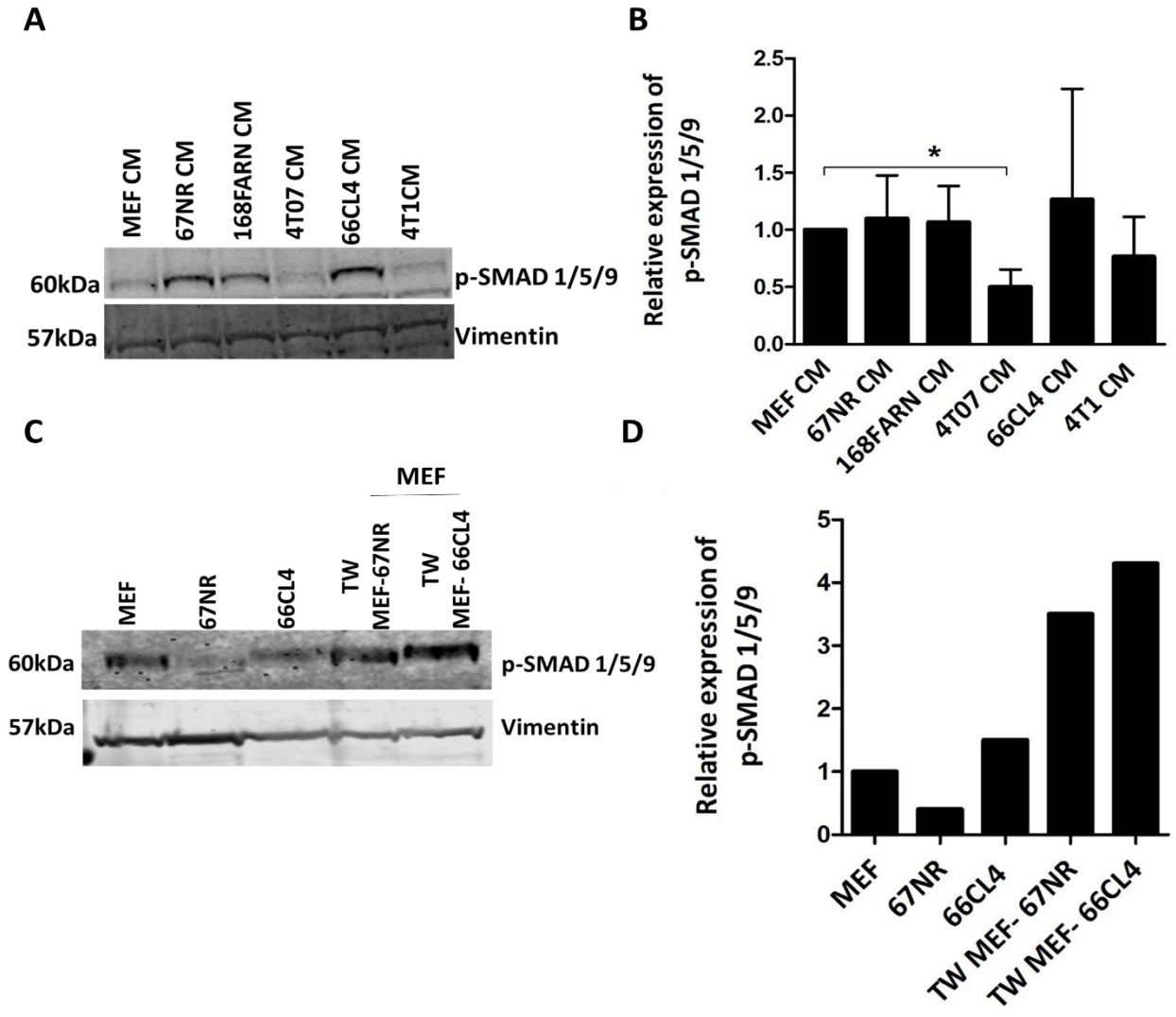

Figure 4.8: Soluble protein secreted by 67NR, 168FARN and 66cl4 of the 4T1 breast cancer model induces SMAD 1/5/9 phosphorylation

*For upper panel **A and B,** CM from 67NR, 168FARN, 4T07, 66cl4 and 4T1 were treated on MEFs for 1hr **A)** Immunoblot detection of p-SMAD1/5/9 with vimentin as loading control **B)** Relative level of p-SMAD1/5/9 when "**A**" is normalize with vimentin and MEFCM set at 1. The results represent three independent experiments displayed as mean ± SEM which was statistically tested by student t-test(*p<0.05). "**A**" is a representative of the blots of three experiment. **C)** Immunoblot detection of p-SMAD 1/5/9 of MEFs grown in monoculture and in transwell with 67NR and 66cl4. Vimentin was used as loading*

*control. **D**) Relative expression of "**C**" when normalize with vimentin and MEF set to 1 **C and D** were carried out once.*

4.4.2 168FARN antagonizes phosphorylated SMAD 1/5/9 signaling in MEF

To test the 4T1 breast cancer model cell lines ability to antagonize p-SMAD 1/5/9 activations, condition medium of the cell lines was harvest, treated on MEFs for 1hr followed by treatment with 1ng/ml rmBMP4 for 30mins at 37°C. MEFs were then harvested with 8M Urea lysis buffer and the lysates analyzed with immunoblotting. The results showed that CM of 168FARN, 66cl4 and 4T1 were able to antagonize the p-SMAD 1/5/9 signaling in MEF to some degree with 168FARN taking it completely down to the basal level of the control (**Figure 4.9 A and B**). CM of 168FARN and 66cl4 cell lines was expected as we have shown that they express and secrete GREM1 on a protein level (**Figure 4.5 A-C**). CM from 4T1 cell line per the data obtained was expected to behave like 67NR CM and 4T07 CM since they did not express GREM1. We can therefore suggest that 4T1 expresses another antagonist of p-SMAD 1/5/9. Furthermore, it was interesting to see some form of activation of p-SMAD 1/5/9 on MEFs that had not received any treatment. We therefore decided to check our genes of focus BMP4 and GREM1 expression on a protein level in MEFs.

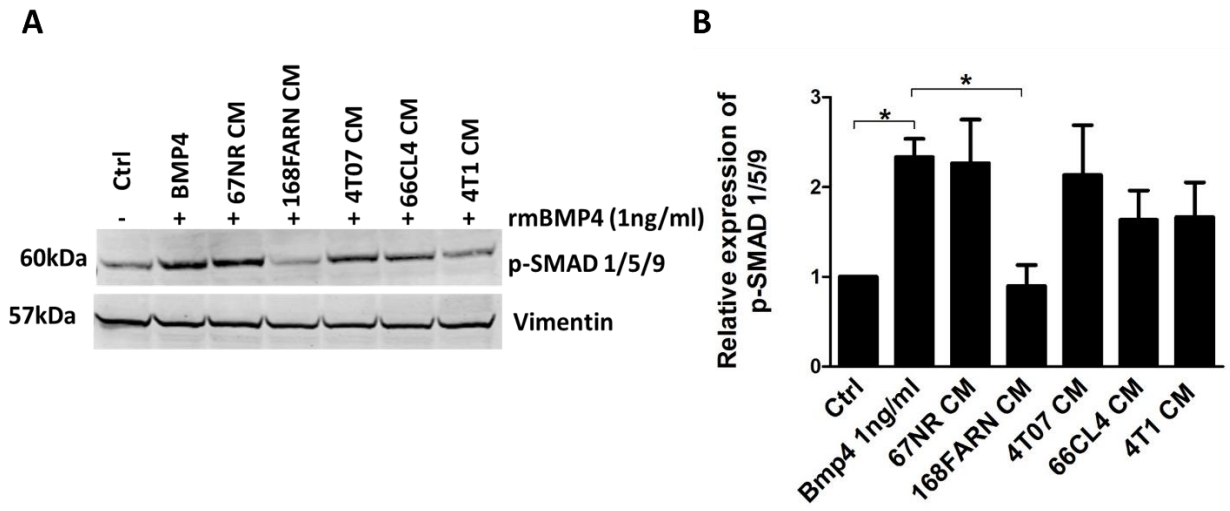

Figure 4.9:168FARN, 66cl4 and 4T1 secretes mediators that antagonizes SMAD 1/5/9 phosphorylation in MEF
*Condition medium (CM) from 67NR, 168FARN, 4T07, 66cl4 and 4T1 were harvested and then treated on MEFs for 1hr followed by rmBMP4(5ng/ml) treatment for 30mins.**A)** Immunoblot detection of p-SMAD 1/5/9 using Vimentin as loading control. This is a representative blot out of three independent experiments*

*done. **B**) Relative expression of "**A**" when normalized with vimentin. The results are mean ± SEM and p-values were obtained via student t-test(*p<0.05).*

4.4.3 MEF expressed BMP4 and GREM1 on protein level

BMP4 and GREM1 have been shown to be expressed in stroma cells (120,121), hence we sought to examine whether MEF expressed BMP4 and GREM1. The results showed that MEF expressed on a protein level both BMP4 and GREM1which was increased with protein transport inhibitor treatment (**Figure 4.10 A-D**). The increment is an indication that the intracellular secretion or transport pathway of the BMP4 and GREM1 has been inhibited thereby accumulating them in the Golgi apparatus or the lumen of the endoplasmic reticulum (122). The co-expression of BMP4 and GREM1 may be suggestive of the importance of BMP4 mediation and regulation by GREM1.

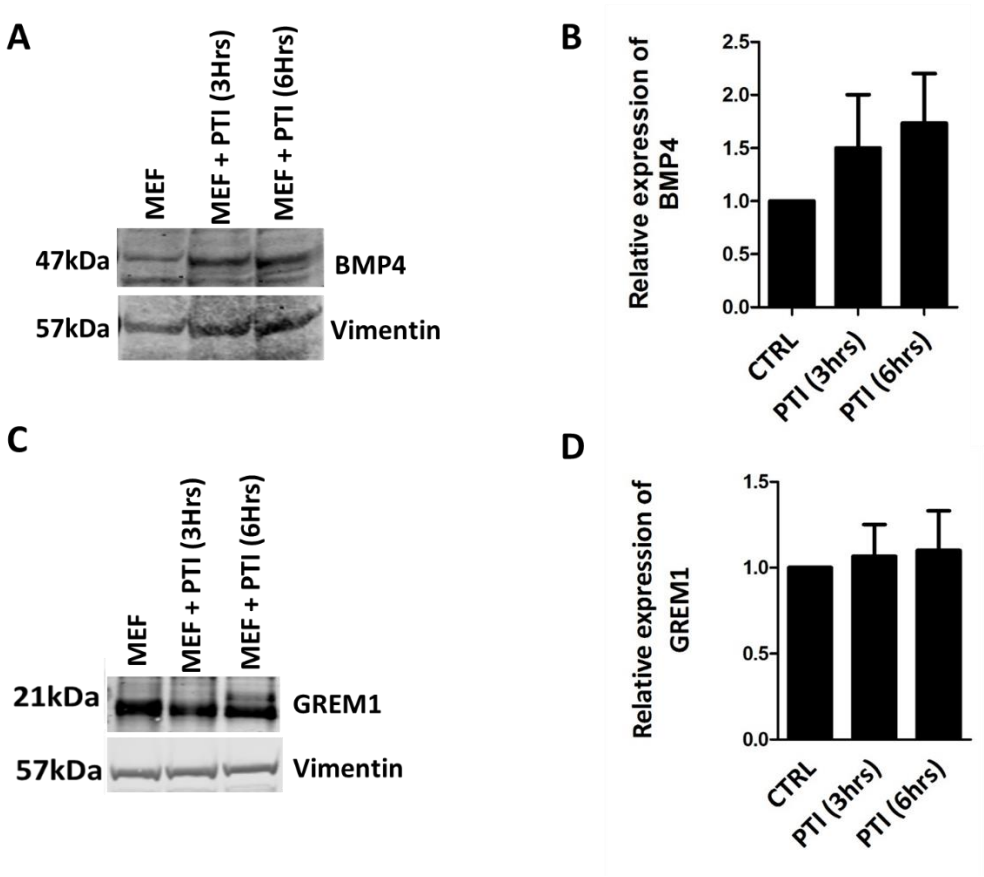

Figure 4.10: MEF expresses BMP4 and GREM1 on a protein level

*MEFs cell were cultured with and without protein transport inhibitor for 3hrs and 6hrs and harvested. BMP4 and GREM1 protein levels were then analyzed. **A)** Immunoblot detection of MEF BMP4 level at 47 kDa using a monoclonal primary BMP4 antibody. (**B**) BMP4 relative expression from "A" normalized to Vimentin. **C**) Immunoblot detection of GREM1 expression in MEF using a polyclonal GREM1 primary antibody and Vimentin as loading control **D**) Relative expression of "C" when normalized to Vimentin.*

Interaction in the tumor microenvironment is a two-way communication by tumor mediators having effects on stroma and vice versa. Since we had treated MEF with CM from the tumor cell lines upon detection of BMP4 to check if its response will be seen in MEF, we decided to also treat the tumor cell lines with MEF CM upon subsequent BMP4 detection to see its effect.

4.4.4 MEF CM enhanced activation of SMAD1/5/9 signaling in 67NR and 4T07 of the 4T1 breast cancer cell lines via secreted mediators

Having seen expression of BMP4 in MEF which is a secreted protein, we investigated the ability of the BMP4 secreted into MEF CM to activate p-SMAD 1/5 signaling on the 4T1 breast cancer model cell lines. The results showed that MEF CM had a tendency to increase phosphorylation of SMAD 1/5/9 in 67NR and 4T07 whiles 168FARN, 66cl4 and 4T1 cell lines showed no effect (**Figure 4.11 A and B**). The increase in phosphorylation of SMAD 1/5/9 could not only be associated to BMP4 production but also to other ligands that signal through SMAD 1/5/9. The results however showing no increased activation in 168FARN and 66cl4 might be due to their expression of GREM1 (**Figure 4.5**) and other parameters antagonizing the soluble mediators secreted into the MEF CM. 4T1 cell line on the other hand showing antagonizing ability to p-SMAD 1/5/9 might be attributed to another antagonist other than GREM1.

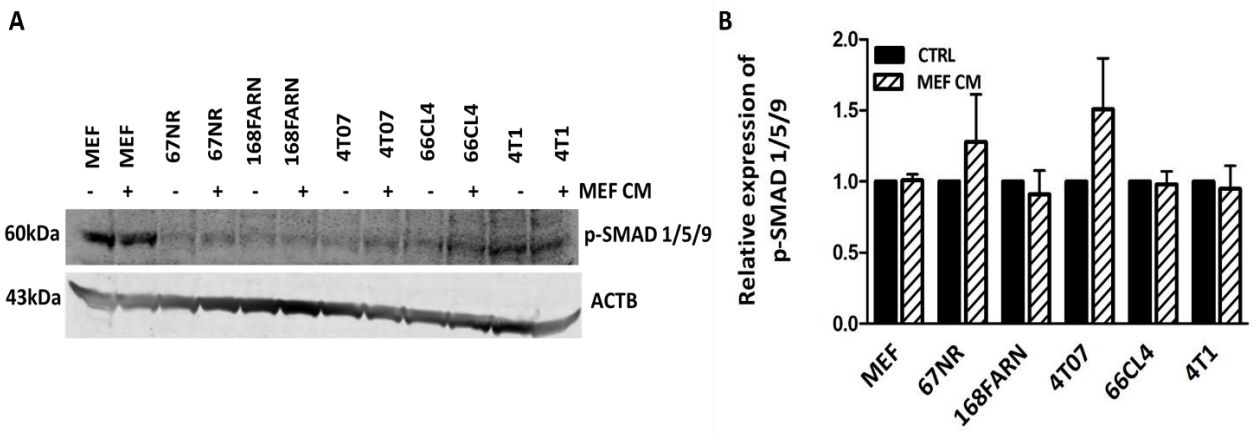

Figure 4.11: MEFs secrets soluble mediators that enhances activation of SMAD 1/5/9 in 67NR and 4T07 cell lines.
MEF CM was treated on the 5 cell lines of the 4T1 breast cancer model for 1hr. Control was established by treating MEF with its own CM. ***A)*** *Immunoblot detection of p-SMAD 1/5/9 antibodies with ATCB as a loading control.* ***B)*** *Relative expression of "A" when normalized with the loading control.*

To mimic the tumor microenvironment of the expression and production of the BMP4 antagonist GREM1 by the tumor cells and MEFs, transwell culture was done.

4.4.5 Transwell culture of tumor cells and MEF enhances their ability to secrete GREM1

Tumor cells recruit fibroblasts to create a conducive environment which enables them to accomplish tumorigenesis and metastasis. To mimic the microenvironment that exhibit two-way communication, and to explore the crosstalk between the fibroblast and the tumor cells, a co-culture study in a transwell system was performed. The tumor cells were seeded in the upper chamber of the transwell whiles MEFs were seeded at the bottom. Both the tumors and the MEFs were harvested, immunoblotted and probed with GREM1 antibody. In the transwell, we observed an increase of GREM1 in all the MEFs compared to their monoculture and the control in transwell which comprised of MEF on both top and bottom (**Figure 4.12)**. This indicated that paracrine communication with the tumor cells triggers MEFs to produce more GREM1. The tumors on the other hand showed increment of GREM1 in 67NR, 168FARN and 66cl4 with 168FARN having about four-fold increase. 4T07 cell lines in transwell cannot however be commented on since there was some form of DNA issue hence might not be a true reflection. This experiment was done only once and will be interesting to repeat to determine if this is a robust and reproducible finding.

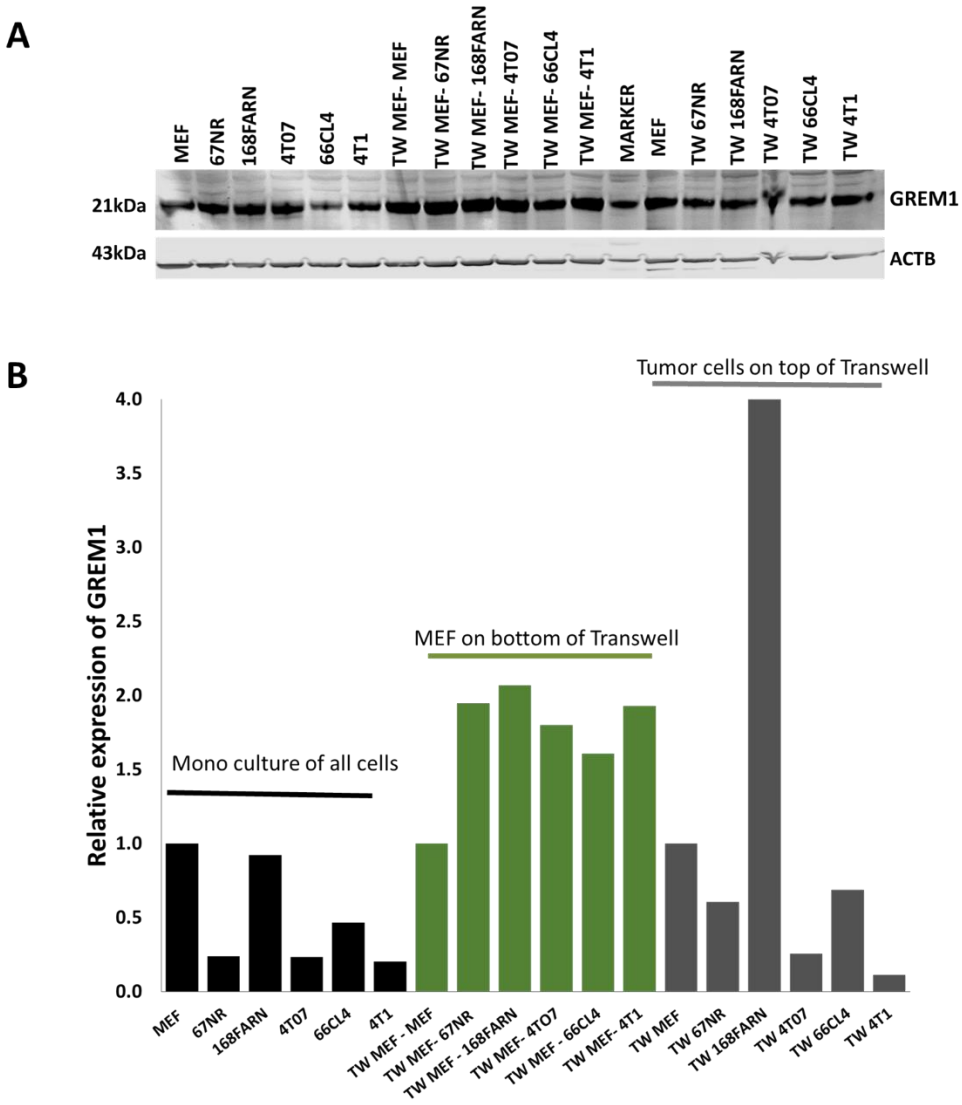

Figure 4. 12: GREM1 expression are increased in transwell culture of MEF and tumor cells/
A) *The five cell lines of the 4T1 breast cancer model was cultured in transwell with MEF for 48hours and both the tumor cells and the MEF were harvested. Each cell in monoculture was also harvest to serve as controls. In transwell, another control was established by growing MEF both on the top and bottom chamber. Immunoblot was run on the lysates and probed with GREM1 antibodies. B-actin was used as a loading control.* ***B)*** *Relative expression of "**A**" when normalized with the loading control.*

The results have shown so far that the five tumor cell lines have different expressions of GREM1 and BMP4. Also, the mRNA data from transcriptome sequencing showed different variations of growth factors and other mediators between the non-metastatic 67NR and metastatic 66cl4. We believe that the differences in metastatic propensity might attribute to the different production of soluble meditators. With regard to fibroblasts, we think the difference in production of soluble

mediation of the tumor cells might have different effects on fibroblast properties such as their activation, migration and proliferation.

4.4.6 MEFs proliferation are influenced by soluble mediators via paracrine crosstalk.

Tumor cells are known to produce stroma-modulating growth factors such as TGF β1,VEGF, PDGF, bFGF that generate a conduction microenvironment through autocrine and paracrine communication (31,32). The soluble mediators secreted by the tumor cells can influence fibroblast properties that aid in tumor progression and metastasis. We therefore hypothesized that the differences in the characteristics of 67NR and 66cl4 cell lines will lead to different production of soluble meditators that vary in effect on fibroblast properties such as proliferation.

To test the hypothesis, we first examined the effects of rmGREM1 and rmBMP4 on fibroblast proliferation. MEFs were cultured in the presence of rmBMP4, rmGREM1 and combination of both for 24 hours. The cell populations of the MEFs were counted using Z1 Beckman counter and then the effects of the various treatments on proliferation were compared. Compared with MEFs that were not treated, those treated with BMP4 showed very minute proliferation increase effect that was not significant ($p>0.005$) (**Figure 4.9A**). The effect increased as the dosage of the rmBMP4 was increased (1 ng/ml and 5 ng/ml). This suggest that a high dosage of rmBMP4 might have had a greater effect. In the presence of GREM1 (250ng/ml) solely, the proliferation rate decreased significantly by half in comparison to the untreated MEF ($p<0.01$) which began to increase when rmGREM1 was combined with rmBMP4. This was an indication that the effect of rmGREM1 was antagonized by BMP4. Morphological changes of the cells were also observed. Fibroblasts that were untreated and/or stimulated by rmBMP4 alone appeared to be more spindle-like when compared with those that were treated with rmGREM1 (**Figure 4.10 A**). The MEFs changed to unnatural circular morphology when treated with rmGREM1 alone which became better when rmGREM1 was in combination with rmBMP4. The circular morphology suggests that rmGREM1 might have caused the MEF to die.

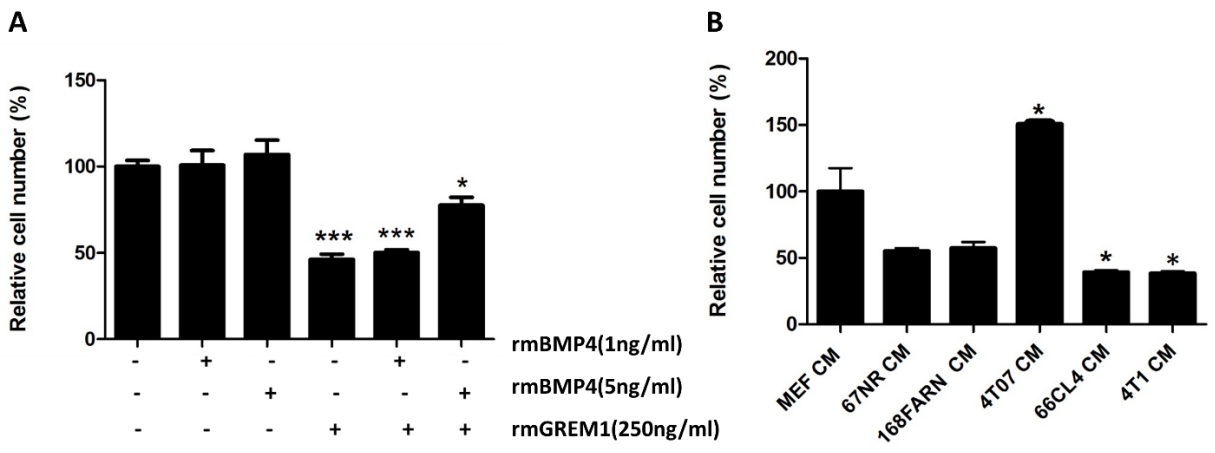

Figure 4.13 Proliferation of MEF is influenced by different stimulation.
*For **A and B**, 8000 cells of MEF were seeded in a 24- well plate and incubated overnight. The cells were then treated with the various stimulants and incubated for another 24hours. Cells numbers were determined using automatic coulter counter. The results were expressed as percent of cell number compared to the control. Results are means of 3 replicates run at the same time and bars are ± SEM.*

The effects of soluble mediators on the proliferation of fibroblasts were also investigated by growing the MEF in CM from the tumor cells. This was to establish if soluble factors secreted by the tumor cells in a paracrine manner institute the proliferation of fibroblasts. As can be seen from the result, 4T07 CM caused MEF to proliferate profoundly ($p<005$) as compared to CM from the other cell lines (**Figure 4.9 B**) which was also evident in their morphology showing large spindle shapes (**Figure 4.10B**). 67NR, 168FARN, 66cl4 and 4T1 CM on the other hand decreased the proliferation rate of MEF as compared to the control which is MEF CM being treated on MEF. The reduction in the proliferation was however not significant for 67NR and 168FARN ($p>0.05$) whiles significant for 66cl4 and 4T1 ($p<0.05$). The reduction in rate might be attributed to the fact that for instance 168FARN, 66cl4 and 4T1 are known to contain antagonists of BMPs and from the initial experiments, rmBMP4 increased proliferation while its antagonist rmGREM1 reduced proliferation. It will however be interesting to see if condition medium of different percentage used will change the effects seen as it can be argued that the necessary mediators for proliferation might have been used up by the tumor cells.

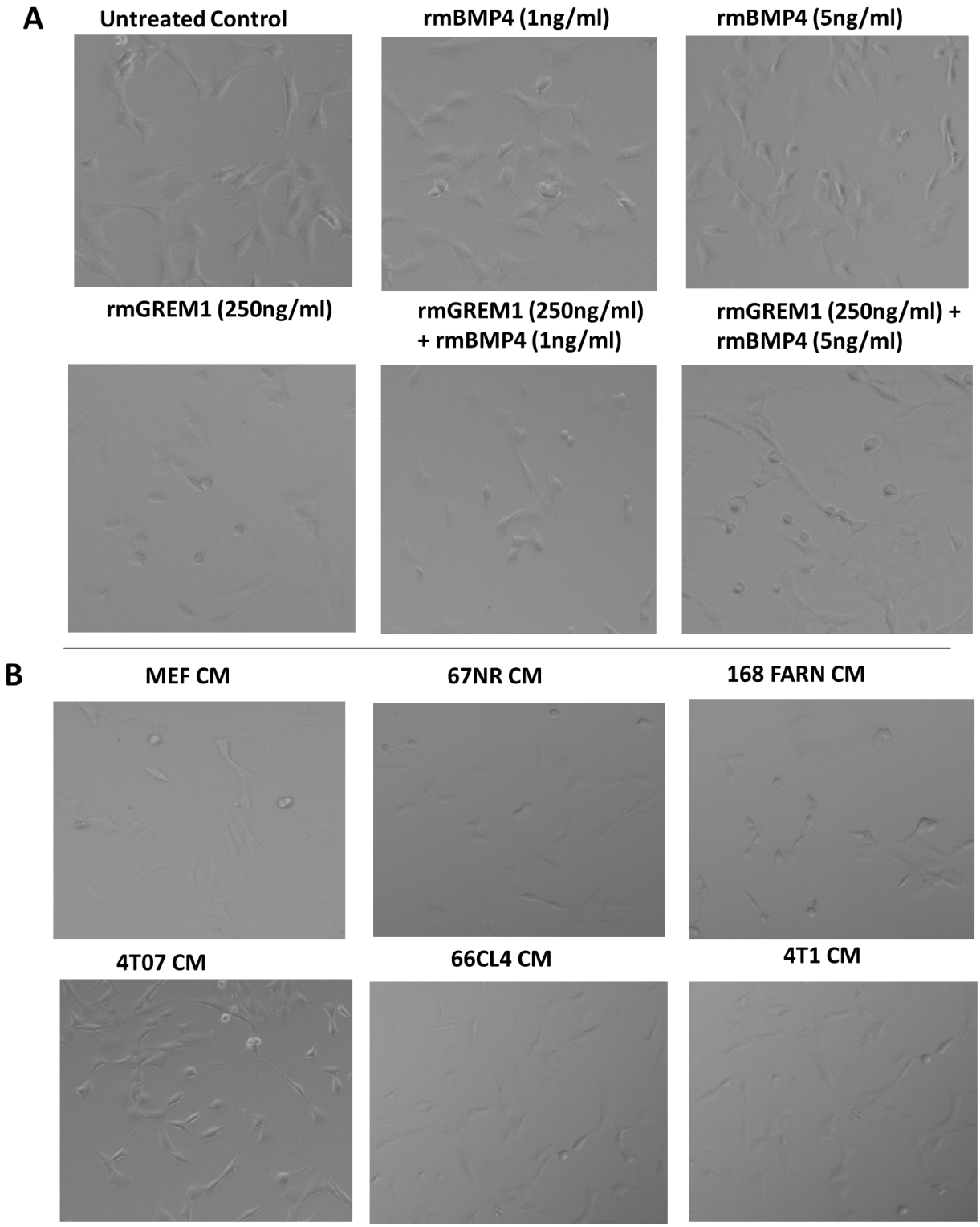

Figure 4.14 Comparison of MEF morphology between untreated MEFs and stimulated MEFs from the proliferation assay in figure 4.9.

A) RmBMP4 and rmGREM1 treatment on MEF with untreated MEF as control B) 5 cell line CM treatment on MEF with MEF CM as control Magnification 20X.

A different method known as MTT assay was used to verify the results. MTT assay correlates the number of cells with the relative metabolic activity of the cell. With regards to the rmBMP4 and rmGREM1, the proliferation rates were all above the untreated MEF, however, in comparison to the rmBMP4 proliferation rate, rmGREM1 treated cells had a lower proliferation rate as seen in the cell count assay (**Appendix VI, A**). The proliferation rate was however increased when rmGREM1 was in combination with rmBMP4. Condition medium treatment from the various 5 cell lines on MEF also showed increased cell viability as compared to the control with the exception of 4T1 CM that was slightly below. 67NR CM exhibited the highest cell viability (**Appendix VI, B)**. After establishing the effect of soluble mediators secreted from the tumor cell lines on proliferation of fibroblast, we also decided to check its effects on migration of fibroblast.

4.5 FIBROBLAST ISOLATED FROM LUNGS DISPLAYED ENHANCED MIGRATION ACTIVITY IN RESPONSE TO SOLUBLE MEDIATORS VIA PARACRINE CROSSTALK.

CAFs are known to modulate breast cancer progression and migration leading to metastasis through paracrine crosstalk by soluble mediators (11,27,38,123). It is equally important to note that tumor cells also influence fibroblast properties such as their activation, proliferation and migration in this way (39,124,125). These properties are diverse based on the wide variety of soluble factors that are secreted from different cancer types. We therefore hypothesized that fibroblasts would migrate differently in response to the different soluble factors that are secreted by the five cell lines of the 4T1 model that have various metastatic potential. To test this hypothesis, the migration property of fibroblast was analyzed using xCELLigence real time analysis.

Lung fibroblasts were used in this experiment. The xCELLigence system was validated using DMEM with and without FBS. The sample with no FBS resulted in base-line cell index level, an indication that there was no migration of lung fibroblast towards the medium (**Figure 4.11 A**). DMEM with FBS on the other hand showed induced migration of the lung fibroblast. To compare the migration ability of lung fibroblasts towards soluble mediators produced by 67NR, 66cl4 and 168FARN, condition medium harvested from these cells were used as chemoattractant placed in the lower chamber of the CIM 16 plate. Lung fibroblast CM was used as a control.

The rate of lung fibroblast migration towards 168FARN CM was highest in comparison to 66cl4 CM and 67NR CM (**Figure 4.11 B**). Lung fibroblast CM serving as a control exhibited some form

of migration even though low. This indicated that lung fibroblast responds with increased migration towards both paracrine soluble factors from some tumor cells. Most of the lung fibroblast migration showed they reached their highest migration point at about 200-250 mins with most showing a decline from 250mins. We also aimed at comparing the migration differences of lung fibroblast towards soluble mediators from CM of the various tumor cell lines interacting with the lung fibroblasts. This was accomplished by seeding 6250cells/well of 67NR, 168FARN and 66cl4 cells in the lower chamber. As shown in **Figure 4.11 C** the lung fibroblasts in culture with the cell lines migrated at different rates as compared to the CM from the cell lines. 168FARN however still was the most potent to attract the lung fibroblasts which continued to increase as a result of cells still proliferating. 67NR and 66cl4 cells also secreted variables that caused migration of the lung fibroblast even though it was lower as compared to the CM. The migration of the lung fibroblast was generally lower for the cell lines serving as chemoattractant. The relative curve area was calculated in other to get a quantitative overview of the various conditions used (**Figure 4.11 D**).

Fibroblasts are known to have different properties based on their origin (126).We therefore decided to check if other types of fibroblasts would respond in a similar way or not. In this respect skin fibroblasts were used. The results of the skin fibroblast were however not reliable as the positive control was on the baseline level, an indication they were not able to migrate properly (**Appendix VII**). Collectively, the results suggest that the tested cancer cells secrete mediators that influence fibroblast differentially.

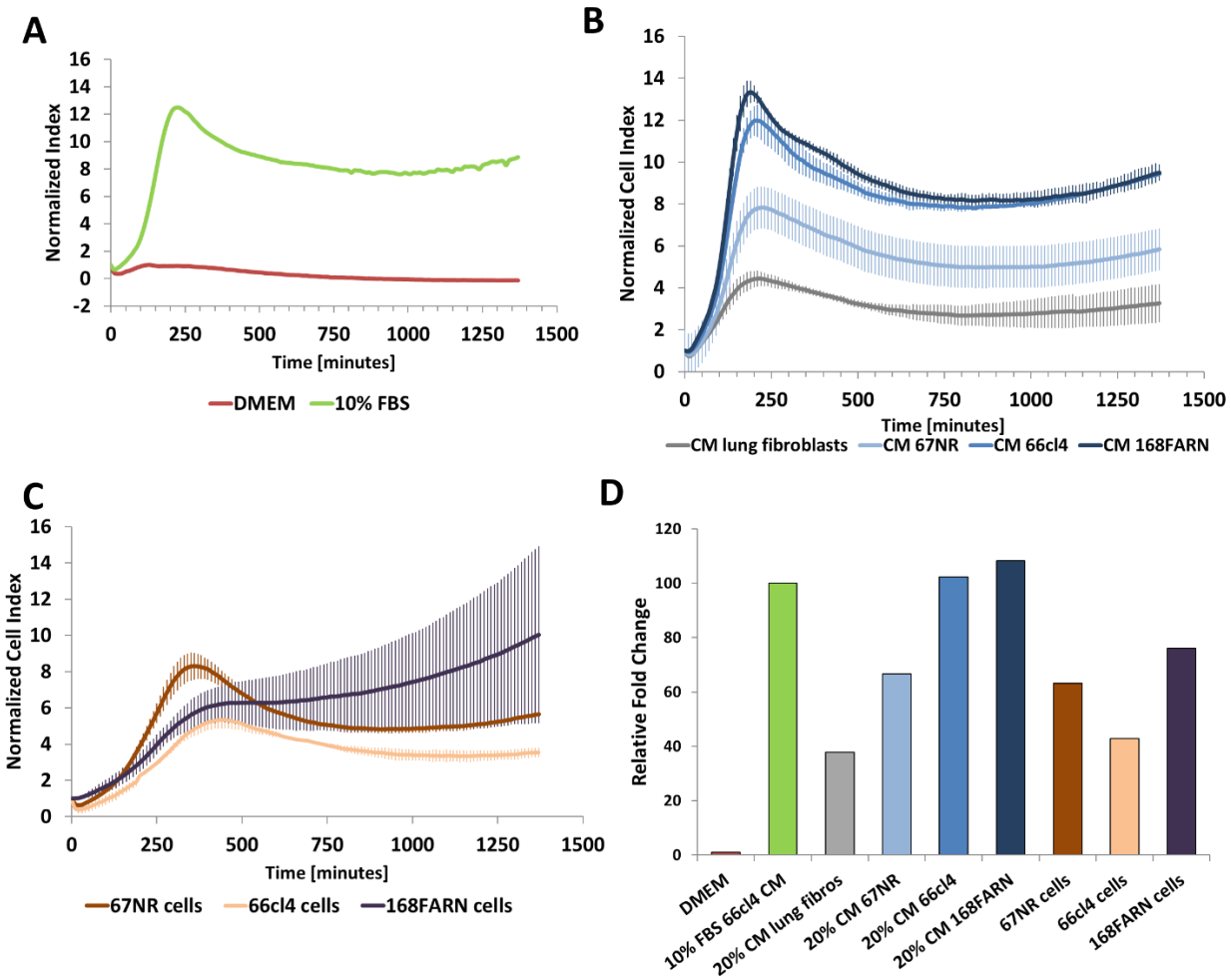

Figure 4.11: Time-dependent migration profiles of Lung fibroblasts.

A) *Validation of system with DMEM that contains no serum (red) or 10% FBS (green).* ***B)*** *Migration curves of lung fibroblasts produced by xCELLigence RTCA with seeding densities of 10000cells/ well (Upper chamber) with condition medium (CM) from 66NR, 66cl4 and 168FARN serving as chemoattractant with lung fibroblast CM as control (lower chamber).* ***C)*** *Same as* ***(B)*** *but with 67NR, 66cl4, 168FARN cells in the lower chamber.* ***D)*** *Total relative curve areas with DMEM with serum being set to 100. All graphs represent mean ± SD from duplicate experiment run parallel with the exception of "****A****".*

5.DISCUSSION

Majority of death of breast cancer (BC) patients is as a result of metastasis (4,5). It is therefore important for us to understand molecular mechanisms and pathways of tumor-stroma cross talk that lead to metastasis (127). This will enable us to develop novel strategies to prevent metastasis. In this study, the 4T1 BC mouse model which involves five cell lines (67NR, 168FARN, 4T07, 66cl4 and 4T1) with different metastatic potential was use in studying the interactions between tumors and fibroblasts. Transcriptome data of the non-metastatic 67NR and metastatic 66cl4 demonstrated that the 66cl4 primary tumor had higher mRNA expression of fibroblast markers and genes as compared to the 67NR. This was an indication that 66cl4 recruited fibroblast more than 67NR. Further search into the transcriptome data for reasons why 66cl4 had higher fibroblast marker and gene expressions lead us to the genes of focus *Bmp4* and *Grem1*. *Bmp4* and its antagonist *Grem1* was also highly expressed in 66cl4 as compared to 67NR. It was interesting to note that among the cell lines only 66cl4 expressed BMP4 whiles both 66cl4 and 168FARN expressed GREM1 on a protein level. With regards to clinical importance, high GREM1 expression was found to be correlated with poor prognosis of BC survival. Except lymph node negative patients that showed correlation with good prognosis, high expression of BMP4 on the showed no correlation. Finally, the interplay of GREM1 and BMP4 on tumor cells and different types of fibroblasts was tested in vitro. RmGREM1 decreasing fibroblast proliferation was antagonized by rmBMP4. Also the CM of 168FARN that secret high GREM1 together with the second highest 66cl4 serve as the highest chemoattractant of fibroblast.

5.1 mRNA expression of CAF markers are upregulated in 66cl4 compared to 67NR

The importance of CAFs in cancer progression through the enhancement of metastatic behavior of tumor cells in the microenvironment has been well demonstrated (39,128,111,38). In this current study, mRNA expression of CAF markers and genes in transcriptome data of non-metastatic 67NR and metastatic 66cl4 was checked. It was found that, 66cl4 primary tumors had higher expression of fibroblast markers (*Acta2, Pdgfra* and *Pdgfrb*,), activation markers (*Cxcl12, Tgf-β1* and *Pdgfb*) and proteases (*Plau, Mmp3, Mmp9* and *Mmp11*) compared to 67NR primary tumors. There were variations in expression of growth factors between 67NR and 66cl4 primary tumors. These variations may be due to the fact that growth factors are produced by both tumors and CAF and not solely by CAF.

The ability of tumors to metastasize requires the function and interaction of stroma cells like CAFs. The 66cl4 tumor in 4T1 breast cancer mouse model metastasizes predominantly to the lung. This might explain why fibroblast markers, activation markers and proteases are higher expressed in the metastasizing 66cl4 than the non-metastasizing 67NR. CAFs contribute to metastasis in diverse ways upon its activation. This includes the release of proteases such as *Mmps* and *Plau*. This soluble factors perform physical function in the microenvironment as they create tunnels in ECM to pave a way for tumor cells to follow suite (42,50,51). The tumor cells then migrate and invade their next organ/site which in this case will be the lungs for the 66cl4 tumor. A similar finding was reported in an unpublished data from our group with macrophages. Markers for macrophages were also highly expressed in 66cl4 as compared to 67NR. The M2 macrophage marker; Arginase1 (*Arg1*), Mannose Receptor C Type 1 (*Mrc1*) and Cluster of Differentiation 163 (*Cd163*) showed this difference. Studies have documented that tumor associated macrophages are associated with tumor progression and are predominantly M2 macrophages (129–131). Thus the upregulation of CAF markers and macrophage markers in 66cl4 may be because 66cl4 requires the function and interaction of stroma cells to accomplish their metastases.

To further understand the mechanisms underlying the increased expression of CAFs in 66cl4, the status of its major activator (*Tgf- β1*) as well as members of the Tgf-β superfamily were evaluated.

5.2 Tgf-β superfamily member, Bmp4 is expressed on mRNA level in 66cl4 cell line in culture and primary tumor

Tgf-β1, a major activator of CAF belongs to the Tgf-β superfamily that is made up of TGFβs, NODAL, Activins, BMPs, GDFs and AMH (56,57). Transcriptome data revealed that, among the Tgf-β superfamily, *Bmp4* and *Tgf- β1* showed the highest expression in the metastatic 66cl4 as compared to non–metastatic 67NR. *Bmp4* was selected due to its high expression in 66cl4 cell line relative to primary tumor.

The expression of BMPs have been reported in several breast cancer cell lines. Amongst the most expressed is BMP4. For example, a study utilizing 39 primary tumor samples and 22 cell lines identified BMP4 as the most highly expressed BMP subtype (62). In addition, another study showed that 66% of breast cancer tissues from 486 patient expressed BMP4 (66). BMP4 is a known regulator of cell migration and invasion (132,64). It has also been associated with the induction of the epithelial mesenchymal transition (EMT) which leads to the mobility of cancer cells as well as

its ability to metastasize (64). This might explain the observed increase in *Bmp4* expression in the metastatic 66cl4 compared to non-metastatic 67NR. The role of BMP4 in metastases together with the observed upregulation in the metastatic 66cl4 tumors made it important to check its clinical relevance.

5.3 BMP4 is associated with good prognosis in lymph node negative breast cancer patients

The clinical relevance of BMP4 was determine using KM plotter and BreastMark database. With regards to KM plotter database, BMP4 showed no correlation to breast cancer prognosis in OS, RFS, DMFS and PPS. Also whole breast cancer for BreastMark showed no correlation. BMP4 not correlating with prognosis does not fit observations made in different studies. BMP4 is known to play a dual role in the suppression and proliferation of tumor cells (66,133,134), as such it is expected to correlate to either poor or good prognosis. However, the lack of correlation might be because BMP4 is involved in other physiological processes such as hematopoiesis, skeletal formation, neurogenesis as well as controlling cellular behaviors that includes apoptosis, differentiation, proliferation and motility (64). Thus, variation in individual patients may mask the overall expression of BMP4 among the population.

A contrary result was seen in BreastMark analysis of BMP4 in lymph node negative BC patients. It was observed that higher expression of BMP4 was related to good prognosis. BMP4 correlation with good prognosis can be connected to its role in breast cancer suppression. A study emphasized BMP4 role in breast cancer suppression when exogenous BMP4 expression reduced accumulation of myeloid-derived suppressor cells (MDSC) (135). MDSC accumulation is known to lead to development of highly metastatic tumors and is associated with poor prognosis of BC (135). Thus, higher expression of BMP4 leads to the suppression of MDSC accumulation which then leads to good prognosis as seen in this study. Another instant where high expression of BMP4 can be associated with good prognosis was seen when BMP4 inhibited growth of several breast cancer cell lines by inducing G1 arrest of the cell cycle (132). The BMP4 induced G1 arrest of the cell cycle in the breast cancer cells was attributed to expression of the cell cycle inhibitor p21 (132,136). In other cancers such as in myeloma and lung cancer, the BMP4-induced growth inhibition was as a result of both G1 arrest as well as increment in the number of apoptotic cells (132) .

BMP4 signaling is regulated extracellularly and intracellularly at various stages by BMP antagonists (69,74,75). A study using the 4T1 model found that a BMP antagonist *Coco*, is important for inducing inactive breast cancer cells to undergo reactivation and metastasize to the lung. Due to this, BMP antagonists were analyzed in this study to find if others were more important than *Coco*.

5.4 GREM1 expression correlates with poor prognosis in breast cancer patients

BMP antagonist plays a significant role in regulating BMP4 activity. It was therefore intriguing to delve into the mRNA transcriptome data to see the interplays of these BMP antagonist between the metastatic 66cl4 and non-metastatic 67NR. Among the BMP antagonist, *Fstl 1*, *Fst*, *Bmper*, *Tsku*, *Bambi* and *Grem1* showed significant upregulation in 66cl4 than 67NR. With the exception of GREM1, all showed no significant correlation with prognosis ($p>0.05$). High expression of GREM1 on the other hand was associated with poor prognosis in OS, RFS, DMFS and PPS for KM plot. BreastMark on the other hand showed variation with for instance whole cancer, luminal A, luminal B, lymph node positive patients and Her2 showing no correlation with prognosis.

BMP4 antagonist GREM1 has been recognized as a moderator of EMT a key element that leads to metastasis in non-cancerous pathologies such as chronic allograft nephropathy (137). GREM1 is also found to be overexpressed in stromal cells that are involved in EMT (121). The observation of high expression of GREM1 to poor prognosis in this current study might be because GREM1 is a modulator of EMT. EMT in cancer has been associated with the advanced stage of the disease that show invasive capabilities and resistance to chemotherapy (138). GREM1 showing no correlation with prognosis can be because of its several roles. GREM1 is not associated with only malignancy function but also plays a critical role in development with regards to embryo patterning and limb development and tissue–specific differentiation (81). The developmental role was implicated in studies where mice that had GREM1 knockout (GREM1-/-) were efficient in kidney and lung development (84,85).

GREM1 and BMP4 showing clinically relevance were now the focus genes of this study. The mRNA expression seen was then verified on a protein level with all five cell lines. This was achieved by subjecting all five cell lines to immunoblotting and ELISA to determine their protein level expression.

5.5 BMP4 and GREM1 expressions in 4T1 Breast cancer model:66cl4 express BMP4 whiles 168FARN and 66cl4 express GREM1

This study demonstrated that the mRNA expression of BMP4 seen in the transcriptome data was equivalent to the protein expression with 66cl4 showing expression and not 67NR. Also, the other metastatic cell lines (168FARN, 4T07 and 4T1) did not express BMP4. BMP4 expression in the 66cl4 might be because it requires it to mediate its migration, invasion and EMT as a result of being a metastatic cell line. Several studies have shown that among most BMPs in breast cancer, BMP4 is mostly expressed and play roles in invasion and metastasis. (62,66). Metastatic cell lines 168FARN, 4T07 and 4T1 not expressing BMP4 might be because they mediate their BMP-dependent migration, invasion and EMT from other BMP sources. 4T07 and 4T1 cell lines for instance are known to express BMP2 and BMP5 (139). Also, several other BMPs such as BMP3, BMP5, BMP6, BMP7 and BMP8 have been shown to be expressed in different breast cancer cell lines (72,140,141).

BMP antagonist, GREM1 was expressed and secreted by only 168FARN and 66cl4 as seen in both immunoblotting and ELISA. Studies have shown that GREM1 is exclusively expressed by stroma cells especially fibroblast and promotes cancer cell survival and proliferation. Exceptions were however seen with some breast samples which expressed GREM1 in a limited manner (121). The tumor cell line diversity with GREM1 expression might be as a result of the various degree of fibroblast recruited in response to signals derived from the tumor. For instance, 67NR not expressing GREM1 might be because it had limited CAF marker expression as compared to 66cl4.

Also with GREM1 being a mediator of EMT (137,121), it can be assumed that BMP4 signaling is essential for normal epithelial tissue integrity that make up the ECM of the breast and hence have to be disrupted during breast cancer development and progression. This could be why the metastatic cell lines 168FARN and 66cl4 express the GREM1 as it is required to disrupt the integrity of the ECM in other to initiate metastasis. An alternative explanation of GREM1 expression in the metastatic 168FARN and 66cl4 is to approach it from the role of BMPs in tumor suppression of breast cancer (136,74,59). The tumor suppression role of BMPs has lead tumors in adapting several mechanisms that enables them to impair this effect. These mechanisms to shut down BMP effects includes genomic mutation of SMAD4 and BMP receptor type II (BMPR2), disposition of epigenetic mechanism for the interruption of BMP signaling and finally, the

production of BMP antagonist (142). The diverse strategies adapted by the tumor are to ensure that the blockage of the tumor suppression role of BMPs is effective in order for the tumor cells to survive and grow. Thus, BMP antagonist expression of GREM1 in metastatic cell lines might be relevant as it has been established for the first time that 168FARN and 66cl4 express GREM1.

Metastasis of BC involves its interaction with CAFs. After determining the expression of BMP4 and GREM1 seen in the metastatic cell lines, its interaction with fibroblast was further studied.

5.6 Interplays of BMP4 and GREM1 in 4T1 breast cancer model and MEFs

BMP4 signaling activation at protein level is measured by p-SMAD 1/5/9 (115,77). The effect of BMP4 and GREM1 expressed by tumor cell lines on MEFs were investigated by observing p-SMAD 1/5/9. It was observed that CM from 67NR, 168FARN and 66cl4 treatment on MEFs activated SMAD 1/5/9 with 66cl4 being the highest. The SMAD 1/5/9 activation seen from 67NR CM is not due to BMPs since mRNA expression from the transcriptome data showed no expression of BMPs for 67NR. However, p-SMAD 1/5/9 from 67NR CM could be attributed to the minimum expression of GDF11 levels seen in 67NR in the mRNA data since GDF11 has been shown to activate its signaling through SMAD 1/5/9 (118). Also, TGF-β has been shown to be activated in endothelial cells via SMAD1/5/9 even though it predominantly signals through SMAD2/3 (143,119). Fibroblasts have the propensity to be originated from endothelial mesenchymal transition hence may have attributes of endothelial cell. Therefore, the expression of Tgf-β1 and Tgf-β3 seen in 67NR in the transcriptome data might have been secreted into 67NR CM and activated SMAD 1/5/9 on MEF. The activation of SMAD 1/5/9 in 66cl4 may have been as a result of BMP4 expression as well as mRNA expression of Tgf-β1 and Tgf-β3 and GDF11 observed in the transcriptome data. 168FARN and 66cl4 activation of SMAD 1/5/9 was however expected to be dampened as a result of BMP antagonist expressed. The antagonizing effect of GREM1 expressed by 168FARN and 66cl4 was not sufficient to inhibit activation of SMAD 1/5/9.

A possible explanation for the low p-SMAD 1/5/9 observed from 4T07 CM and 4T1 CM may be as a result of low production of soluble mediators that activate SMAD1/5/9. For instance it has been shown that 4T07 and 4T1 express low BMP2 and BMP5(139). Also a study demonstrated BMP-induced SMAD2/3 signaling in 4T1 breast cancer model (144). BMP signaled through SMAD 2 but not SMAD 3 in 67NR whiles contrary to the metastatic cell lines (168FARN, 4T07, 66cl4 and 4T1), BMP signaled through both SMAD2 and SMAD 3(144). Thus, BMPs 2 and 5

expressed by 4T07 and 4T1 may have activated through SMAD 2/3 leading to their low p-SMAD 1/5/9 activations.

To mimic more of the tumor microenvironment, 67NR and 66cl4 was cultured in transwell with MEF and p-SMAD1/5/9 was checked. SMAD 1/5/9 activations were increased in transwell as compared to monoculture for both cells. This might be because the tumors secreted Tgf-β1 to activate MEFs which was signaled through SMAD 1/5/9. The activation of the MEFs by the tumor cells might be as a result of requiring the MEFs to produce mediators (e.g. growth factors) that enables them to grow.

The interaction of GREM1 expressed by the tumor cells on MEF was also studied. CM from all five cell lines were treated on MEF that had been stimulated with rmBMP4. 168FARN, 66cl4 and 4T1 were able to antagonized BMP4 signal on MEF to some extent especially for 168FARN. It cannot however be concluded that the antagonizing effect is as a result of only GREM1 (168FARN and 66cl4) and COCO (4T1). These cell lines might also express other forms of BMP antagonist as seen in the *Fstl 1, Fst, Bmper, Tsku, Bambi* upregulation in 66cl4 in the transcriptome data. In addition, GREM1 in cancer cells has been shown to be overexpressed when they interact with stroma cells (128). Due to this MEF was cultured in transwell with tumor cells to see if GREM1 will be overexpressed both in the tumor cells and MEF. GREM1 expression was increased when 168FARN and 66cl4 were co-cultured with MEFs. Also, GREM1 level of MEFs increased in the transwell with all the tumor cell lines. This might be as a result of paracrine communication between MEFs and tumor cells. They may have communicated by secretion of soluble factors to increase MEF's expression of GREM1 to suppress activity that can lead to tumor cells growth inhibition. GREM1 expression was also observed on untreated controls. This was an indication that MEFs produce GREM1. Literature also shows that GREM1 and BMP4 is secreted by the stroma cells, especially fibroblasts (121,120), for this reason GREM1 and BMP4 in MEFs was checked.

5.7 BMP4 and GREM1 are co-expressed in MEF

MEF was found to express GREM1 and BMP4 on protein level which were increased with PTI treatment. The increment is an indication that the intracellular secretion or transport pathway of the BMP4 and GREM1 has been inhibited thereby accumulating them in the Golgi apparatus or

the lumen of the endoplasmic reticulum (122). The co-expression of BMP4 and GREM1 may be suggestive of the importance of BMP4 mediation and regulation by GREM.

The expression of the GREM1 in MEFs was to be expected as GREM1 was first observed from a v-mos- transformed rat fibroblast cell line (80) and GREM1 has been documented to be overexpress in stroma cells (121). Furthermore, Cancer invasion front (CIF) is the area where tumor-host cells interacts mostly in a paracrine and mechanical fashion (137,150). CAF is known to be the majority of CIF cells (128,142). CIF cells express GREM1 as it provides them an advantage to shift their differentiation to a more mesenchymal and stem-like phenotype (86,121,128,142,145). This might be why GREM1 has been found to be expressed by CAF and in this study MEF (121).

BMP signaling activated in the microenvironment is said to be away from the CAF-instilled microenvironment due to CAFs GREM1 expression (145,146). However, the co-expression of BMP4 seen in MEF can enable BMP4 signaling to be activated in CAF instilled microenvironment in an autocrine manner. After observing BMP4 and GREM1 expression in MEFs, it was presumed that BMP4 and GREM1 might be secreted into MEF CM. This resorted in the treatment of tumor cell lines with MEF CM to observe activation of SMAD 1/5/9. P-SMAD 1/5/9 was increased in 67NR and 4T07. The expression of BMP antagonists GREM1 and COCO in 168FARN, 66cl4 and 4T1 might explain why MEF CM had no effect in these cells. It is however important to note that they may also be due other antagonists as seen from the expression of BMP antagonist in transcriptome data for 66cl4. This suggest the activation of SMAD 1/5/9 from the soluble factors of MEFs might be associated with tumor suppressive activity. Thus for the 168FARN, 66cl4 and 4T1 to be able to metastasize prevents SMAD 1/5/9 activation. This finding correlates again with tumors adapting several mechanisms to impair the tumor suppression role of BMPs as vividly described in section 5.5.

5.8 Influence of BMP4, GREM1 and tumor soluble mediators on fibroblast proliferation and migration properties

Metastatic ability or aggressiveness varies from different tumors and is dependent on the tumors ability to recruit, activate and enhance growth of CAF among other stroma cells (147). Metastatic progression relies on CAFs ability to migrate within the tumor microenvironment and through the tumor compartment to the new site (147). The recruitment, migration and proliferation of the CAF

depends on the metastatic propensity of the tumor cells. This leads to different production of signals and soluble factors that forms a paracrine feedback loop (147). In this current study, the ability of soluble factors from tumor cells as well as rmBMP4 and rmGREM1 ability to proliferate and migrate fibroblast was also checked.

The findings suggested MTT and Cell counting did not show the same result as rmBMP4 showed no proliferation effect in counting but increased proliferation of MEF in MTT. The increase in fibroblast per MTT assay has been documented with previous studies reporting BMP4 both inhibiting and enhancing growth of epithelial cells and mammary fibroblasts (132,115). This phenomenon of dual role has been associated with superfamily members TGF-β. They are known to have the inhibition factor of epithelia cell proliferation which is lost during cancer progression (140). RmBMP4 was also able to antagonize rmGREM1 inhibiting MEF proliferation. RmGREM1 did not only inhibit invasion but distorted the normal spindle shape of fibroblast and indication the MEF might be dying. RmGREM1 inhibition of MEF proliferation was contrary to a study that showed increment in cell proliferation of normal lung fibroblast and epithelial cell lines after they had been transfected with GREM1 (88). CM from 67NR, 168FARN, 66cl4 and 4T1 however showed inhibition in growth and indication of soluble factors that inhibit MEF proliferation. MTT pattern of the CM treatment were not exactly what reflected in the counting assay method and this might be due to the 50%CM used. It is also worth noting that the MTT assay does not directly reflect cell numbers as in the counting assay but cell metabolism which can be influenced by changes such as pH in the culture medium and the physiology of the cells (148,149). This was however one experiment; hence a firm conclusion cannot be made since it was not repeated with different batches of CM from the tumor cells. It will therefore be interesting to repeat and also vary the concentration of the CM to see if the same effect will be seen.

Migration of the Fibroblast was determined using xCELLigence cell migration assay. In general, the CM from 168FARN and 66cl4 migrated lung fibroblast than the 67NR CM. Studies have shown GREM1 can increase epithelial cell migration and invasion. This might be why 168FARN and 66cl4 attracted lung fibroblast more since they express and secrete GREM1. The study showed that human lung adnocarcinoma transfected epithelial *cell* line (A549 cells) with GREM1 increased their migration and invasion (87). Also, lung fibroblast in culture with the tumor cells migrated at different rates as compared to the CM from the tumor cells. The general lower

migration of the lung fibroblast was as a result of cells in culture serving as chemoattractant. This is because of the influences caused by the rate of growth of the cell, difference in cell number and the amount of soluble factors produced.

The findings from these experiments provide basics of information concerning BMP4 and GREM1 in the 4T1 tumor cell lines. This can be further research to aid in improving breast cancer therapy by providing information that will serve in targeting cytokines like BMP4 and GREM1.

6. CONCLUSION AND FUTURE PLANS

6.1 Conclusion

CAF mediate direct and indirect tumorigenesis and tumor progression effects through secretion and expression of several factors. Thus, tumors ability to recruit CAF increases its ability to metastasize as CAF are known to be EMT mediators and CIF cells. Furthermore, GREM1 is a known EMT mediator that function to increase tumor cell migration and metastasis. GREM1 is also known to antagonize BMP-dependent tumor suppression. Due to this, the study shows high GREM1 expression is attributed to the poor cancer prognosis in breast cancer. This study has also shown for the first time that 168FARN and 66cl4 metastatic cell lines of the 4T1 breast cancer mouse model express GREM1. The GREM1 expression aid in 168FARN and 66cl4 recruitment of CAF that leads to their metastatic ability. Further research into the interplays of GREM1 in 4T1 breast cancer mouse model may provide information that will serve in targeting GREM1 to help tumor cells to metastasize.

6.2 Future Plans

From the outcomes of this study, GREM1 expression might be a key player in aiding the recruiting of fibroblast that facilitates the differences in metastatic behavior of the five cell lines. In order to have a confirmed reason for these observations, all experiments can be carried out with different primary fibroblast to see if same responses will be seen. The xCELLigence RTCA migration assay should also be repeated since it was done once in other to ascertain if the results seen are consistent. In addition, quantitative RT-PCR should be used to identify factors causing effect in the various experiments.

Furthermore, to check if GREM1 is really important for tumor formation and/or metastases a knockdown/knockout of GREM1 in the 4T1 tumor cell lines especially 168FARN and 66cl4 should be done. BMP4 knockout can also be done for 66cl4. The knockout cell line can then be injected into BALB/c mice to see how well tumors form will be metastasized. All experiments carried out in this study can then be repeated with the knocked out cell lines. Epigenetic analysis of GREM1 promoters such as ChIP-qPCR-analysis in the different cell lines to access if the promoters are poised for different regulation can also be carried out. This is important because genes are regulated by several epigenetic mechanisms such as post-translational modifications of histone proteins and DNA methylation.

Fibroblasts are known to express GREM1 and it has been shown that 67NR contain about 40% stroma cell. It was therefore surprising to see no mRNA expression of GREM1 in the transcriptome data. To verify this, fibroblast could be stained both in 66cl4 and 67NR tumors. Fluorescence-activated cell sorting (flow cytometer) can also be use in analyzing the amount of fibroblast.

REFERENCE

1. Ferlay J, Soerjomataram I, Ervik M, Dikshit R, Eser S, Mathers C, Rebelo M, Parkin DM, Forman D, Bray F. GLOBOCAN 2012 v1.0, Cancer Incidence and Mortality Worldwide: IARC CancerBase No. 11 [Internet] [Internet]. Lyon, France: International Agency for Research on Cancer. 2013 [cited 2015 Sep 20]. Available from: http://globocan.iarc.fr
2. Tazhibi M, Feizi a. Awareness levels about breast cancer risk factors , early warning signs , and screening and therapeutic approaches among Iranian adult women : a large population based study using latent class analysis . PubMed Commons. 2015;2014:2014–5.
3. Ovcaricek T, Frkovic S, Matos E, Mozina B, Borstnar S. Triple negative breast cancer - prognostic factors and survival. Radiol Oncol [Internet]. 2011;45(1):46–52. Available from: http://www.degruyter.com/view/j/raon.2011.45.issue-1/v10019-010-0054-4/v10019-010-0054-4.xml
4. Studebaker AW, Storci G, Werbeck JL, Sansone P, Sasser a. K, Tavolari S, et al. Fibroblasts isolated from common sites of breast cancer metastasis enhance cancer cell growth rates and invasiveness in an interleukin-6-dependent manner. Cancer Res. 2008;68(21):9087–95.
5. Wu W, Wu J. Signal Transduction in Cancer Metastasis. Livre [Internet]. 2010;15(701):103–18. Available from: http://link.springer.com/10.1007/978-90-481-9522-0
6. Kozłowski J, Kozłowska A, Kocki J. Breast cancer metastasis – insight into selected molecular mechanisms of the phenomenon. Postepy Hig Med Dosw. 2015;69:447–51.
7. Subramanian A, Manigandan A, Sivashankari A, Sethuraman S. Development of nanotheranostics against metastatic breast cancer — A focus on the biology & mechanistic approaches. Biotechnol Adv [Internet]. Elsevier B.V.; 2015;33(8):1897–911. Available from: http://dx.doi.org/10.1016/j.foodres.2011.04.025
8. American Cancer Society. What is breast cancer ? What causes breast cancer ? [Internet]. American Cancer Society. 2015 [cited 2016 Jan 23]. p. 1–13. Available from: http://www.cancer.org/acs/groups/cid/documents/webcontent/003090-pdf.pdf
9. Ali S, Coombes RC. Endocrine-Responsive Breast Cancer and Strategies for Combating Resistance. Nat Rev Cancer [Internet]. 2002;2(2):101–12. Available from: http://www.nature.com/doifinder/10.1038/nrc721
10. Polyak K. Science in medicine Breast cancer : origins and evolution. Cell [Internet]. 2007;117(11):3155–63. Available from: http://www.pubmedcentral.nih.gov/articlerender.fcgi?artid=2045618&tool=pmcentrez&rendertype=abstract
11. Khamis ZI, Sahab ZJ, Sang Q-XA. Active roles of tumor stroma in breast cancer metastasis. Int J Breast Cancer [Internet]. 2012;2012:574025. Available from: http://www.pubmedcentral.nih.gov/articlerender.fcgi?artid=3296264&tool=pmcentrez&rendertype=abstract
12. Weigelt B, Peterse JL, van 't Veer LJ. Breast cancer metastasis: markers and models. Nat Rev Cancer. 2005;5(August):591–602.
13. Wirtz D, Konstantopoulos K, Searson PCPPC. The physics of cancer: the role of physical

interactions and mechanical forces in metastasis. Nat Rev Cancer [Internet]. Nature Publishing Group; 2011;11(7):512–22. Available from: http://dx.doi.org/10.1038/nrc3080

14. Steeg PS. Tumor metastasis: mechanistic insights and clinical challenges. Nat Med. 2006;12(8):895–904.

15. Yersal O. Biological subtypes of breast cancer: Prognostic and therapeutic implications. World J Clin Oncol [Internet]. 2014;5(3):412. Available from: http://www.wjgnet.com/2218-4333/full/v5/i3/412.htm

16. Madden SF, Clarke C, Gaule P, Aherne ST, O'Donovan N, Clynes M, et al. BreastMark: an integrated approach to mining publicly available transcriptomic datasets relating to breast cancer outcome. Breast Cancer Res [Internet]. BioMed Central Ltd; 2013;15(4):R52. Available from: http://www.pubmedcentral.nih.gov/articlerender.fcgi?artid=3978487&tool=pmcentrez&rendertype=abstract

17. Reis-filho JS, Pusztai L. Gene expression profiling in breast cancer : classification , prognostication , and prediction. Lancet (London, England). England; 2011 Nov;378(9805):1812–23.

18. Schnitt SJ. Classification and prognosis of invasive breast cancer: from morphology to molecular taxonomy. Mod Pathol [Internet]. Nature Publishing Group; 2010;23(S2):S60–4. Available from: http://www.nature.com/doifinder/10.1038/modpathol.2010.33

19. Sorlie T, Perou CM, Tibshirani R, Aas T, Geisler S, Johnsen H, et al. Gene expression patterns of breast carcinomas distinguish tumor subclasses with clinical implications. Proc Natl Acad Sci U S A [Internet]. 2001;98(19):10869–74. Available from: http://www.pubmedcentral.nih.gov/articlerender.fcgi?artid=58566&tool=pmcentrez&rendertype=abstract

20. Rivenbark AG, O'Connor SM, Coleman WB. Molecular and Cellular Heterogeneity in Breast Cancer [Internet]. The American Journal of Pathology. 2013. p. 1113–24. Available from: http://dx.doi.org/10.1016/j.ajpath.2013.08.002\npapers2://publication/doi/10.1016/j.ajpath.2013.08.002

21. Russnes HG, Navin N, Hicks J, Borresen-Dale AL. Insight into the heterogeneity of breast cancer through next-generation sequencing. J Clin Invest. 2011;121(10):3810–8.

22. Meric-Bernstam F, Mills GB. Overcoming implementation challenges of personalized cancer therapy. Nat Rev Clin Oncol. England; 2012 Sep;9(9):542–8.

23. Bayer Research Institute. Personalized medicine against cancer [Internet]. Available from: http://www.research.bayer.com/en/23-personalized-medicine.pdfx

24. Polyak K. Heterogeneity in breast cancer. J Clin Invest. 2011;121(10):2011–3.

25. Nature. Cancer microenvironment [Internet]. Nature. [cited 2016 Mar 31]. Available from: http://www.nature.com/subjects/cancer-microenvironment

26. Joyce J a, Pollard JW. Microenvironmental regulation of metastasis. Nat Rev Cancer [Internet]. 2009;9(4):239–52. Available from: http://www.nature.com/doifinder/10.1038/nrc2618

27. Koontongkaew S. The tumor microenvironment contribution to development, growth, invasion and metastasis of head and neck squamous cell carcinomas. J Cancer. 2013;4(1):66–83.

28. Meng M, Wang W, Yan J, Tan J, Liao L, Shi J, et al. Immunization of stromal cell targeting fibroblast activation protein providing immunotherapy to breast cancer mouse model. Tumor Biol [Internet]. 2016; Available from: http://link.springer.com/10.1007/s13277-016-4825-4

29. Morandi A, Chiarugi P. Metabolic implication of tumor:stroma crosstalk in breast cancer. J Mol Med (Berl) [Internet]. 2014;92(2):117–26. Available from: http://www.ncbi.nlm.nih.gov/pubmed/24458539

30. Brennen WN, Isaacs JT, Denmeade SR. Rationale Behind Targeting Fibroblast Activation Protein-Expressing Carcinoma-Associated Fibroblasts as a Novel Chemotherapeutic Strategy. Mol Cancer Ther. 2012;11(2):257–66.

31. Mueller MM, Fusenig NE. Friends or foes - bipolar effects of the tumour stroma in cancer. Nat Rev Cancer. 2004;4(11):839–49.

32. Wan L, Pantel K, Kang Y. Tumor metastasis: moving new biological insights into the clinic. Nat Med [Internet]. 2013;19(11):1450–64. Available from: http://www.nature.com.proxy.library.adelaide.edu.au/nm/journal/v19/n11/full/nm.3391.html

33. Pietras K, Östman A. Hallmarks of cancer: Interactions with the tumor stroma. Exp Cell Res [Internet]. Elsevier Inc.; 2010;316(8):1324–31. Available from: http://dx.doi.org/10.1016/j.yexcr.2010.02.045

34. Micke P, Ostman A. Exploring the tumour environment: cancer-associated fibroblasts as targets in cancer therapy. Expert Opin Ther Targets. 2005;9:1217–33.

35. Anderberg C, Pietras K. On the origin of cancer-associated fibroblasts. Cell Cycle [Internet]. 2009;8(10):1461–5. Available from: http://www.tandfonline.com/doi/abs/10.4161/cc.8.10.8557

36. Hanahan D, Weinberg RA. The hallmarks of cancer. Cell. United State; 2000 Jan;100(1):57–70.

37. Yu Y, Xiao C-H, Tan L-D, Wang Q-S, Li X-Q, Feng Y-M. Cancer-associated fibroblasts induce epithelial-mesenchymal transition of breast cancer cells through paracrine TGF-β signalling. Br J Cancer [Internet]. 2014;110(3):724–32. Available from: http://www.ncbi.nlm.nih.gov/pubmed/24335925

38. Räsänen K, Vaheri A. Activation of fibroblasts in cancer stroma. Exp Cell Res [Internet]. Elsevier Inc.; 2010;316(17):2713–22. Available from: http://dx.doi.org/10.1016/j.yexcr.2010.04.032

39. Kalluri R, Zeisberg M. Fibroblasts in cancer. Nat Rev Cancer. 2006;6(5):392–401.

40. Chang HY, Chi J-T, Dudoit S, Bondre C, van de Rijn M, Botstein D, et al. Diversity, topographic differentiation, and positional memory in human fibroblasts. Proc Natl Acad Sci U S A. United States; 2002 Oct;99(20):12877–82.

41. Rothschild E, Banerjee D. Subverting Subversion : A Review on the Breast Cancer

Microenvironment and Therapeutic Opportunities. 2015;9.

42. De Veirman K, Rao L, De Bruyne E, Menu E, Van Valckenborgh E, Van Riet I, et al. Cancer associated fibroblasts and tumor growth: Focus on multiple myeloma. Cancers (Basel). 2014;6(3):1363–81.

43. Kojima Y, Acar A, Eaton EN, Mellody KT, Scheel C, Ben-Porath I, et al. Autocrine TGF- and stromal cell-derived factor-1 (SDF-1) signaling drives the evolution of tumor-promoting mammary stromal myofibroblasts. Proc Natl Acad Sci [Internet]. 2010;107(46):20009–14. Available from: http://www.pubmedcentral.nih.gov/articlerender.fcgi?artid=2993333&tool=pmcentrez&rendertype=abstract

44. Massague J. TGFbeta signalling in context. Nat Rev Mol Cell Biol. England; 2012 Oct;13(10):616–30.

45. Massagué J. TGFβ signalling in context. Nat Rev Mol Cell Biol [Internet]. Nature Publishing Group; 2012;13(10):616–30. Available from: http://dx.doi.org/10.1038/nrm3434

46. Olumi AF, Grossfeld GD, Hayward SW, Carroll PR, Tlsty TD, Cunha GR. Carcinoma-associated fibroblasts direct tumor progression of initiated human prostatic epithelium. Cancer Res. 1999;59(19):5002–11.

47. Trimis G, Chatzistamou I, Politi K, Kiaris H, Papavassiliou AG. Expression of p21waf1/Cip1 in stromal fibroblasts of primary breast tumors. Hum Mol Genet. 2008;17(22):3596–600.

48. Fleming JM, Miller TC, Quinones M, Xiao Z, Xu X, Meyer MJ, et al. Research article The normal breast microenvironment of premenopausal women differentially influences the behavior of breast cancer cells in vitro and in vivo. BMC Med. England; 2010;8:27.

49. Tyan SW, Kuo WH, Huang CK, Pan CC, Shew JY, Chang KJ, et al. Breast cancer cells induce cancer-associated fibroblasts to secrete hepatocyte growth factor to enhance breast tumorigenesis. PLoS One. 2011;6(1):1–9.

50. Gupta GP, Massagu J. Cancer Metastasis: Building a Framework. Cell. 2006;127(4):679–95.

51. Gaggioli C, Hooper S, Hidalgo-Carcedo C, Grosse R, Marshall JF, Harrington K, et al. Fibroblast-led collective invasion of carcinoma cells with differing roles for RhoGTPases in leading and following cells. Nat Cell Biol. 2007;9(12):1392–400.

52. Kessenbrock K, Plaks V, Werb Z. Matrix metalloproteinases: regulators of the tumor microenvironment. Cell. United States; 2010 Apr;141(1):52–67.

53. Orimo A, Gupta PB, Sgroi DC, Arenzana-Seisdedos F, Delaunay T, Naeem R, et al. Stromal fibroblasts present in invasive human breast carcinomas promote tumor growth and angiogenesis through elevated SDF-1/CXCL12 secretion. Cell. United States; 2005 May;121(3):335–48.

54. Balkwill F. Cancer and the chemokine network. Nat Rev Cancer [Internet]. 2004;4(7):540–50. Available from: http://www.nature.com/doifinder/10.1038/nrc1388

55. Duda DG, Duyverman AMMJ, Kohno M, Snuderl M, Steller EJA, Fukumura D, et al.

Malignant cells facilitate lung metastasis by bringing their own soil. Proc Natl Acad Sci U S A [Internet]. National Academy of Sciences; 2010 Dec 14;107(50):21677–82. Available from: http://www.ncbi.nlm.nih.gov/pmc/articles/PMC3003109/

56. Fabregat I, Fernando J, Mainez J, Sancho P. TGF-beta signaling in cancer treatment. Curr Pharm Des. Netherlands; 2014;20(17):2934–47.

57. Tirado-Rodriguez B, Ortega E, Segura-Medina P, Huerta-Yepez S. TGF- beta: an important mediator of allergic disease and a molecule with dual activity in cancer development. J Immunol Res. United States; 2014;2014:318481.

58. Karagiannis GS, Treacy A, Messenger D, Grin A, Kirsch R, Riddell RH, et al. Expression patterns of bone morphogenetic protein antagonists in colorectal cancer desmoplastic invasion fronts. Mol Oncol [Internet]. Elsevier B.V; 2014;8(7):1240–52. Available from: http://dx.doi.org/10.1016/j.molonc.2014.04.004

59. Owens P, Pickup MW, Novitskiy S V, Giltnane JM, Gorska a E, Hopkins CR, et al. Inhibition of BMP signaling suppresses metastasis in mammary cancer. Oncogene [Internet]. Nature Publishing Group; 2014;34(May):1–13. Available from: http://www.ncbi.nlm.nih.gov/pubmed/24998846

60. Yanagita M. BMP antagonists: Their roles in development and involvement in pathophysiology. Cytokine Growth Factor Rev. 2005;16(3 SPEC. ISS.):309–17.

61. Rothhammer T, Poser I, Soncin F, Bataille F, Moser M, Bosserhoff A-K. Bone Morphogenic Proteins Are Overexpressed in Malignant Melanoma and Promote Cell Invasion and Migration. Cancer Res [Internet]. 2005;65(2):448–56. Available from: http://cancerres.aacrjournals.org/content/65/2/448.long\nhttp://www.ncbi.nlm.nih.gov/pubmed/15695386

62. Alarmo EL, Kuukasjärvi T, Karhu R, Kallioniemi A. A comprehensive expression survey of bone morphogenetic proteins in breast cancer highlights the importance of BMP4 and BMP7. Breast Cancer Res Treat. 2007;103(2):239–46.

63. Sun J, Zhuang FF, Mullersman JE, Chen H, Robertson EJ, Warburton D, et al. BMP4 activation and secretion are negatively regulated by an intracellular Gremlin-BMP4 interaction. J Biol Chem. 2006;281(39):29349–56.

64. Kallioniemi A. Bone morphogenetic protein 4-a fascinating regulator of cancer cell behavior. Cancer Genet [Internet]. United States: Elsevier Inc.; 2012 Jun;205(6):267–77. Available from: http://dx.doi.org/10.1016/j.cancergen.2012.05.009

65. Furuta Y, Hogan BLM. BMP4 is essential for lens induction in the mouse embryo. Genes Dev [Internet]. Cold Spring Harbor Laboratory Press; 1998 Dec 1;12(23):3764–75. Available from: http://www.ncbi.nlm.nih.gov/pmc/articles/PMC317259/

66. Alarmo E-L, Huhtala H, Korhonen T, Pylkkänen L, Holli K, Kuukasjärvi T, et al. Bone morphogenetic protein 4 expression in multiple normal and tumor tissues reveals its importance beyond development. Mod Pathol [Internet]. 2013;26(1):10–21. Available from: http://www.ncbi.nlm.nih.gov/pubmed/22899288

67. Brazil DP, Church RH, Surae S, Godson C, Martin F. BMP signalling: agony and antagony in the family. Trends Cell Biol [Internet]. Elsevier Ltd; 2015;1–16. Available from: http://dx.doi.org/10.1016/j.tcb.2014.12.004

68. Walsh DW, Godson C, Brazil DP, Martin F. Extracellular BMP-antagonist regulation in development and disease: Tied up in knots. Trends Cell Biol [Internet]. Elsevier Ltd; 2010;20(5):244–56. Available from: http://dx.doi.org/10.1016/j.tcb.2010.01.008

69. Lowery JW, de Caestecker MP. BMP signaling in vascular development and disease. Cytokine Growth Factor Rev [Internet]. Elsevier Ltd; 2010;21(4):287–98. Available from: http://dx.doi.org/10.1016/j.cytogfr.2010.06.001

70. Wakefield LM, Hill CS. Beyond TGFβ: roles of other TGFβ superfamily members in cancer. Nat Rev Cancer [Internet]. Nature Publishing Group; 2013;13(5):328–41. Available from: http://www.nature.com/nrc/journal/v13/n5/full/nrc3500.html\nhttp://www.nature.com/nrc/journal/v13/n5/pdf/nrc3500.pdf

71. Karagiannis GS, Musrap N, Saraon P, Treacy A, Schaeffer DF, Kirsch R, et al. Bone morphogenetic protein antagonist gremlin-1 regulates colon cancer progression. Biol Chem. 2015;396(2):163–83.

72. Rodriguez-Martinez A, Alarmo E-L, Saarinen L, Ketolainen J, Nousiainen K, Hautaniemi S, et al. Analysis of BMP4 and BMP7 signaling in breast cancer cells unveils time-dependent transcription patterns and highlights a common synexpression group of genes. BMC Med Genomics [Internet]. BioMed Central Ltd; 2011;4(1):1–16. Available from: http://www.biomedcentral.com/1755-8794/4/80

73. Cao Y, Slaney CY, Bidwell BN, Parker BS, Johnstone CN, Rautela J, et al. BMP4 Inhibits Breast Cancer Metastasis by Blocking Myeloid-Derived Suppressor Cell Activity. Cancer Res [Internet]. 2014;74(18):5091–102. Available from: http://cancerres.aacrjournals.org/cgi/doi/10.1158/0008-5472.CAN-13-3171

74. Alarmo E-L, Kallioniemi A. Bone morphogenetic proteins in breast cancer: dual role in tumourigenesis? Endocr Relat Cancer. 2010;17(2):R123–39.

75. Liu A, Niswander L a. Bone morphogenetic protein signalling and vertebrate nervous system development. Nat Rev Neurosci. 2005;6(12):945–54.

76. Massagué J, Seoane J, Wotton D. Smad transcription factors Smad transcription factors. 2005;2783–810.

77. Miyazono K, Kamiya Y, Morikawa M. Bone morphogenetic protein receptors and signal transduction. J Biochem. 2010;147(1):35–51.

78. Topol LZ, Modi WS, Koochekpour S, Blair DG. DRM/GREMLIN (CKTSF1B1) maps to human chromosome 15 and is highly expressed in adult and fetal brain. Cytogenet Genome Res [Internet]. 2000;89(1-2):79–84. Available from: http://www.karger.com/DOI/10.1159/000015568

79. Wordinger RJ, Zode G, Clark AF. Focus on Molecules: Gremlin. Exp Eye Res. 2008;87(2):78–9.

80. Topol LZ, Marx M, Laugier D, Bogdanova NN, Boubnov N V, Clausen PA, et al. Identification of drm, a novel gene whose expression is suppressed in transformed cells and which can inhibit growth of normal but not transformed cells in culture. Mol Cell Biol [Internet]. 1997;17(8):4801–10. Available from: http://dx.doi.org/10.1128/MCB.17.8.4801

81. Topol LZ, Bardot B, Zhang Q, Resau J, Huillard E, Marx M, et al. Biosynthesis , Post-

translation Modification , and Functional Characterization of Drm / Gremlin *. J Biol Chem [Internet]. 2000;275(12):8785–93. Available from: http://dx.doi.org/10.1074/jbc.275.12.8785

82. Rodrigues-Diez R, Rodrigues-Diez RR, Lavoz C, Carvajal G, Droguett A, Garcia-Redondo AB, et al. Gremlin activates the smad pathway linked to epithelial mesenchymal transdifferentiation in cultured tubular epithelial cells. Biomed Res Int. 2014;2014.

83. Church RH, Krishnakumar A, Urbanek A, Geschwindner S, Meneely J, Bianchi A, et al. Gremlin1 preferentially binds to bone morphogenetic protein-2 (BMP-2) and BMP-4 over BMP-7. Biochem J [Internet]. 2015;466(1):55–68. Available from: http://www.ncbi.nlm.nih.gov/pubmed/25378054

84. Khokha MK, Hsu D, Brunet LJ, Dionne MS, Harland RM. Gremlin is the BMP antagonist required for maintenance of Shh and Fgf signals during limb patterning. Nat Genet. United States; 2003 Jul;34(3):303–7.

85. Michos O, Panman L, Vintersten K, Beier K, Zeller R, Zuniga A. Gremlin-mediated BMP antagonism induces the epithelial-mesenchymal feedback signaling controlling metanephric kidney and limb organogenesis. Development. England; 2004 Jul;131(14):3401–10.

86. Namkoong H, Shin SM, Kim HK, Ha S-A, Cho GW, Hur SY, et al. The bone morphogenetic protein antagonist gremlin 1 is overexpressed in human cancers and interacts with YWHAH protein. BMC Cancer [Internet]. 2006;6(1):1–13. Available from: http://dx.doi.org/10.1186/1471-2407-6-74

87. Kim M, Yoon S, Lee S, Ha SA, Kim HK, Kim JW, et al. Gremlin-1 induces BMP-independent tumor cell proliferation, migration, and invasion. PLoS One. 2012;7(4).

88. Mulvihill MS, Kwon Y-W, Lee S, Fang LT, Choi H, Ray R, et al. Gremlin is overexpressed in lung adenocarcinoma and increases cell growth and proliferation in normal lung cells. PLoS One [Internet]. 2012;7(8):e42264. Available from: http://www.pubmedcentral.nih.gov/articlerender.fcgi?artid=3411619&tool=pmcentrez&rendertype=abstract

89. Nolan K, Thompson TB. The DAN family: Modulators of TGF-?? signaling and beyond. Protein Sci. 2014;23(8):999–1012.

90. Mitola S, Ravelli C, Moroni E, Salvi V, Leali D, Ballmer-Hofer K, et al. Gremlin is a novel agonist of the major proangiogenic receptor VEGFR2. Blood. 2010;116(18):3677–80.

91. Eckhardt BL, Parker BS, van Laar RK, Restall CM, Natoli AL, Tavaria MD, et al. Genomic analysis of a spontaneous model of breast cancer metastasis to bone reveals a role for the extracellular matrix. Mol Cancer Res [Internet]. 2005;3(1):1–13. Available from: http://www.ncbi.nlm.nih.gov/pubmed/15671244

92. Hollern DP, Honeysett J, Cardiff RD, Andrechek ER. The E2F Transcription Factors Regulate Tumor Development and Metastasis in a Mouse Model of Metastatic Breast Cancer. Mol Cell Biol [Internet]. 2014;34(17):3229–43. Available from: http://www.ncbi.nlm.nih.gov/pubmed/24934442

93. Hennighausen L. Mouse models for breast cancer. Oncogene [Internet]. 2000;19(8):966–7. Available from: http://www.ncbi.nlm.nih.gov/pubmed/10713679

94. Vargo-Gogola T, Rosen JM. Modelling breast cancer: one size does not fit all. Nat Rev Cancer [Internet]. 2007;7(9):659–72. Available from: http://www.ncbi.nlm.nih.gov/entrez/query.fcgi?cmd=Retrieve&db=PubMed&dopt=Citation&list_uids=17721431

95. ASLAKSON CJ, MILLER FR. Selective Events in the Metastatic Process Defined By Analysis of the Sequential Dissemination of Subpopulations of a Mouse Mammary-Tumor. Cancer Res. 1992;52(6):1399–405.

96. Lou Y, Preobrazhenska O, Auf Dem Keller U, Sutcliffe M, Barclay L, McDonald PC, et al. Epithelial-Mesenchymal Transition (EMT) is not sufficient for spontaneous murine breast cancer metastasis. Dev Dyn. 2008;237(10):2755–68.

97. Iorns E, Drews-Elger K, Ward TM, Dean S, Clarke J, Berry D, et al. A New Mouse Model for the Study of Human Breast Cancer Metastasis. PLoS One. 2012;7(10).

98. Gyorffy B, Lanczky A, Eklund AC, Denkert C, Budczies J, Li Q, et al. An online survival analysis tool to rapidly assess the effect of 22,277 genes on breast cancer prognosis using microarray data of 1,809 patients. Breast Cancer Res Treat. Netherlands; 2010 Oct;123(3):725–31.

99. BreastMark. BreastMark: Breast Cancer Survival Analysis Tool. [Internet]. [cited 2016 Nov 24]. Available from: http://glados.ucd.ie/?BreastMark/?index.?htm

100. Seluanov A, Vaidya A, Gorbunova V. Establishing Primary Adult Fibroblast Cultures From Rodents. J Vis Exp [Internet]. MyJove Corporation; 2010 Oct 5;(44):2033. Available from: http://www.ncbi.nlm.nih.gov/pmc/articles/PMC3185624/

101. Zhang M, Xu G, Liu W, Ni Y, Zhou W. Role of fractalkine/CX3CR1 interaction in light-induced photoreceptor degeneration through regulating retinal microglial activation and migration. PLoS One. United States; 2012;7(4):e35446.

102. Towbin H, Staehelin T, Gordon J. Electrophoretic transfer of proteins from polyacrylamide gels to nitrocellulose sheets: procedure and some applications. Proc Natl Acad Sci U S A. United States; 1979 Sep;76(9):4350–4.

103. West S. Western Blotting Handbook and Troubleshooting Guide. Pierce [Internet]. 2004;1–52. Available from: http://www.socochim.ch/Catalogs/Compl_PIERCE/WB1600990.pdf#search='western+blotting+handbook+and+troubleshooting+guide'\nwww.piercenet.com.

104. Mahmood T, Yang PC. Western blot: Technique, theory, and trouble shooting. N Am J Med Sci. 2012;4(9):429–34.

105. Thermo Scientific. ELISA technical guide and protocols. Manual. 2010;0747(815).

106. EBioscience. Enzyme Linked Immunosorbent Assay (ELISA) Enzyme Linked Immunosorbent Assay (ELISA). 2014;4–9.

107. American Type Culture Collection. MTT Cell Proliferation Assay Instruction Guide. Components. 2011;6597:1–6.

108. Biosciences A. xCELLigence RTCA DP [Internet]. [cited 2016 Apr 22]. Available from: http://www.aceabio.com/product/rtca-dp/

109. ACEA Biosciences. xCELLigence RTCA DP Instrument for Flexible Real-Time Cell

Monitoring [Internet]. 2014. Available from: http://www.aceabio.com/wp-content/uploads/xCELLigence-RTCA-DP-Instrument-CIM-Plate.pdf

110. Roche. Real Time Cell Analysis system - xCELLigence Cell Response Profiling Technology [Internet]. Xcelligence. [cited 2016 Apr 4]. Available from: http://icob.sinica.edu.tw/pubweb/data/xCelligence_???pdf

111. Östman A, Augsten M. Cancer-associated fibroblasts and tumor growth - bystanders turning into key players. Curr Opin Genet Dev. 2009;19(1):67–73.

112. KM plot. KM plot [Internet]. [cited 2016 Jan 5]. Available from: http://kmplot.com/analysis/

113. Koussounadis A, Langdon SP, Um IH, Harrison DJ, Smith VA. Relationship between differentially expressed mRNA and mRNA-protein correlations in a xenograft model system. Sci Rep [Internet]. Nature Publishing Group; 2015;5(May):10775. Available from: http://www.nature.com/srep/2015/150608/srep10775/full/srep10775.html

114. Maier T, Güell M, Serrano L. Correlation of mRNA and protein in complex biological samples. FEBS Lett [Internet]. Federation of European Biochemical Societies; 2009;583(24):3966–73. Available from: http://dx.doi.org/10.1016/j.febslet.2009.10.036

115. Owens P, Polikowsky H, Pickup MW, Gorska AE, Jovanovic B, Shaw AK, et al. Bone Morphogenetic Proteins Stimulate Mammary Fibroblasts to Promote Mammary Carcinoma Cell Invasion. PLoS One. 2013;8(6):1–12.

116. Hayashi H, Ishisaki A, Imamura T. Smad mediates BMP-2-induced upregulation of FGF-evoked PC12 cell differentiation. FEBS Lett. Netherlands; 2003 Feb;536(1-3):30–4.

117. Kuo W-J, Digman MA, Lander AD. Heparan sulfate acts as a bone morphogenetic protein coreceptor by facilitating ligand-induced receptor hetero-oligomerization. Mol Biol Cell. United States; 2010 Nov;21(22):4028–41.

118. Zhang Y-H, Cheng F, Du X-T, Gao J-L, Xiao X-L, Li N, et al. GDF11/BMP11 activates both smad1/5/8 and smad2/3 signals but shows no significant effect on proliferation and migration of human umbilical vein endothelial cells. Oncotarget. 2016;7(11):12063–74.

119. Nurgazieva D, Mickley A, Moganti K, Ming W, Ovsyi I, Popova A, et al. TGF-β1, but not bone morphogenetic proteins, activates Smad1/5 pathway in primary human macrophages and induces expression of proatherogenic genes. J Immunol [Internet]. United States; 2015 Jan;194(2):709–18. Available from: http://www.ncbi.nlm.nih.gov/pubmed/25505291

120. Martinovic S, Mazic S, Kisic V, Basic N, Jakic-razumovic J, Borovecki F, et al. Expression of Bone Morphogenetic Proteins in Stromal Cells from Human Bone Marrow Long-term Culture The Journal of Histochemistry & Cytochemistry. 2004;52(9):1159–67.

121. Sneddon JB, Zhen HH, Montgomery K, van de Rijn M, Tward AD, West R, et al. Bone morphogenetic protein antagonist gremlin 1 is widely expressed by cancer-associated stromal cells and can promote tumor cell proliferation. Proc Natl Acad Sci U S A. 2006;103(40):14842–7.

122. eBioscience. Protein Transport Inhibitor Cocktail (500X). Ebioscience. 2015;1–2.

123. Quail DF, Joyce J a. Microenvironmental regulation of tumor progression and metastasis. Nat Med [Internet]. 2013 Nov;19(11):1423–37. Available from:

http://www.ncbi.nlm.nih.gov/pmc/articles/PMC3954707/

124. Cirri P, Chiarugi P. Cancer associated fibroblasts: the dark side of the coin. Am J Cancer Res [Internet]. 2011;1(4):482–97. Available from: http://www.pubmedcentral.nih.gov/articlerender.fcgi?artid=3186047&tool=pmcentrez&rendertype=abstract

125. Liu M, Xu J, Deng H. Tangled fibroblasts in tumor-stroma interactions. Int J Cancer. 2011;129(8):1795–805.

126. Lindner D, Zietsch C, Becher PM, Schulze K, Schultheiss HP, Tschöpe C, et al. Differential expression of matrix metalloproteases in human fibroblasts with different origins. Biochem Res Int. 2012;2012.

127. Gangadhara S, Barrett-Lee P, Nicholson RI, Hiscox S. Pro-metastatic tumor-stroma interactions in breast cancer. Future Oncol. England; 2012 Nov;8(11):1427–42.

128. Karagiannis GS, Poutahidis T, Erdman SE, Kirsch R, Riddell RH, Diamandis EP. Cancer-Associated Fibroblasts Drive the Progression of Metastasis through both Paracrine and Mechanical Pressure on Cancer Tissue. Mol Cancer Res. 2012;1403–19.

129. Movahedi K, Laoui D, Gysemans C, Baeten M, Stange G, Van den Bossche J, et al. Different tumor microenvironments contain functionally distinct subsets of macrophages derived from Ly6C(high) monocytes. Cancer Res. United States; 2010 Jul;70(14):5728–39.

130. Obeid E, Nanda R, Fu YX, Olopade OI. The role of tumor-associated macrophages in breast cancer progression (review). Int J Oncol. 2013;43(1):5–12.

131. Hao NB, Lü MH, Fan YH, Cao YL, Zhang ZR, Yang SM. Macrophages in tumor microenvironments and the progression of tumors. Clin Dev Immunol. 2012;2012.

132. Ketolainen JM, Alarmo E-L, Tuominen VJ, Kallioniemi A. Parallel inhibition of cell growth and induction of cell migration and invasion in breast cancer cells by bone morphogenetic protein 4. Breast Cancer Res Treat. Netherlands; 2010 Nov;124(2):377–86.

133. Owens P, Pickup MW, Novitskiy S V., Chytil A, Gorska AE, Aakre ME, et al. Disruption of bone morphogenetic protein receptor 2 (BMPR2) in mammary tumors promotes metastases through cell autonomous and paracrine mediators. Proc Natl Acad Sci U S A [Internet]. National Academy of Sciences; 2012 Feb 21;109(8):2814–9. Available from: http://www.ncbi.nlm.nih.gov/pmc/articles/PMC3286911/

134. Hardwick JC, Kodach LL, Offerhaus GJ, van den Brink GR. Bone morphogenetic protein signalling in colorectal cancer. Nat Rev Cancer [Internet]. Nature Publishing Group; 2008 Oct;8(10):806–12. Available from: http://dx.doi.org/10.1038/nrc2467

135. Cao Y, Slaney CY, Bidwell BN, Parker BS, Johnstone CN, Rautela J, et al. BMP4 inhibits breast cancer metastasis by blocking myeloid-derived suppressor cell activity. Cancer Res. United States; 2014 Sep;74(18):5091–102.

136. Ampuja M, Jokimäki R, Juuti-Uusitalo K, Rodriguez-Martinez A, Alarmo E-L, Kallioniemi A. BMP4 inhibits the proliferation of breast cancer cells and induces an MMP-dependent migratory phenotype in MDA-MB-231 cells in 3D environment. BMC Cancer [Internet]. 2013;13:429. Available from: http://www.pubmedcentral.nih.gov/articlerender.fcgi?artid=3848934&tool=pmcentrez&rendertype=abstract

137. Carvajal G, Droguett A, Burgos ME, Aros C, Ardiles L, Flores C, et al. Gremlin: a novel mediator of epithelial mesenchymal transition and fibrosis in chronic allograft nephropathy. Transplant Proc. United States; 2008 Apr;40(3):734–9.

138. Tamminen JA, Parviainen V, Rönty M, Wohl AP, Murray L, Joenväärä S, et al. Gremlin-1 associates with fibrillin microfibrils in vivo and regulates mesothelioma cell survival through transcription factor slug. Oncogenesis [Internet]. 2013;2(July):e66. Available from: http://dx.doi.org/10.1038/oncsis.2013.29

139. Gao H, Chakraborty G, Lee-Lim AP, Mo Q, Decker M, Vonica A, et al. The BMP inhibitor Coco reactivates breast cancer cells at lung metastatic sites. Cell [Internet]. Elsevier Inc.; 2012;150(4):764–79. Available from: http://dx.doi.org/10.1016/j.cell.2012.06.035

140. Alarmo EL, Kallioniemi A. Bone morphogenetic proteins in breast cancer: dual role in tumourigenesis? Endocr Relat Cancer [Internet]. 2010;17. Available from: http://dx.doi.org/10.1677/ERC-09-0273

141. Davies SR, Watkins G, Douglas-Jones A, Mansel RE, Jiang WG. Bone morphogenetic proteins 1 to 7 in human breast cancer, expression pattern and clinical/prognostic relevance. J Exp Ther Oncol. United States; 2008;7(4):327–38.

142. Karagiannis GS, Berk A, Dimitromanolakis A, Diamandis EP. Enrichment map profiling of the cancer invasion front suggests regulation of colorectal cancer progression by the bone morphogenetic protein antagonist, gremlin-1. Mol Oncol [Internet]. Elsevier B.V; 2013;7(4):826–39. Available from: http://dx.doi.org/10.1016/j.molonc.2013.04.002

143. Daly AC, Randall RA, Hill CS. Transforming growth factor beta-induced Smad1/5 phosphorylation in epithelial cells is mediated by novel receptor complexes and is essential for anchorage-independent growth. Mol Cell Biol. United States; 2008 Nov;28(22):6889–902.

144. Holtzhausen A, Golzio C, How T, Lee Y-H, Schiemann WP, Katsanis N, et al. Novel bone morphogenetic protein signaling through Smad2 and Smad3 to regulate cancer progression and development. FASEB J Off Publ Fed Am Soc Exp Biol. United States; 2014 Mar;28(3):1248–67.

145. Sneddon JB. The contribution of niche-derived factors to the regulation of cancer cells. Methods Mol Biol. United States; 2009;568:217–32.

146. Sneddon JB, Werb Z. Location, Location, Location: The Cancer Stem Cell Niche. Cell Stem Cell. 2007;1(6):607–11.

147. Karagiannis GS, Schaeffer DF, Cho CKJ, Musrap N, Saraon P, Batruch I, et al. Collective migration of cancer-associated fibroblasts is enhanced by overexpression of tight junction-associated proteins claudin-11 and occludin. Mol Oncol [Internet]. Elsevier B.V; 2014;8(2):178–95. Available from: http://dx.doi.org/10.1016/j.molonc.2013.10.008

148. Riss T. Is Your MTT Assay Really the Best Choice? Promega Corp. 2014;1983(1):1–7.

149. Berridge M V, Tan AS. Characterization of the cellular reduction of 3-(4,5-dimethylthiazol-2-yl)-2,5-diphenyltetrazolium bromide (MTT): subcellular localization, substrate dependence, and involvement of mitochondrial electron transport in MTT reduction. Arch Biochem Biophys. United State; 1993 Jun;303(2):474–82.

APPENDIX

APPENDIX I: Buffers for Immunoblotting

Buffer	Stock Solution	Final Solution
10X TBS	Trisbase (121.1 g/mol) NaCl (58.4g/mol) Deionized Water	0.2M 1.37M Add to volume Adjust with 37% HCL to pH 7.6
1X TBS		1 part of 10X TBS to 9 part deionized water
TBST		100ml 10X TBS 900ml H_2O 10ml 10% Tween
Transfer buffer	NuPAGE 20X transfer buffer	Total volume of 1liter 850ml dH_2O 50ml NuPAGE 20X transfer buffer 100ml 100% methanol
MOPS	NuPAGE MOPS SDS Running Buffer (20X)	50ml 20x MOPS 950ml dH_20

APPENDIX II: A representative of Standard Curve of Elisa

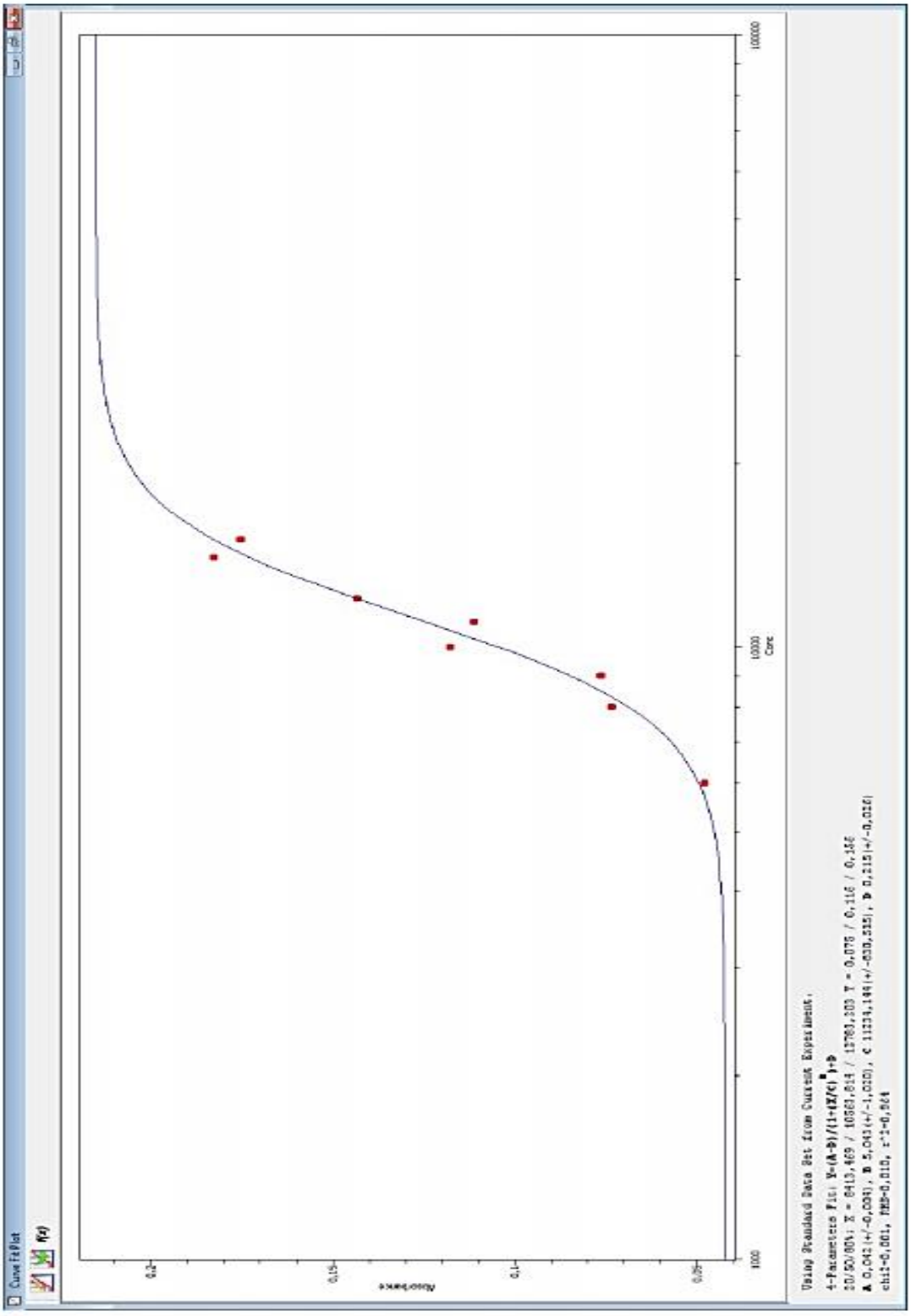

APPENDIX III: A) Transcriptome Data Analysis. Markers and mRNA expression level factors associated to CAF function in tumor growth and metastasis.

-		Comparison of cell lines				Comparison of primary tumors			
	Gene	**66cl4**	**67NR**	**Log_2**	**p-value**	**66cl4**	**67NR**	**Log_2**	**p-value**
Markers	Vim	1456.4	2921.7	-1.00	0.0001	2009.5	0.0	17.62	1.00
	Fap	0.1	0.0	2.55	1.0	0.9	1.5	-0.72	0.0558
	S100a4/FSP1	16368.9	0.0	20.64	1.0	0.0	0.0	0.00	1.00
	Acta2	0.0	0.0	2.72	1.0	8.7	3.5	1.34	0.0002
	Pdgfra	4.0	14.2	-1.83	0.0001	60.6	28.9	1.07	0.0002
	Pdgfrb	5.9	4.1	0.51	0.0001	27.6	6.2	2.14	0.0002
Activation Markers	Tgfb1	18.7	3.2	2.57	0.00012	44.6	24.6	0.86	0.0002
	Tnc	0.0	16.7	-13.39	0.30392	2.1	5.6	-1.41	0.0002
	Thy1	0.0	0.0	-2.65	1.0	23.1	25.0	-0.11	0.5554
	Pdgfb	1.1	0.0	7.40	0.00423	8.5	5.3	0.70	0.0005
	Cspg4/Ng2	0.0	0.0	-1.81	1.0	0.6	0.5	0.36	0.3041
	Pald1	2.9	3.6	-0.30	0.03636	10.3	8.5	0.27	0.1055
	Tsp-1	112.7	12.4	3.19	0.00012	177.8	11.3	3.98	0.0002
Proteases	Plau	0.0	0.0	-0.89	1.0	51.6	27.9	0.89	0.0002
	Mmp1a	0.0	0.1	-2.18	1.0	0.0	0.0	-0.92	1.00
	Mmp1b	0.2	0.5	-1.70	0.00012	0.0	0.0	0.87	1.00
	Mmp2	0.2	0.1	0.50	1.0	8.9	35.5	-2.00	0.0002
	Mmp3	3.8	21.2	-2.47	0.00012	68.8	38.3	0.85	0.0002
	Mmp7	0.0	0.0	0.00	1.0	0.0	0.0	0.51	1.00
	Mmp9	1.0	0.2	2.44	0.00012	33.5	14.2	1.24	0.0002
	Mmp11	3.2	0.8	2.00	0.00012	11.8	1.7	2.82	0.0002
	Mmp12	0.0	0.0	0.58	1.0	3.7	0.4	3.30	0.0002
	Mmp13	0.3	0.1	1.51	0.00012	4.3	2.0	1.10	0.0002
	Mmp14	22.8	23.5	-0.04	0.77655	81.8	77.8	0.07	0.6737

APPENDIX III: B) Transcriptome Data Analysis. Markers and mRNA expression level factors associated to CAF function in tumor growth and metastasis

		Comparison of cell lines				Comparison of primary tumors			
	Gene	**66cl4**	**67NR**	**Log_2**	**p-value**	**66cl4**	**67NR**	**Log_2**	**p-value**
Growth Factors	Vegfa	14.3	19.1	-0.41	0.00161	16.6	25.0	-0.58	0.0010
	Vegfb	36.8	37.4	-0.02	0.87254	25.1	26.2	-0.06	0.7864
	Vegfc	4.5	0.0	9.26	0.30444	20.3	0.8	4.74	0.0002
	Hgf	0.0	0.0	-0.94	1.0	0.8	1.1	-0.40	0.3588
	Fgf2/bFgf	0.0	1.2	-6.96	0.00012	0.1	1.9	-3.80	0.0045
	Igf1	0.0	0.0	-0.30	1.0	5.0	3.7	0.44	0.0907
	Igf2	0.2	0.1	1.23	0.00012	3.2	0.9	1.78	0.0002
	Egf	0.1	0.1	0.08	1.0	0.3	0.1	1.06	0.0460
	Pdgfc	0.1	1.1	-4.17	0.00012	3.4	6.0	-0.81	0.0002
Other factors	Tnf	0.0	0.0	-1.36	1.0	1.3	1.1	0.26	0.6140
	Csf1	249.3	130.8	0.93	0.00012	154.4	65.4	1.24	0.0002
	Csf2	0.0	0.0	-1.11	1.0	0.1	0.2	-0.89	1.0
	Il12a	0.0	0.0	-0.18	1.0	0.0	0.2	-1.91	1.0
	Il1a	0.0	0.0	0.98	1.0	0.6	0.2	1.65	0.0276
	Il4	0.0	0.0	0.00	1.0	0.1	0.2	-1.97	0.2727
	Il6	0.3	0.1	2.41	0.03091	0.7	1.2	-0.83	0.1522
	Cxcl12	143.0	31.6	2.18	0.00012	205.1	75.2	1.45	0.0002
	Sparc	161.9	557.2	-1.78	0.00012	424.5	629.8	-0.57	0.0016
	Lox	0.1	0.0	3.36	1.0	2.1	1.7	0.32	0.3042
	Fn1	58.2	67.0	-0.20	0.14507	0.0	394.5	-15.27	1.0
	Cxcl9	0.0	0.0	0.92	1.0	13.4	29.5	-1.14	0.0002
	Cxcl10	126.0	1.9	6.05	0.00012	15.5	47.7	-1.62	0.0002

APPENDIX IV: BreastMark prognosis results of BMP4 and GREM1

	Breast Cancer Subtype	p-Value	Hazard ratio
BMP4	Luminal A	0.870	0.9795(0.7935-1.257)
	Luminal B	0.356	0.9179(0.7648-1.102)
	Lymph node positive	0.064	0.8091(0.6463-1.013)
	Her2	0.413	1.149(0.8252-1.599)
	Basal	0.314	1.171(0.8612-1.592)
GREM1	Luminal A	0.515	1.086(0.8475-1.391)
	Luminal B	0.822	0.9798(0.8198-1.171)
	Lymph node positive	0.770	1.034(0.8276-1.291)
	Whole cancer	0.012	1.162(1.033-1.306)
	Her2	0.232	1.234(0.8735-1.742)

APPENDIX V: Relevant Bmp antagonist family correlation with prognosis- Km plotter (Overall Survival)

Gene	Affymetrix ID	p-Value	Hazard ratio
BMPER	241986	0.80	1.05(0.73-1.49)
FST	226847	0.57	0.90(0.63-1.29)
FSTL1	208782	0.18	0.85(0.67-1.08)
BAMBI	203304	0.72	1.04(0.83-1.32)
TSKU	218245	0.50	0.92(0.73-1.17)

APPENDIX VI

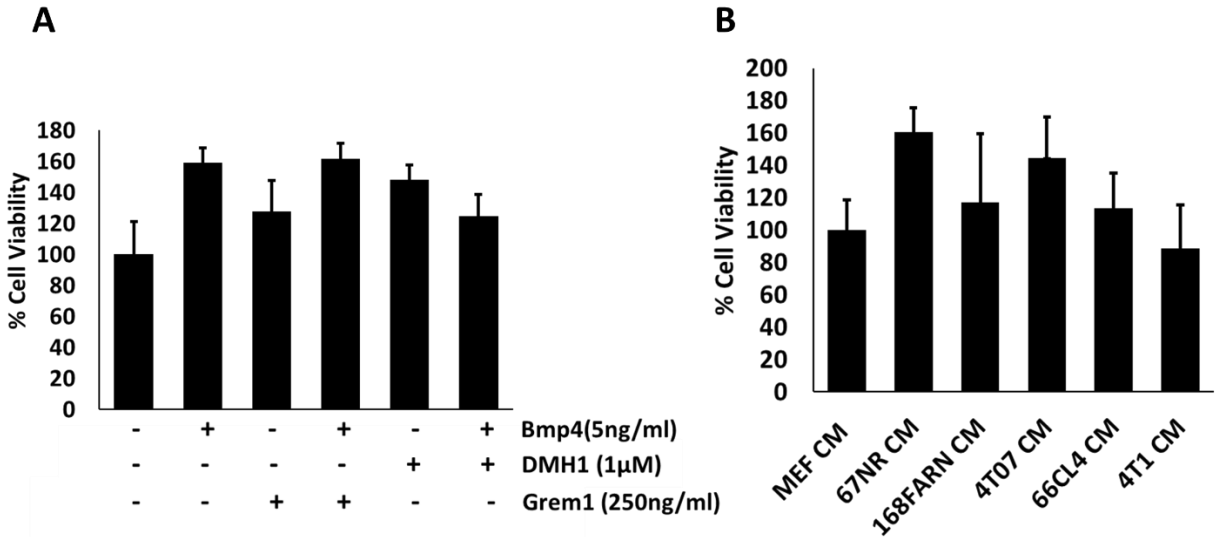

Appendix VI: Proliferation of MEF is influenced by different stimulation.
*For **A and B** 2000 cells/well were seeded in 96-well culture plates and incubated overnight. The cells were then treated with the various stimulants and incubated for another 24hours. Cell viability was then measured by MTT assay. The results were expressed as percentage of cell viability compared to the control which is MEFs in its own medium. Results are means of 10 parallel experiment and bars are ±SD.*

APPENDIX VII: Time-dependent migration profiles of Lung Fibroblast

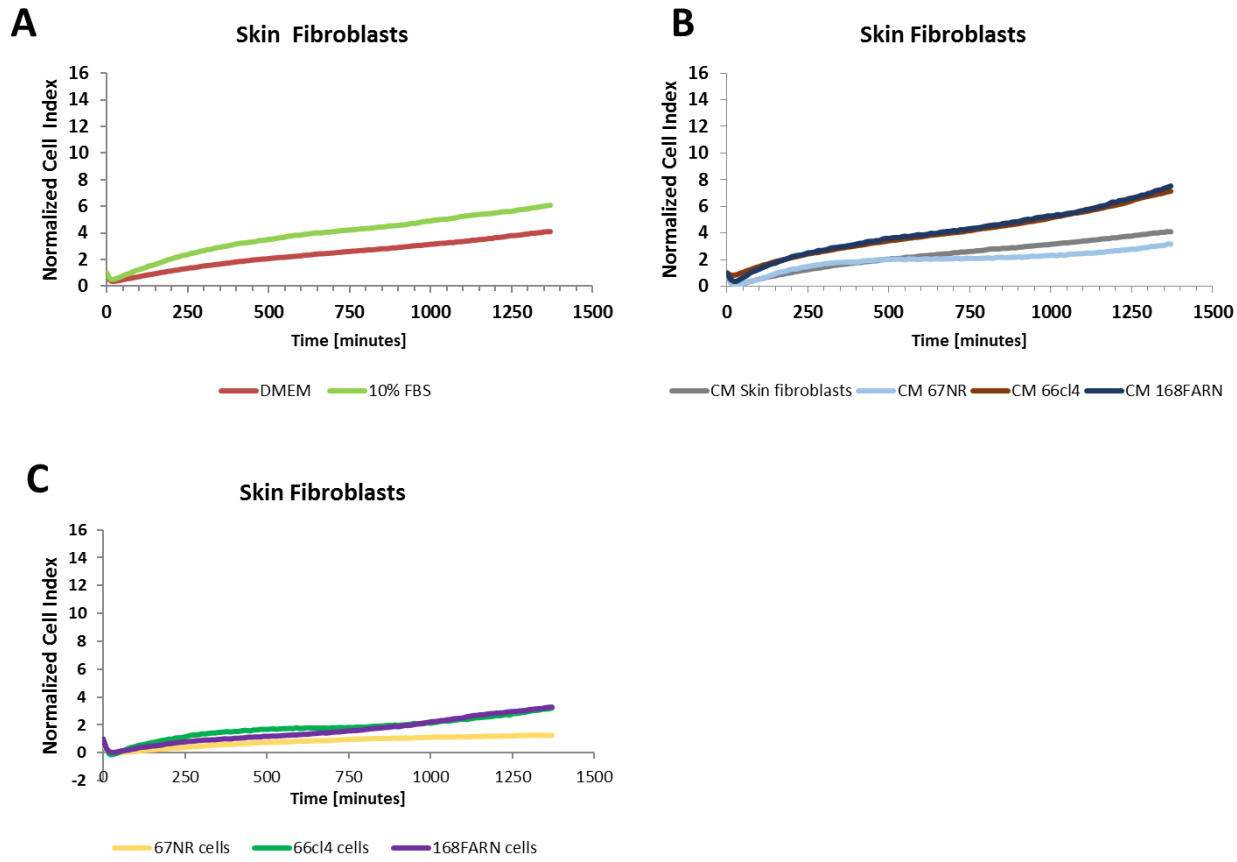

Appendix VII: Time-dependent migration profiles of Lung Fibroblast.

A) *Validation of system with DMEM that has no serum (red) and one that contain 10% FBS (green).* ***B)*** *Migration curves of Skin Fibroblast cells produced by xCELLigence RTCA with seeding densities of 10000cells/ well (Upper chamber) with condition medium (CM) from 66NR, 66cl4 and 168FARN serving as chemoattractant with lung fibroblast CM as control (lower chamber).* ***C)*** *Same as* ***(B)*** *but with 67NR, 66cl4, 168FARN cells instead of CM in the lower chamber. All graphs represent mean ± SD from duplicate experiment run parallel with the exception of "****A****".*